INAUGURAL - DISSERTATION

submitted to the

Combined Faculties of the Natural Sciences and Mathematics,

Ruperto-Carola University of Heidelberg, Germany

for the degree of

Doctor of Natural Sciences

Transition-Metal Complexes as Enzyme-Like Reagents for Protein Cleavage

Dina Pavlović Rosman

Heidelberg, 2005

INAUGURAL - DISSERTATION

submitted to the

Combined Faculties for the Natural Sciences and for Mathematics,

Ruperto-Carola University of Heidelberg, Germany

for the degree of

Doctor of Natural Sciences

presented by

Dipl. -Chem. Dina Pavlović Rosman,

born in Zagreb, Croatia

Oral examination: 21st December 2005

Transition-Metal Complexes as Enzyme-Like Reagents for Protein Cleavage

Referees: Prof. Dr. Nils Metzler-Nolte

Prof. Dr. Andres Jäschke

This work was carried out between March 2002 and August 2005 at the

Institut for Pharmacy and Molecular Biotechnology,

Faculty for Biosciences,

University of Heidelberg,

Germany

I am grateful to so many people who helped, on their own ways, this research to be done. Specially I am thankful to:

Prof. Dr. Nils Metzler-Nolte, for the opportunity to work in his group, helpful "tea-time" discussions, his fascination in chemistry and many lab and teaching skills;

Dr. Thomas Weyhermüller for the numerous X-ray crystal structure determinations;

My colleagues Fozia Noor, Srećko Kirin, Xavier de Hatten, Andrea Maurer, Merja Neukamm, Tim Kersebohm, Ulli Schatzschneider, Ulli Hoffmans and Stephanie Cronje for always unpredictable working atmosphere;

Heiko Rudy and Peter Weyrich for excellent MS skills and technical support in general;

Ute Hertle and Tobias Timmermann for running the NMR experiments with enthusiasm, specially during my "hydrolysis time";

Viola Funk and Karin Weiß, our secretaries, for very good organisation, helpfulness and the most important – good mood;

Annette Wüstholz for her perfectionism, which helped me during my first few semesters of teaching pharmacy students;

Marcus Buchholz, for his persistence in searching for the "perfect" crystal.

I am also greatful to my croatian friends for making me feel like home everywhere I go. Wonderful feeling. Special thanks to:
Dagmar and Tamara, for their quiet and good kind; Davorka, for advices she told me; Marko, for many things. You are still my hero, don`t you know?; Miro, who thought me "Silence is golden"; Mirela for thousands of e-mails and jokes she sent me. Where do you get it from?

But most of all, I would like to thank those whom I deeply love, respect and admire, and whom I dedicate this thesis – my family:

My parents, for ease and beauty of their character, trust and patience, and for the most precious thing - their unconditional love;

My brother and his family, for all good vibrations and positive energy;

My Guido, for this wonderful journey we go through since ten years;

My Timon, for making me stop and think, for bringing me sunshine every single day……and much, much more…

od srca…

mojoj obitelji

Table of Contents

Abstract

Pavlović Rosman, Dina Dipl. Chem. 21st December 2005

„Transition-Metal Complexes as Enzyme-Like Reagents for Protein Cleavage"

Referees: Prof. Dr. Nils Metzler-Nolte
Prof. Dr. Andres Jäschke

In this thesis, metal-promoted hydrolytic cleavage of the amide bond in histidine-containing dipeptides, has been studied.
Transition-metal complexes are emerging as new reagents for selective cleavage of unactivated amide bonds in proteins. Such complexes bind to the side chains of methionine and histidine forming an inert complex with the *N*-terminal amino acid in the peptide. This binding is a prerequisite for subsequent cleavage, which occurs near these "anchoring" residues.
We designed transition metal complexes for the cleavage of the first peptide bond downstream from the anchoring side chain of histidine. For this purpose, a series of ligands and their corresponding metal complexes, containing various divalent metal ions, such as Pd(II), Zn(II), Cu(II), Co(II), Ni(II) and Cd(II) have been synthesized. To complete their characterization, beside ^{1}H and ^{13}C NMR data, FAB/ESI-MS data and elemental analysis, crystallographic data of nine complexes have been obtained. They gave further insight into the geometry and nature of binding in synthesized metal complexes.
In the course of this thesis, the role of the synthesized transition metal complexes as the promotores in the cleavage of the amide bond in small peptides, was examined. To supress the formation of hydrolytically inactive promoter-substrate complexes, the *N*-terminus of the dipeptides was protected by the acetylation. The histidine residue was placed either on the *N*- (AcHisGly) or C-terminus (AcβAlaHis) of the dipeptides. The rate of cleavage was monitored by following the ^{1}H NMR resonances of free glycine.
In addition, the possibilities to couple one of the new ligands with NTA (*N*-nitrilotriacetic acid) moiety, were investigated. In that compound, metal complex of the ligand could act as a peptidase, while the NTA moiety is known as an important and well characterized chelator for the oligo-histidine tag. It could be shown that, in this case, the carbodiimide method and mixed anhydride method are coupling methods of choice.

To summerize, in this study a new Pd(II) complex was identified, which showed very good regioselectivity in promoting hydrolytic cleavage of dipeptides. Using this complex, almost 80% of the peptide was cleaved after five days. Our results prove that a scissile bond on the carboxylic side of the anchoring histidine residue is necessary for hydrolysis: when the peptide bond is on the *N*-terminus of the anchoring histidine residue, no hydrolytic cleavage was observed.

Zusammenfassung

Pavlović Rosman, Dina Dipl. Chem. 21.12.2005

„Übergangsmetallkomplexe als Peptidase-Mimetika“

Gutachter: Prof. Dr. Nils Metzler-Nolte
Prof. Dr. Andres Jäschke

Diese Doktorarbeit beschäftigt sich mit der Metall-katalysierten Hydrolyse von Histidin-haltigen Dipeptiden.
In den letzten Jahren sind koordinativ ungesättigte Übergangsmetallkomplexe als neue Reagentien für die selektive Spaltung nicht-aktivierter Amid-Bindungen in Peptiden entwickelt worden. Solche Komplexe binden an die Donorgruppen von Aminosäure-Seitenketten wie Methionin oder Histidin. Dies ist eine Voraussetzung für die nachfolgende Spaltung des Peptidrückrats, welche in der Nähe der Bindungsstelle erfolgt.
Wir haben Metallkomplexe für die Hydrolyse der Peptidbindung entwickelt, die sich auf der C-terminalen Seite einer Histidin-Ankergruppe befindet. Es wurde eine Serie von Liganden und ihre Komplexe mit divalenten Übergangsmetallen wir Pd(II), Zn(II), Cu(II), Co(II), Ni(II) und Cd(II) synthetisiert. Alle Verbindungen wurden mit Elementaranalyse, ^{1}H und ^{13}C NMR sowie FAB-/ESI-Massenspektrometrie vollständig charakterisiert. Von neun der Verbindungen konnten zusätzlich Kristalle erhalten werden, die für eine Röntgenstrukturanalyse geeignet waren. Dies erlaubte weitergehende Einblicke in die Geometrie und Bindungsverhältnisse der synthetisierten Verbindungen.
Anschließend wurde die Eignung dieser Metallkomplexe als Katalysatoren für die Spaltung der Amidbindung in den Dipeptiden AcHisGly und AcβAlaHis untersucht. Um die Bildung inaktiver Katalysator-Peptid-Komplexe zu unterdrücken, wurde der *N*-Terminus der Dipeptide durch Acetylierung geschützt. Während AcβAlaHis unter den gewählten Bedingungen stabil war, konnte die Hydrolyserate von AcHisGly NMR-spektroskopisch durch zeitabhängige Messung der Intensität des Signals des freigesetzten Glycins verfolgt werden.
Für eine mögliche Anwendung dieser Metallkomplexe als Werkzeuge für die hydrolytische Abspaltung der in der Äffinitätschromatographie von Proteinen häufig verwendeten Oligo-Histidin-Tags wurden Konjugate der synthetisierten Liganden mit NTA (Nitrilotriessigsäure) hergestellt, da NTA-Metallkomplexe an 6xHis-Tags binden. Dabei erwiesen sich die Carbodiimid- und Mixed-Anhydrid-Methode als gut geeignet.

Im Rahmen dieser Arbeit konnte insbesondere ein neuer Palladium(II)-Komplex identifiziert werden, der eine sehr hohe Regioselektivität bei der hydrolytischen Spaltung von Dipeptiden aufweist. Innerhalb von fünf Tagen hydrolysiert diese Verbindung nahezu 80% eines vorgelegten Peptids. Wie erwartet, wird nur die Amidbindung auf der C-terminalen Seite der Histidin-Ankergruppe gespalten. Befindet sich die Peptidbindung auf der *N*-terminalen Seite des Histidins, so ist keine Hydrolyse zu beobachten.

Abbreviations

Å	angström
Ac	acetyl
Ar	aryl group
B	magnetic field
bh	background hydrolysis
bz	benzyl
C	celsius
cm	cenitmeter
CT	charge transfer
CV	cyclic voltametry
d	doublet
dd	doublet doublet
δ	chemical shift
EPR	electron paramgnetic renonace
equiv.	equivalent
Esd	estimated standard deviation
ESI	electro-spray interface
Et	ethyl
ε	molar extinction coefficient
FAB	fast atom bombardment
G	Gauss
g	gram
h	hour
HOMO	highest occupied molecular orbital
HPLC	high performance liquid chromatography
Hz	hertz
I	nuclear spin
IMAC	Immobilized Metal Ion Affinity Chromatography
IR	infrared radiation
J	coupling constant
K	kelvin
L	ligand

LUMO	lowest unoccupied molecular orbital
λ	wavelenght
m	multiplet, meter, milli-
M	molar, mega-, metal
Me	methyl
min	minute
MO	molecular orbital
MS	mass spectrometry
m/z	mass per charge ratio
NMR	nuclear magnetic resonance
ppm	parts per million
py	pyridine
q	quartet
rt	room temperature
S	spin
s	singlet
sol	solvent
SOMO	single occupied molecular orbital
σ	standard deviation
T	temperature
t	triplet
TLC	thin-layer chromatography
tert	tertiary
UV	ultra violet
Vis	visible
vs.	Versus

Abbreviations for chemicals and solvents

Aa	amino acid
Ala	alanine
BNPS	3-bromo-3-methyl-2-(2`-nitrophenylsulfenyl)-indolenine
Cys	cysteine
DCC	dicyclohexylcarbodiimide
DCM	dichloromethane
DIPEA	*N*, *N*-diisopropylethylamine
DMAP	4-(dimethylamino)pyridine
DMF	dimethylformamide
DMSO	dimethyl sulfoxid
dtco	1,5-dithiacyclooctane
edda	ethylenediamine-*N*,*N*`-diacetate
en	ethylenediamine
EtOAc	ethylacetate
EtOH	ethanol
Fmoc	fluorenyl-9-methoxycarbonyl
Gly	glycine
HBTU	O-(benzotriazole-1-yl)-*N*,*N*,*N*`,*N*`-tetramethyluronium hexafluorophosphane
HEPES	*N*-(2-hydroxyethyl)-piperazine-*N*'-2-ethanesulfonic acid
His	histidine
HOBt	*N*-hydroxybenzotriazole
iBCF	isobutyl chloroformate
Lys	lysine
MeOH	methanol
3-NBA	3-nitrobenzyl alcohol
NEt_3	triethylamine
NHS	*N*-hydroxysuccinimide
NTA	*N*-nitrilotriacetic acid
py	pyridine
TBTU	O-(benzotriazole-1-yl)- *N*,*N*,*N*`,*N*`-tetramethyluronium tetrafluoroborate
TFA	trifluoro-acetic acid

THF	tetrahydrofurane
TMS	tetramethylsilane
tren	tris(2-aminoethyl)amine
trien	triethylenetetramine
TSPSA	3-(trimethylsilyl) propane sulfonic acid Na salt
Z	Benzyloxycarbonyl

1

Introduction

1.1 Peptide Bond

Peptides, from the Greek πεπτοζ – "digestable", are the family of molecules formed from the linking, in a defined order, of various amino acids. They are an increasingly important class of molecules in medicinal chemistry, biochemistry, physiology and molecular biology. The bond between one amino acid residue and the next one is an amide or peptide bond.

Owing to about 40% double-bond character in the carbon-nitrogen bond, peptide groups are planar, and the α carbon atoms, and hence the amide oxygen and nitrogen atoms, most often adopt a trans disposition. Since oxygen is more electronegative than nitrogen, the delocalized electrons of the peptide bond are shifted toward oxygen. For this reason, the peptide bond is polar. In amides, both C-N and C-O bonds possess comparable amounts of single- and double-bond character, resulting in appreciable delocalization of negative charge on the amide carbonyl oxygen atom. Because of partial negative charge of the carbonyl

oxygen, it can serve as a hydrogen acceptor in hydrogen bonds. The nitrogen has a partial positive charge, so that the weakly acidic –NH group can serve as a hydrogen donor in hydrogen bonds. Measurements reveal that the carbon-nitrogen bond of a peptide group is somewhat shorter than a typical carbon-nitrogen single bond: bond length of 132 pm for the peptide bond is intermediate between 145 pm for single and 124 pm for double bonds.

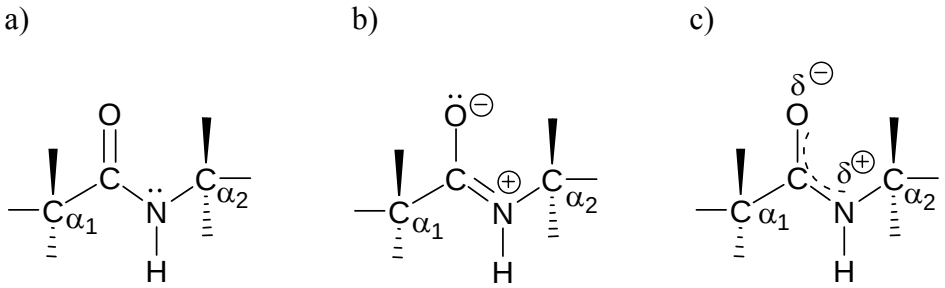

Scheme 1.1 *Structure of the peptide bond: a) peptide bond as a single carbon-nitrogen bond; b) peptide bond as a double bond, and the bond between carbon and oxygen is a single bond; c) resonance hybrid, probably a truer representation of the peptide bond.*

Through almost the entire pH range, the amide group is neutral. It is such a weak acid that quantitative equilibrium measurments are difficult. Proton loss from the amide nitrogen to give a negatively charged species does not occure until > 1 M hydroxide, pK_a = 15. The amide group is also a very weak base, undergoing protonation only in 1 M acid. For an anionic amide, protonation and metalation occur at the nitrogen. For a neutral amide, both protonation and metalation occur at the amide oxygen atom. Bond length changes in the peptide bond upon metalation are small and variable[1].

Metal ions interact only very weakly with an isolated amide group, owing to the very weak basicity of the amide oxygen atom (pK_a = -1). In aqueous solutions water provides a competitive oxygen donor. Substitution of the amide hydrogen atom by a metal ion would furnish a strong bond to the amide nitrogen, but the strong competition of the proton for the very basic amide nitrogen (pK_a = 15) prevents most metal ions from dissplacing the proton, except in strongly basic solutions. The extent of metal ion interaction in peptides may increase by initital anchoring of the metal ion[2]. Potential anchors include the side chains of histidine and cysteine, but in most cases only a weak chelation occurs at the peptide oxygen atom. Metal ions can also anchor at the amino terminus, followed by formation of a five-membered chelate ring at the first amide oxygen.

1.2 Hydrolysis of Peptide Bonds

Selective cleavage of peptides and proteins is an important procedure in biochemistry and molecular biology. The half-life for the hydrolysis of the peptide bonds is 7-600 years at room temperature and pH 4-8[3].

The mechanism of metal-promoted amide hydrolysis is less certain. Sayre[4] has suggested five different mechanisms by which peptide bond may be hydrolyzed by metal complexes. His research and research of some other laboratories[5, 6] have aimed at distinguishing between two kineticaly equivalent pathways leading to the tetrahedral intermediate (TI): the electrophilic activation of the carbonyl moiety by metal (Scheme 1.2a) and provision of better nucleophile – Metal hydroxide mechanism (Scheme 1.2b).

a) b)

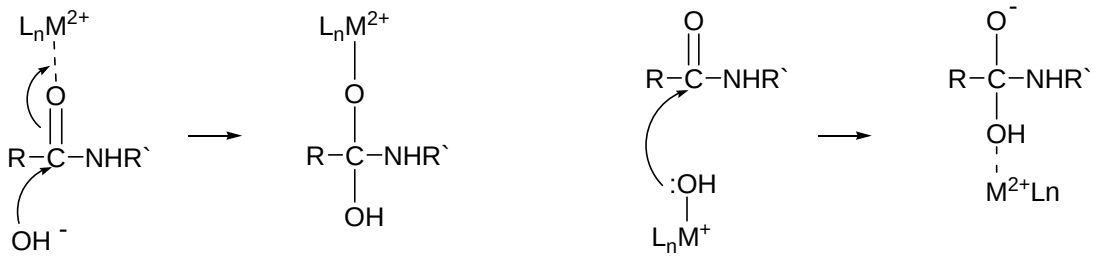

Scheme 1.2 *a) Electrophilic activation; b) Metal hydroxide nucleophile.*

However, later research of Pocker et al.[7] raised the possibility of simultaneous carbonyl activation and M-OH participation (Scheme 1.3a) or general base catalysis (Scheme 1.3b).

a) b)

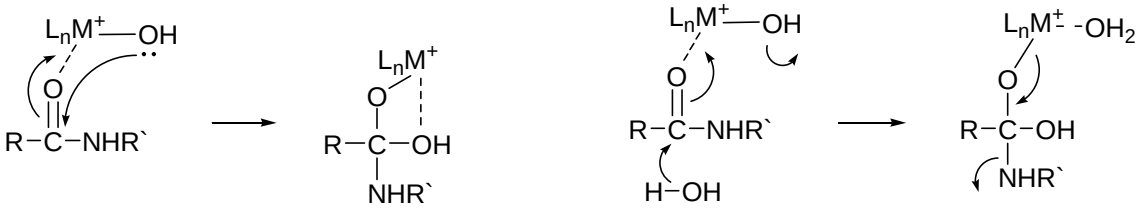

Scheme 1.3 *a) Electrophilic activation/ Metal hydroxide nucleophile; b) Electophilic activation/ General base catalysis.*

Another possibility, which is rarely considered[8], is that M-OH_2 could initiate a general acid catalysis (GAC) for C-N cleavage and a mechanism, that is an extension of Scheme 1.3b, has been proposed (Scheme 1.4).

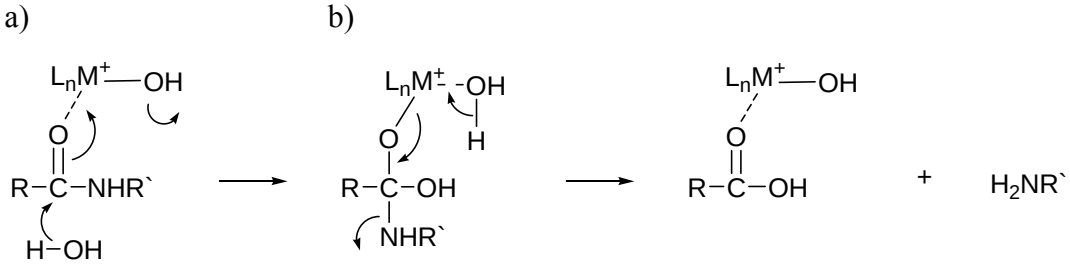

Scheme 1.4 *a) Electophilic activation/ General Base Catalysis; b) General Acid Catalysis.*

In contrast to ester hydrolysis, which involves relatively facile expulsion of an alkoxide leaving group, amide hydrolysis proceeds according to a rate-limiting TI breakdown mechanism, involving a poor leaving group, which must be protonated either prior to or simultaneously with C-N cleavage.

1.3 Synthetic Peptidases

1.3.1 Why Develop Synthetic Peptidases?

Since the peptide bond is extremely unreactive towards hydrolysis, relatively fast methods of artificial cleavage are needed. Although numerous naturally occuring peptidases are known, the development of a synthetic one would be of great utility and importance.

Traditionally, sequence analysis has been done with a small number of proteolytic enzymes, but among them only trypsin is highly regioselective[9]. The available proteases usually effect selective and catalytic cleavage under mild conditions, but they are sometimes inapplicable because they cleave at too many sites and produce fragments that are too short. In addition to proteolytic enzymes, the most commonly used chemical cleavage reagent is cyanogen bromide[3] (CNBr) which cleaves proteins on the carboxylic side of methionine residues and, because these residues are relatively rare, usually produces long fragments. It has also several shortcomings: it is volatile and toxic, requires harsh conditions and often produces incomplete cleavage. CNBr requires 70% formic acid as the solvent and causes various side reactions. The protein fragments created by CNBr are no longer native, because the methionine residues in them are irreversibly converted to serine lactones. There is also a number of other reagents, such as *N*-bromosuccinimide and 3-bromo-3-methyl-2-(2`-nitrophenylsulfenyl)-indolenine (BNPS-skatole), that are used for tryptophan-selective cleavage[10, 11]. Cleavage by *N*-bromosuccinimide requires harsh conditions that might result in substrate degradation. Reactions with BNPS-skatole are effective only in the presence of a high excess of the cleaver. Therefore, new selective chemical (nonenzymatic) reagents are needed for the improvement of hydrolysis procedures.

Synthetic peptidases could also find utility as conformational probes. The three-dimensional structure of proteins and nucleic acids is gained from X-ray crystallography and NMR – two powerful techniques, each of them requires large amounts of material and obtaining X-ray-quality crystals is very difficult. To avoid these difficulties, the artificial hydrolases could be designed to recognize certain conformations or turn regions between two α-helices.

Beside this, synthetic peptidases could be helpful in elucidating the role of metal ions in natural hydrolases. Although many hydrolases utilize metal ions, the precise role of the metal ion in the hydrolysis reactions is not known. Most probably, metal ions could promote

hydrolysis by providing a) a scaffold to ensure proper conformation; b) activation of the carbonyl bond; and/or c) charge neutralizatioon to facilitate nucleophilic attack and stabilize the leaving group[12]. Obtaining a better understanding of the function of metal ions in synthetic systems would provide a deeper knowledge of the role of metal ions in natural peptidases and in addition aid in the development of more efficient synthetic hydrolases.

Some transition-metal complexes are emerging as new reagents for selective hydrolysis of peptides and proteins[13-15]. These readly available and small molecules can hydrolyze amide bonds in peptides and proteins, though their regioselectivity is still the most important task and challenge. Many researchers have demonstrated metal-promoted hydrolysis of peptides with metal ions such as palladium(II), platinum(II), copper(II), zinc(II) and cobalt(III). Some of the most important examples of the metal complexes as synthetic peptidases are summerized in the following chapters 1.3.2 – 1.3.5.

1.3.2 Palladium(II) and Platinum(II) Complexes as Synthetic Peptidases

Palladium, platinum and their complexes have many medicinal, chemical and industrial applications. Interaction of Pd(II) and Pt(II) with biological molecules is of great medical interest, mostly because some of these complexes are anticancer drugs[16]. Their most common oxidation state is +II where they have d^8 electron configuration, and therefore diamagnetic. Complexes of Pd(II) and Pt(II) are mostly square planar. Pt(II) is inert to ligand substitution, while Pd(II) is considerably more labile. The ligand substituiton rates for Pd(II) are usually 10^5 times greater than for Pt(II) in complexes with similar ligands[17]. Both metal ions are “soft” Lewis acid and prefer “soft” ligands, such as CN^- or sulfur donors, to “hard” ligands, such as oxygen donors. Research from the laboratory of T. G. Appleton[18] reports about binding of both metals to many biological ligands, such as peptides and proteins. They form stable complexes with the peptide backbone and with the side chains of methionine, cysteine, histidine and other amino acids[17, 19]. Pd(II) and Pt(II) can coordinate to peptides in several modes, *but none of those studies report about cleavage of the peptides upon coordination*!

Kostić`s lab reported for the first time 1991. about the selective hydrolysis of non-activated peptide bonds, promoted by platinum(II) complexes anchored to amino acid side chains[20]. Although their first studies were carried out with Pt(II), they soon switched to the more labile Pd(II) complexes.

1.3.2.1 Cleavage Reagents and Their Regioselectivity

In his early studies[21-25], Kostić has realized that in hydrolytically active Pd(II) and Pt(II) complexes at least two of four coordination sites must be available: one for anchoring to the side chain of the amino acid in the peptide, another for interaciton with the proximate peptide bond to be cleaved. Therefore, at least two coordination sites in the complex should be occupied by weak ligands that can be readily replaced. The remaining two sites are occupied by a bidentate ligand to forestall additional substitution and hydrolysis equilibria. Figure 1.1 shows the most effective cleavage reagents tested.

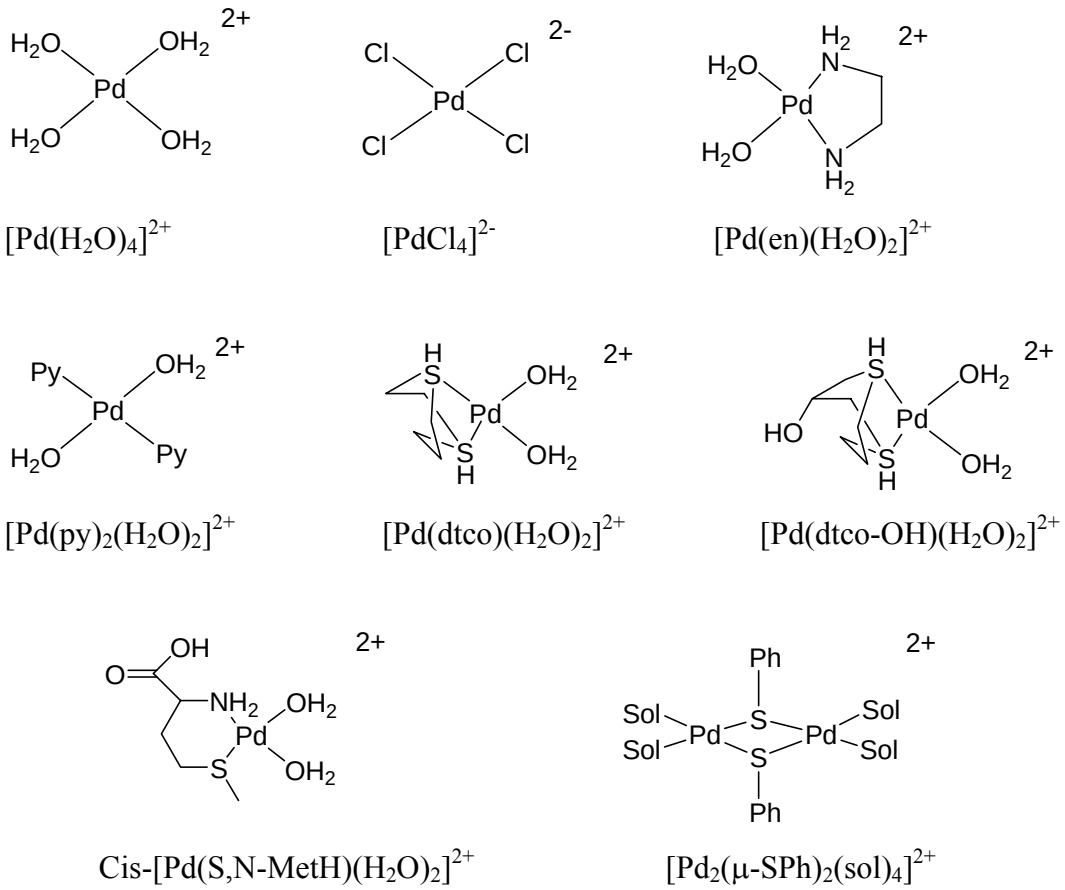

Figure 1.1 *Most effective complexes of Pd(II) and Pt(II) as cleavage reagents of peptides and proteins.*

The simpliest cleavage reagent is $[Pd(H_2O)_4]^{2+}$. However, this complex oligomerizes at pH>2, via OH^- bridges. To overcome this problem, the complex should be kept in solution of the noncoordinating $HClO_4$, which supresses the oligomerization. Coordinating anions may displace the aqua ligand and decrease the availability of the two coordination sites required for the cleavage. This is the case also for $[PdCl_4]^{2-}$, which is less effective than $[Pd(H_2O)_4]^{2+}$

as a cleavage reagent, because the need for prior aquation of Cl^- ligands decreases the amount of the hydrolytically active aqua complex.

Complexes of Pd(II) can bind to the thioether group in methionine and to the imidazole group in histidine[26]. In the small peptides of general formula AcHisAa and AcMetAa (in which Ac is acetyl group and Aa is a leaving amino acid), the anchored Pd(II) ion hydrolyzes the amide bond involving the carboxylic group of the anchoring amino acid, that is, the first peptide bond downstream from the anchor (Scheme 1.5). However, in the proteins and oligopeptides, the anchored Pd(II) ion hydrolyzes the second amide bond upstream from the anchor.

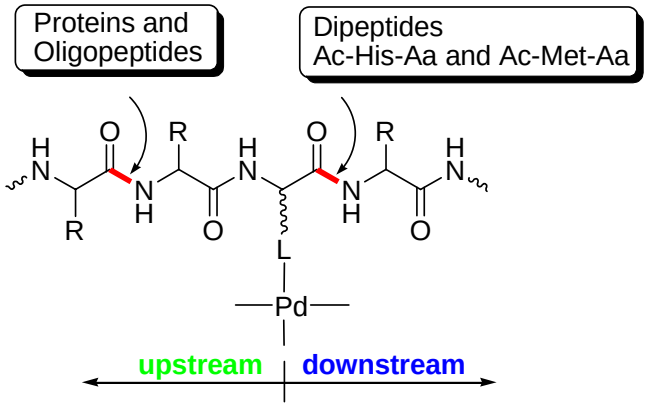

Scheme 1.5 *Palladium(II) complexes act with different regioselectivity in the cleavage of dipeptides and proteins (The sites of cleavage are highlighted. The anchoring side chain is coordinated to the Pd(II) ion via the group L; the remaining three ligands are not specified).*

Furthermore, the kinetics and regioselectivity of cleavage of histidine-containing peptides can be controlled by the choice of ligands in Pd(II) complexes[27]. In the presence of $[PdCl_4]^{2-}$ glycine was completely released from the peptide AcHisGly, which means only the first amide bond downstream, not the first amide bond upstream, was cleaved. However, upon mixing AcHisGly with $[Pd(H_2O)_4]^{2+}$ both amide bonds are cleavaed. Why the $[PdCl_4]^{2-}$ complex does not cleave the "left" amide bond? Under assumption that both amide bonds in the same peptide are cleaved by the same mechanism, the difference between $[Pd(H_2O)_4]^{2+}$, which cleaves both amide bonds, and $[PdCl_4]^{2-}$, which cleaves only the "right" one, may be due to steric factors.

The former complex is smaller and presumably may approach the scissile bonds more closely. The group is more effective than the $PdCl_3^-$ group in both limiting mechanisms for hydrolysis – external attack and internal delivery. The Pd(II) ion in the cationic complex is stronger Lewis acid, therefore better able to activate the amide group for external attack, than

the ion in the anionic complex. For the internal delivery of a water molecule, the aqua complex is obviously also better suited than the chloro complex: because the $Pd(H_2O)_3^{2+}$ group attached to the imidazole ring in the dipeptide contains several aqua ligands, conformations that bring one of them near the scissile amide bond are likely to exist. These expectations are confirmed by the molecular-dynamics simulations.

For both Pd(II) and Pt(II) reagents, Kostić identified the hydrolytically active complexes and different cleavage selectivity of Pd(II) and Pt(II) complexes, shown in Scheme 1.6. A weakly acidic solution is necessary to suppress their conversion to inactive complexes.

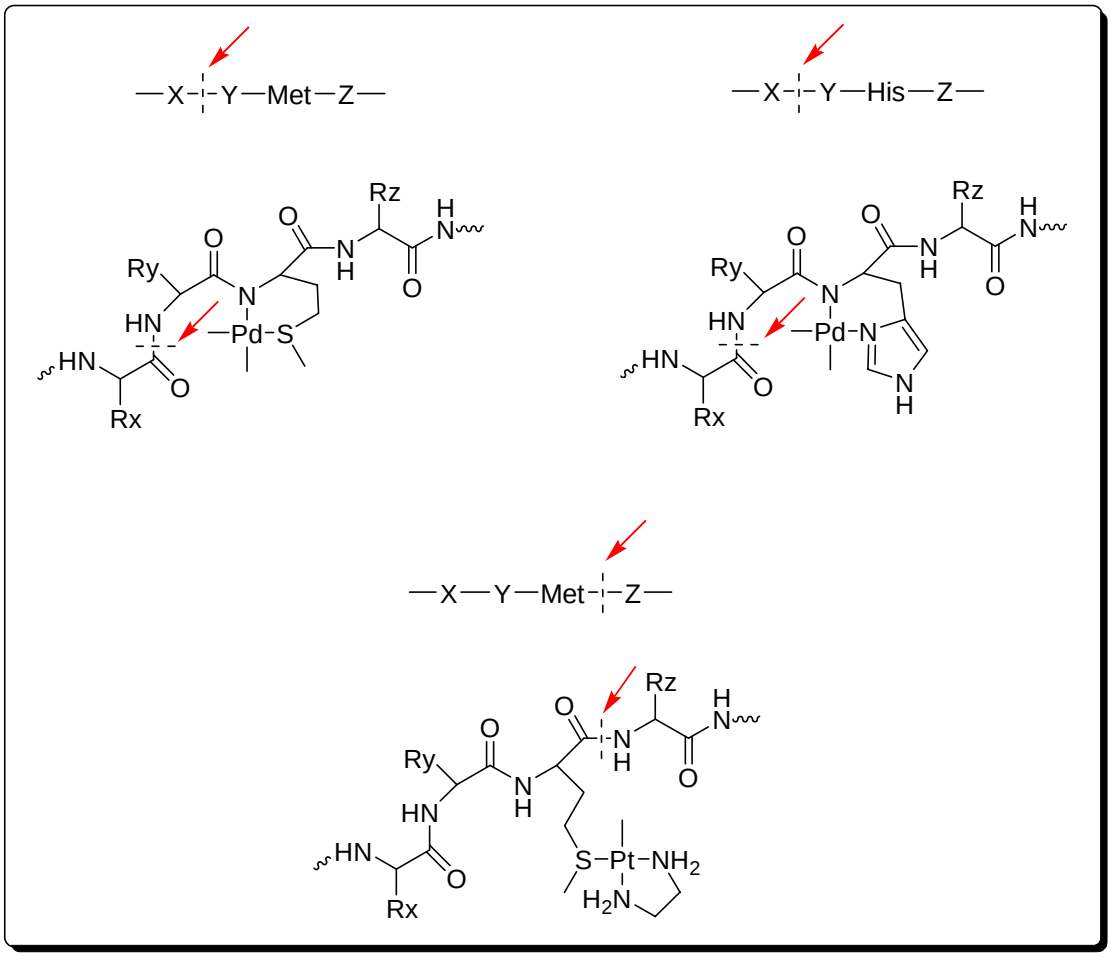

Scheme 1.6 *Different Cleavage Selectivity of Pd(II) and Pt(II) Complexes.*

Study of the regioselectivity of the Pt(II) promoters resulted with the conclusion, that the overall selectivity of peptide cleavage can be altered by changing the solvent: in the presence of Pt(II) promoter, cleavage will occur near histidine and methionine in aqueous solution[28], but near tryptophan in acetone solution[29].

1.3.2.2 Mechanism of Cleavage

The first event in cleavage of amide bond in peptides and proteins is anchoring of the metal complex, the promoter, to the side chain.

Both Pd(II) and Pt(II) have a high affinity for sulfur and nitrogen ligands and readily coordinate to the side chains of Cys, Met and His[21, 23, 30-33]. In this way, the metal ion gets in the vicinity of the peptide bond to be cleaved. Because the amide group is a poor ligand for transition-metal ions in aqueous solution, this group in peptides and proteins interacts only with a metal ion that is already anchored to the side chain or to the terminal amino group.

There are two general mechanisms for the cleavage of the scissile peptide bond promoted by the metal complexes (see also Scheme 1.2-1.4).

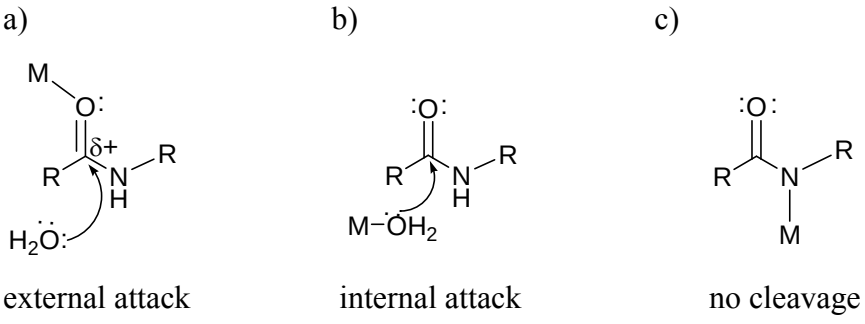

Scheme 1.7 *Possible interactions between anchored Pd(II) or Pt(II) Ion (M) and proximate amide group: a) Binding to the nitrogen atom requires deprotonation of the NH group and results in the inhibition of the hydrolytic cleavage; b) Binding to the oxygen atom enhances the electrophilicity of the carbon atom and activates the amide group toward hxdrolytic cleavage by solvent water; c) Close approach by the metal ion aids delivery of its aqua ligand to the carbon atom and thus promotes hydrolytic cleavage of the amide bond.*

In the *external attack mechanism*, the anchored metal ion binds to the oxygen atom in the amide group (Scheme 1.7 a), so that this binding enhances the electrophilicity of the amide carbon atom, stabilazes the tetrahedral intermediate formed in the nucleophilic attack by an external water molecule, and thus promotes cleavage of the peptide bond[34].

In the *internal attack mechanism*, the anchored metal ion delivers its aqua ligand to the scissile peptide bond internally, in a cyclic transition state (Scheme 1.7b). The critical difference between the two mechanisms is the origin of the water molecule – from the solvent, or from the coordination sphere of the metal.

If, however, the anchored metal ion deprotonates the amide NH group and binds the nitrogen atom of the resulting amidate group, then the coordination of the amidate anion

strengthens the C-N bond, protects the amide carbon from nucleophilic attack and thus inhibits hydrolysis of this peptide bond (Scheme 1.7c)[35].

Molecular-dynamics calculations showed that different complexes of Pd(II) prefer one or the other mechanism (Scheme 1.7a; Scheme 17b)[27]. External attack may be preferred when a favorable ring can be formed. This may be the case in the hydrolysis of S-methylglutathione, for which the chelate ring is six-membered. The internal delivery may be favored when the length of the side chain permits approach of the coordinated water to the scissile peptide bond, and also disfavors the external attack because the chelate ring involved in this mechanism would be larger than six-membered. This may be the case for AcMetGly and other Met-containing substrates, which would have to form seven-membered S,O-chelate rings. Regioselectivity of cleavage, therefore, depends on the mode of attachment of substrate to the metal complexes and on the proximity of the attachment site to the scissile amide bond.

1.3.3 Synthetic Copper(II) Peptidases

The first clue that Cu(II) was effective in accelerating the hydrolysis of simple peptides was reported in 1953 by Newton[36]. Newton studied Cu(II)-promoted hydrolysis of both glycine amide and diglycine. He found that, at low pH, the presence of Cu(II) ions accelerated the hydrolysis of both substrates by a factor of between 2 and 30. Few years later, Meriwether and Westheimer[37] observed that both Cu(II) and Ni(II) ions accelerated the hydrolysis of glycine amide and phenylglycine amide. After 24h, nearly 95% of glycine amide was hydrolyzed in the presence of Cu(II), compared with 60% of the same substrate hydrolyzed in the presence of Ni(II).

As research progressed in the use of defined substrates to test the ability of metal ions to promote amide hydrolysis, other work focused on the use of defined metal complexes as synthetic peptidases. Application of defined metal complexes was an attempt to provide small-molecule versions of metallopeptidases. Although free metal ions are effective in promoting the hydrolysis of amides, the use of free metal ions has limitations due to their reactivity, solubility and stability.

Groves et al.[38] studied the metal-promoted hydrolysis of amides, peptides and proteins by metal complex Cu(II)triazacyclononane (1).

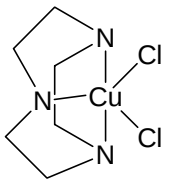

(1)

Figure 1.2 *Structure of Cu(II)triazacyclononane (1)*

They reported about the hydrolysis of substrates by Cu(II) complex, where this complex was effective at promoting cleavage of amide bond of an activated amide containing a metal binding site.

Burstyn et al.[39] reported the hydrolysis of diglycine promoted by the same complex (1). The reaction was catalytic, with the observation of greater than stoichometric hydrolysis and no loss in rate after 28 days. The hydrolysis was highly buffer-dependent. The reactions performed at pH 8.1 in 50 mM $NaHCO_3$ buffer resulted in the hydrolysis of diglycine promoted by the Cu(II)triazacyclononane (1); however, when analogous reactions were performed at pH 8.1 but in 50 mM HEPES buffer (*N*-(2-hydroxyethyl)-piperazine-N'-2-ethanesulfonic acid), no detectable hydrolysis was observed. The greater rate observed with phosphate buffer was attributed to the buffer`s ability to act as a bifunctional catalyst to aid in the transfer of a proton and facilitate the breakdown of the tetrahedral intermediate.

There are many other examples of Cu(II) complexes as promoters of amide bond hydrolysis. While the salicylic acid complex of Cu(II) (2) reacted with glycine and diglycine to form the stable Schiff base complex (3), in the case of triglycine it showed unexpected hydrolysis with the formation of (3) and the liberation of free glycine[40].

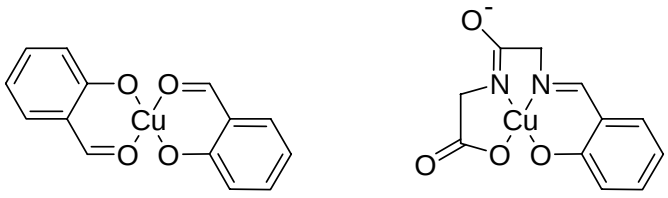

(2) (3)

Figure 1.3 *Structure of salicylic acid complex of Cu(II) (2) complexed with glycine and diglycine to form stable Schiff base complex (3)*

To determine the specificity of the hydrolysis reactions promoted by (2), the tripeptides Gly-Gly-Ala and Ala-Gly-Gly were used as substrates[41]. Hydrolysis occurred primarily at the C-terminal amide bond: in the reaction of (2) with Gly-Gly-Ala, the products were (3) and free Ala; in the reaction of (2) with Ala-Gly-Gly, the products were Cu(II)-

bound Schiff base adduct of salicylate with Ala-Gly and free Gly. These observations were consistent with complexation of the metal ion to the amino terminus of the tripeptide.

1.3.4 Cobalt(III)-Promoted Hydrolysis of Amides and Small Peptides

As described before (Chapters 1.2 and 1.3.2.2), there are many possible mechanisms for amide bond hydrolysis. The above possibilities have been recognized and investigated over many years, but it is still difficult to establish beyond reasonable doubt which mechanism is actually operating. Therefore, Co(III) chemistry has been also done to provide a possible way out. The "hard" Co(III) center behaves as an excellent, though not unusual, Lewis acid, and the reduced lability of coordinated ligands allows the two mechanisms to be distinguished and examined, often separately. The Co(III) center is slightly more polarizing than other first-row transition metals, and in this sense it may be more effective in the external attack mechanism.

It was shown that the Co(III) complex (4) was the effective reagent and the β_2 configuration of the product chelate (5) showed that initial coordination of the *N*-terminal amino group occurred at this positon (compound (6))[42].

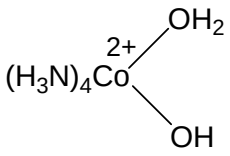

(4)

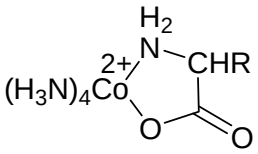

(5)

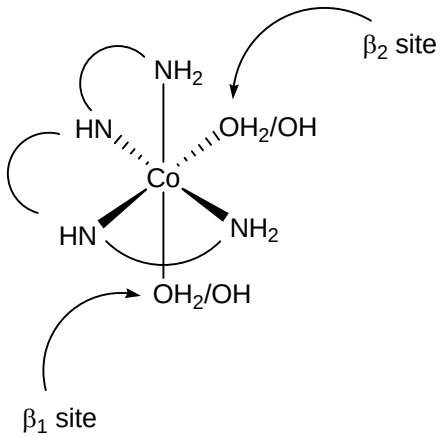

(6)

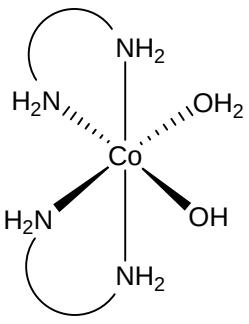

(7)

Figure 1.4 *Co(III) complexes with β_1 and β_2 configurations.*

Other results[43-45] showed that the β_1 site is preferred in the case of sterically "simple" dipeptides, and with more sterically constrained dipeptides, the β_2 site is preferred. These studies showed that both the β_1 and β_2 site are reasonably labile, and this was shown to dictate the hydrolysis mechanism for this particular Co(III) reagent. The $[Co(en)_2(OH/OH_2)]^{2+/3+}$ system (7) was also examined[46], but it has been shown that its considerably slower coordination rate and ability to undergo cis-trans isomerization resulted in a multitude of products.

Kimura, Young and Collman[47] published a comparative study of the β-trien and tren (8) systems in 1970. They found the tren system to be less reactive but more selective for the *N*-terminal residue. Oh and Storm[48] reported that the $[Co(edda)(OH)(OH_2)]$ complex (9) is more reactive at pH 10 than the β-trien complex, but at this pH the latter is present in its less reactive dihydroxo form.

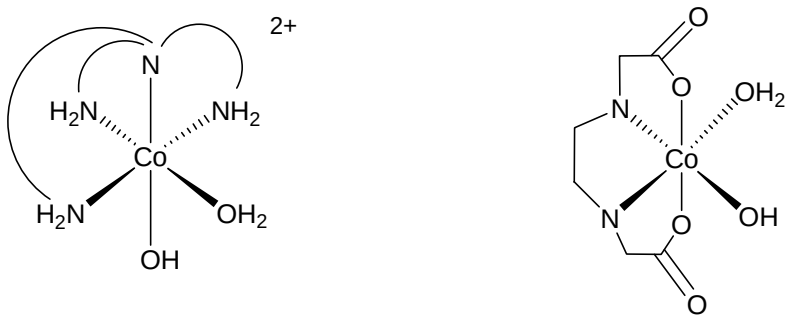

(8) (9)

Figure 1.5 *Structures of tren system (8) and [Co(edda)(OH)(OH$_2$)] complex (9).*

1.3.5 Synthetic Analogues of Zinc Enzymes

Zinc plays an essential role in biological systems, because it is constituent of more than 300 enzymes. Many studies[49-53] of synthetic analogues of zinc enzymes (small molecules that resemble the enzyme active site) have been done in order to understand why different zinc enzymes utilize different amino acid residues at the active site, and to understand how the chemistry of zinc is modulated by its coordination environment.

The active sites of many of Zn-containing enzymes feature a tetrahedrally coordinated zinc center that is attached to the protein backbone by three amino acid residues, with a fourth site being occupied by a water molecule (Figure 1.6)[54, 55].

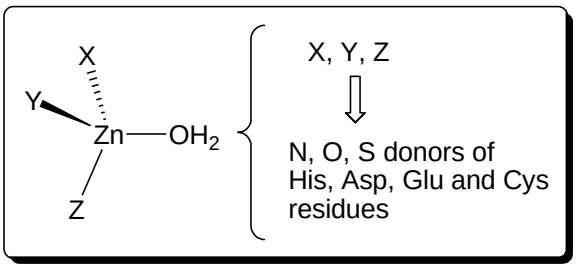

Figure 1.6 *A common structural feature of zinc enzymes.*

The residues which bind zinc to protein are typically His, Glu, Asp and Cys. The nature of these residues and the amino acid spacer lengths between the active site residues, dictate the specific function performed by each of enzymes.

Which are the properties of Zn(II) that are pertinent to its role in enzymes? First of all, that are its redox properties: Zn(II) ion is very stable with respect to oxidation and reduction and so it does not participate in redox reactions, in contrast to Cu, Fe or Mn. The second very important property of Zn(II) is its coordination geometry: the d^{10} configuration of Zn^{2+} indicates that zinc complexes are not subject to ligand field stabilization effects and so coordination number and geometry is only dictated by ligand size and charge. In enzymes, zinc shows strong preference for tetrahedral coordination, which enhances both the Lewis acidity of the zinc center, and the Brönsted acidity of coordinated water molecules. In its ligand binding properties, zinc shows its favour to bind to nitrogen, sulphur and oxygen atoms, and therefore zinc can strongly bind to many proteins. What is also very important is that anions, such as OH^-, OR^- and SR^-, retain a nucleophilic character when coordinated to zinc.

The most frequent motif of the active site in Zn(II) containing enzymes is a mononuclear tetrahedral site of the type $[\{XYZ\}Zn^{II}\text{-}OH_2]$, therefore the investigation of synthetic analogues for Zn-enzymes should contain this motif. A rational approach towards obtaining synthetic analogues is to use tridentate ligands which incorporate the requisite X, Y and Z donor groups to mimic the protein ligation. A further refinement of this approach is to use a tripodal ligand in which the X, Y and Z groups are attached to a common tetrahedral (or trigonal pyramidal) center. Although the most prevalent coordination motif is tetrahedral, other coordination geometries are known, in part due to the ability of ligands, such as aspartate and glutamate, to bind in a bidentate manner. There are also polynuclear sites, where the zinc centers are often bridged by a water molecule and an aspartate residue[56-58].

The first enzyme recognized to contain zinc was carbonic anhydrase. It has played a pivotal role in the development of zinc enzymology[59]. X-ray diffraction studies demonstrate

that the zinc center of the active site is coordinated to the protein by the imidazol groups of three histidine residues and a water molecule following the [$(His)_3Zn^{II}$-OH_2] motif . Although there are many studies performed using tridentate nitrogen donor ligands to model the stucture and function of the active site[60-69], only very few of those studies have successfully enabled the isolation of structurally characterized mononuclear four-coordinated zinc-hydroxide or zinc-aqua complexes that mimic the active site[70-72]. Complexes which represent a major advance in bioinorganic zinc chemistry by providing the first well characterized tetrahedral zinc hydroxide complexes, are the [$Tp^{RR`}$]ZnOH complexes (10), where [$Tp^{RR`}$] is the tris(pyrazolyl)borate ligand system.

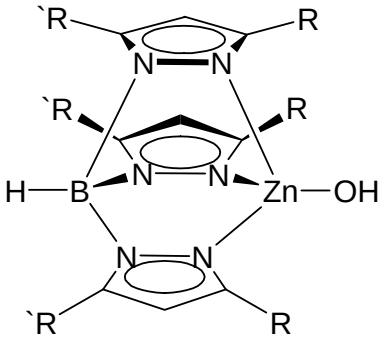

(10)

Figure 1.7 *The tris(pyrazolyl)borate ligand system, [$Tp^{RR`}$]ZnOH (10).*

The strucutre of some other zinc proteases follow the [$(His)_2(Glu)Zn^{II}$-OH_2] motif. The most important examples are carboxypeptidase, thermolysine and neutral proteases. Those zinc proteases are responsible for catalyzing the hydrolysis of peptide bonds. The active sites of those three proteases contain zinc center being bound to the protein by a combination of one glutamate and two histidine residues. Efforts to obtain synthetic analogues of these enzymes have focused on the use of a variety of tridentate ligands with [N_2O] donor arrays[73-75].

The active site of bacteriophage T7 lysozyme, a zinc enzyme which destroys bacteria by cleaving the amide bond between L-alalnine and *N*-acetylmuramate moieties of polysaccharide components within their cell walls, consists of a tetrahedral zinc center which is bound to the protein backbone via one sulfur and two nitrogen donors of cystein and histidine residues, with a fourth site site bein occupied by a water molecule - [$(His)_2(Cys)Zn^{II}$-OH_2] motif[76].

Another interesting example is alcohol dehydrogenase, which catalyzes the biological oxidation of primary and secondary alcohols. X-ray diffraction studies show that the active site consists of a zinc center which is coordinated in a distored tetrahedral manner to a histidine and two cysteine residues: [(His) $(Cys)_2Zn^{II}$-OH_2] motif.

The unusual composition of the active site - [$(Cys)_3Zn^{II}$-OH_2] – possesses a zinc dependent enzyme 5-aminolevulinate dehydratase, which catalyzes the dimerization of 5-aminolevulinic acid to porphobilinogen[77].

In addition to the [{XYZ}Zn^{II}-OH_2] motif, where the coordinated water molecule plays a critical role, recent studies[78] indicate that zinc may also play an important role by activating thiols towards nucleophilic attack. For example, alkylation of zinc thiolates has been proposed to be a step in the mechanism of action of the Ada DNA repair protein. The active site of the Ada DNA repair protein possesses a [$(Cys)_4Zn$] motif.

1.4 Immobilised Metal-Ion Affinity Chromatography (IMAC)

Immobilised metal-ion affinity chromatography is a versatile separation procedure that exploits differences in the affinities exhibited by many biopolymers for metal ions. It was introduced by Porath et al.[79] as a new tool for the purification of proteins and peptides. Since that time IMAC has been used in the isolation of proteins[80], peptides[81] and nucleic acids[82]. This technique involves the chelation of a suitable metal ion onto a solid support matrix, whose surface has previously been chemically modified with a polydentate ligand. The resulting metal ion chelating ligate then has the potential to coordinate with electron donor groups resident on the surface of the interacting protein[83-85]. The separation selectivity is then achived on the basis of differences in the thermodynamic stabilites of the protein-metal ion chelating ligate complexes. Proteins which form adsorption complexes of low stability will be eluted first, while protein that form stable complexes will be eluted later. As the differences in the equilibrium association constants increase for the respective protein-metal ion chelating ligate coordination complexes, better resolution will be obtained. As a result, proteins with very similar properties with respect to charge, molecular size and amino acid composition, but with differences in their tertiary structures or surface array of specific amino acid residues, may be separated.

Much of the research interest into the use of IMAC over the past 20 years has revolved around the appliciation of first row, transition metal ions, such as Ni^{2+}, Cu^{2+} and Zn^{2+}. The metal ion is complexed and immobilized by a chelator, which is covalently linked to a solid matrix. The metal complex contains free coordination sites, which can be occupied by additional electron donor groups. Of special interest are histidine residues on protein surfaces[86]. Combining this principle with protein engineering leads to an elegant strategy for identification and rapid one-step purification of gene products expressed as fusion proteins with an oligo-histidine tag. The oligo-histidine tag should serve as a high affinity binding sequence for the purification of any fusion protein via metal chelating adsorbents. An important and well characterized chelator for the oligo-histidine tag is the *N*-nitrilotriacetic acid (NTA) derivative *N*-(1-carboxy-5-aminopentyl)iminodiacetic acid[87].

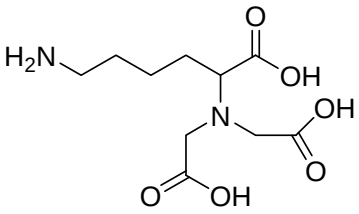

Figure 1.8 *Chelator N-(1-carboxy-5-aminopentyl)iminodiacetic acid.*

The most frequently method used for separation (purification) of recombinant proteins is the one which employs an NTA-attached resin to immobilize nickel ions and to separate recombinant proteins that are engineered to have six consecutive histidine residues (Figure 1.9).

Figure 1.9 *Immobilization scheme for histidine-tagged proteins using NTA.*

A hydrophobic polystyrene matrix interacts over the hydrophobic block ( ) with a hydrophilic NTA block, which extends into solution, creating an activity-preserving interface to which histidine-tagged proteins bind through chelated metal ions[88]. Nickel ions chelated by the NTA group have coordination sites free to bind to electron-donating side chains, particulary histidine residues, on the protein surface.

Immobilization of histidine-tagged proteins by IMAC has several merits: his-tags are small and therefore structurally and functionally benign; his-tags can be added to either the

amino- or carboxyl-terminus, and in the middle of the recombinant proteins, which allows control of immobilization orientation; the interaction between histidines and chelated Ni^{2+} has high binding stability, the K_d can be as low as 10^{-13}; the interaction is reversible, immobilized proteins can be eluted by lowering the pH or competitively eluted with imidazole or free chelators[89]. The metal ion and ligand binding properties of the chelator lipid interfaces as well as their dependency on ionic strenght, pH, and temperature was examined in details[90, 91].

Several approaches using chelated metal ions have been reported that allow histidine-tagged proteins to be immobilized at several types of interfaces, such as lipid interfaces and lipid monolayers with metal-chelating lipids[92, 93], gold surfaces with self-assembling monolayers formed with metal-chelating alkanethiols[94], and oxide surfaces with metal-chelating silanes[95].

Specific docking of peptides[96, 97] and proteins to chelator lipids was demonstrated not only via histidine tag, but also via surface histidines[98]. A designed model peptide[99] as well as a DNA binding protein[100] could be organized in two dimensions by phase-segregated chelator lipids. The his-tagged protein was found to be fully functional with respect to its specific DNA recognition. Two-dimensional crystallization of proteins at chelator lipid monolayers was reported[101-104]. Metal-chelating interfaces can be produced either by coating with chelator lipids, or by modification of different surfaces with NTA[105].

2

Objectives of Thesis

Selective cleavage of the amide bond in peptides and proteins is an important reaction in biochemistry and molecular biology. However, the peptide bond is extremly unreactive towards hydrolysis (7-600 years at room teperature and pH 4-8). Since many of chemical cleavage reagents are still inapplicable, the design and development of new synthetic peptidases would be of great utility.

In this research, the role of different metal complexes as synthetic peptidases should be investigated. Therefore, different ligand structures and the influence of their rigidness on the formation of the corresponding metal complexes, should be examined.

To this end, the first objective in this thesis will be the synthesis and characterization of the ligands and their corresponding transition metal complexes. All ligands should contain a substituted pyridyl-ring with a possibility to form chelate complexes with transition metal ions. Where possible, X-ray crystal structure determinations of metal complexes and/or ligands should be obtained to gain a detailed structural insight.

After synthesis and structural characterization of the ligands and their metal complexes, the next objective will be the investigation of the peptide hydrolysis promoted by the synthesized metal complexes. For this purpose, dipeptides will be used that contain one histidine residue as the anchor for the metal complexes. The regioselectivity, as well as the rate of cleavage, will be investigated in dependence of:

a) ligand structure and
b) nature of the metal ion.

These goals mentioned above should be the main objectives of this thesis. As an extension of these projects, we will investigate reaction conditions and coupling reagents for the synthesis of the compound which could take a part in immobilization of peptides and proteins (Immobilized Metal Ion Affinity Chromatography - IMAC) and their immediate selective hydrolysis.

3

Results and Discussion

3.1 Synthesis and spectroscopic properties: Ligands and Corresponding Metal Complexes

In the structure of all ligands synthesized during this research, there is either the pyrdyl-unit substituted on the position 2, or quinoline unit substituted on the position 8, leaving two carbon atoms as spacers between the aromatic and aliphatic amine. An exception is the commercially available dipyridyle amine, ligand which contains pyridine ring substituted on the position 2, but leaving only one carbon spacer.

a) b) c)

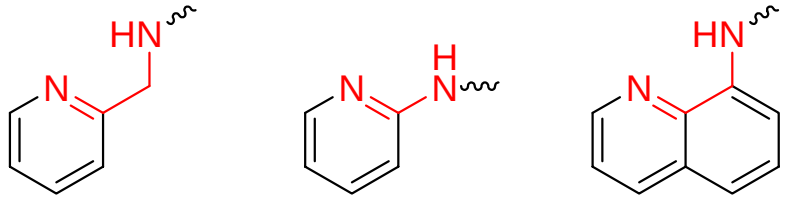

Figure 3.1 *Structural units in the ligands, substitued on the position 2: a) pyridyl unit leaving two carbon spacer between aromatic and aliphatic amine; b) pyridyl unit leaving only one carbon spacer; c) quinoline unit leaving two carbon spacer.*

3.1.1 Derivatives of 2-Picolylamine

In the synthesis of the ligand **2**, instead of direct introduction of the carboxylic moiety, the ester **1** was synthesized, purified and the ester hydrolysed in a later step (Scheme 3.1). A convenient synthesis was the reaction of two equivalents of 2-picolylamine with one equivalent of α-bromo-toluic acid methyl ester in THF in the presence of NEt_3. After refluxing the reaction mixture for 2 hours and cooling down to room temperature, the white precipitation $HNEt_3Br$ was removed by filtration and solvent was removed under reduced pressure. The product **1** was further purified by the coloumn chromatography ($CHCl_3$: MeOH : EtOAc, 5 : 5 : 2). Hydrolysis of the methyl ester moiety of **1** was achivied by stirring of compound **1** for 2.5 hours at room temperature in a $MeOH/H_2O$ mixture containing excess NaOH, leading to the carboxylate derivative in solution. To obtain the acid the pH was adjusted to 7 by dropwise addition of diluted hydrochloric acid, followed by removal of the solvent under reduced pressure. The brown sticky residue was found to be the desired compound but in impure form. By addition of CH_3CN and vigorous stirring, the ligand **2** separated as a white solid.

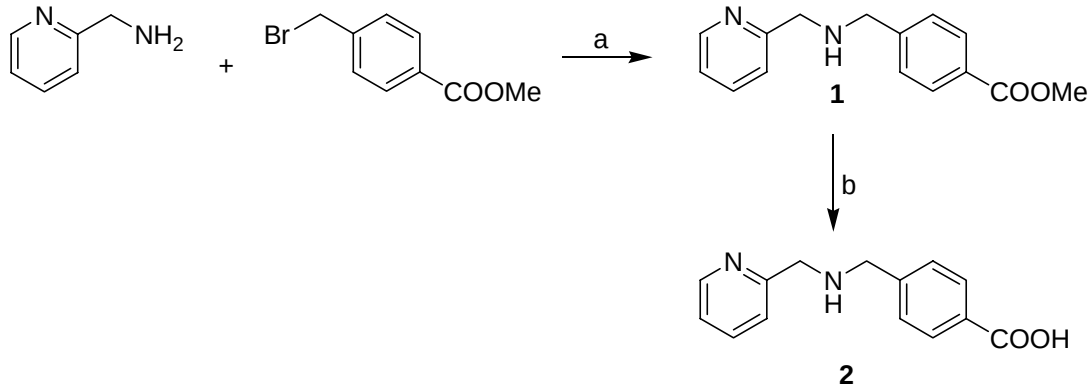

Scheme 3.1 *Synthesis of compounds **1** and **2**: a) NEt_3 in THF, reflux, 2h; b) NaOH in $MeOH/H_2O$, reflux, 2.5h, HCl pH = 7.*

Ligand **3** was synthesized according to an alkylating procedure similar to the one proposed by Chaouk H. et al.[106] but with some modifications. Instead of alkylation of 2-picolylamine with chloroacetic acid during 9 h, the alkylation with bromoacetic acid, previously neutralised with an aqueous solution of NaOH, was achivied even after 5 h at 60°C (Scheme 3.2). After evaporation of the solvent, the solid was washed with diethylether to remove remaining amine.

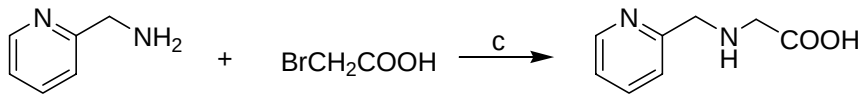

3

Scheme 3.2 *Synthesis of compound **3**: c) NaOH/H_2O, 60°C, 6h.*

The ^{1}H NMR spectrum of the ligand **1** showed two methylene singlets in the vicinity of δ 3.7 ppm: the singlet at 3.77 ppm can be attributed to the methylene group on the pyridine ring, and the singlet at 3.73 ppm can be assigned to the benzyl methylene group. The singlet at 2.11 ppm in the ^{1}H NMR and 52.01 ppm in the ^{13}C NMR attributed to the methyl ester group, disappeared after hydrolysis of the ester moiety. Two methylene groups of the ligand **3**, one on the pyridine ring and one on the acetate moiety, appeared at 3.87 ppm and 3.22 ppm, respectively.

The aromatic signals of the ligand **2** in ^{1}H NMR spectra appeared between 8.47 and 7.24 ppm (Figure 3.2): doublets at 8.47 and 7.45 ppm, as well as triplets at 7.75 and 7.24 ppm can be attributed to the four proton signals of the pyridine ring, while two doublets at 7.85 and 7.34 ppm were assigned to the four protons of the benzyl ring (see Chapter 4.3.1).

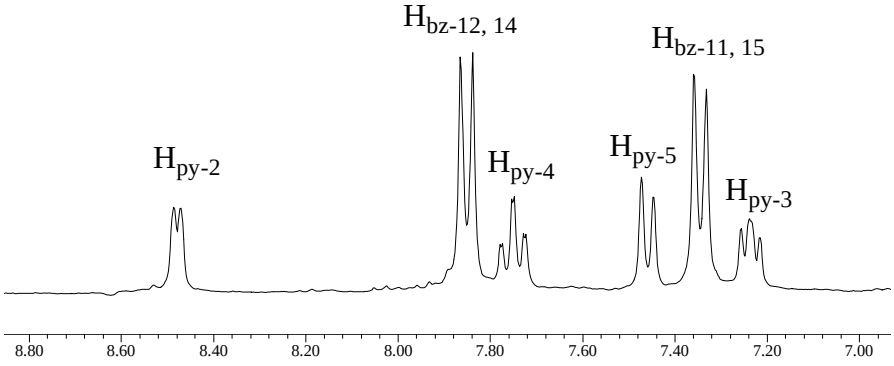

Figure 3.2 *^{1}H NMR spectra of the ligand **2**: Ar and py region.*

MS-FAB spectra of **1** and **2** showed the molecular peaks at *m/z* 257 and 243, respectively, which corresponded exactly to the $[M + H]^+$ ion.

In addition, the commercially available dipyridyl amine **4** was also used as a ligand in the complexation reactions and later in the peptide hydrolysis experiments.

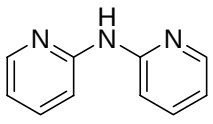

4

Figure 3.3 *Dipyridyl amine as a ligand **4**.*

Complexes **5** - **18** were prepared by the reaction of the ligand **2** - **4** with the corresponding metal(II) nitrates/chlorides in methanol (Scheme 3.3-3.5). The reaction mixture was left few hours at room temperature and then the next few days at 7°C. In the synthesis of Pd(II), Co(II) and Ni(II) complexes, the precipitation occurred immidiately after mixing the ligand with the corresponding metal(II) nitrates/chlorides. However, after mixing metal and ligand for the synthesis of Zn(II) and Cu(II) complexes, no precipitation was observed. Therefore, these clear solutions of Zn(II) and Cu(II) complexes with ligand **2** were left at 7°C for days, where the crystallization started after 6 and 2 days, respectively. Crystals of Zn(II) complex **9** and Cu(II) complex **10** were suitable for the X-ray structure analysis.

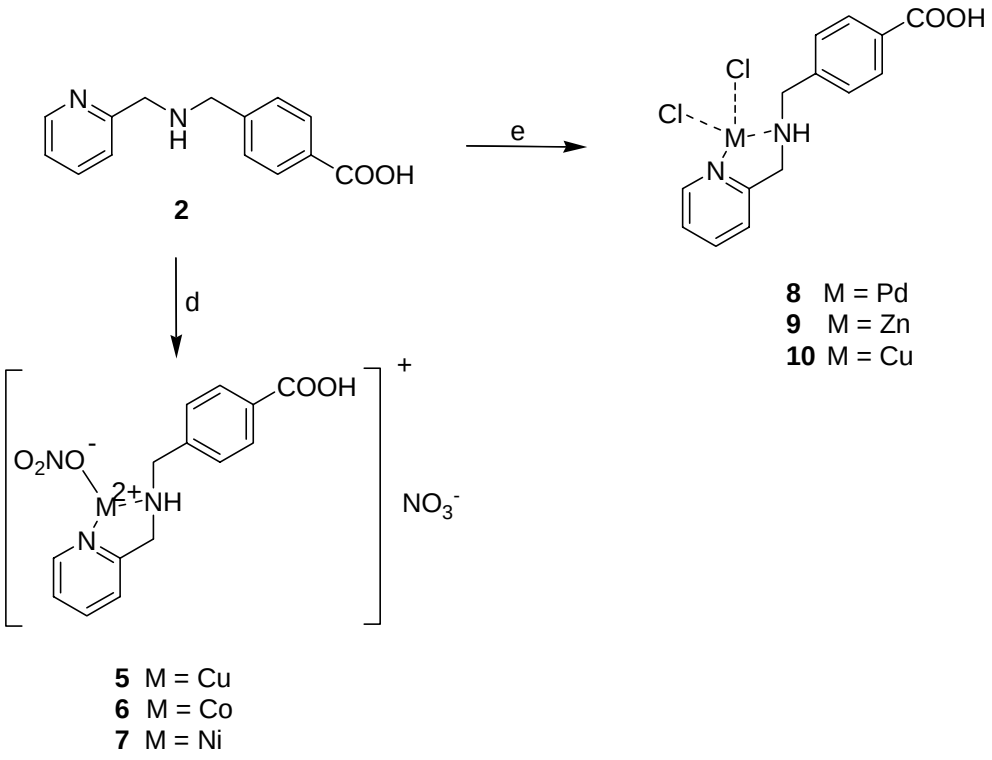

Scheme 3.3 *Synthesis of metal complexes of the ligand **2**: d) $M(NO_3)_2$ x nH2O in hot MeOH; c) Na_2PdCl_4 in hot MeOH for **8**; MCl_2 in hot MeOH for **9** and **10**.*

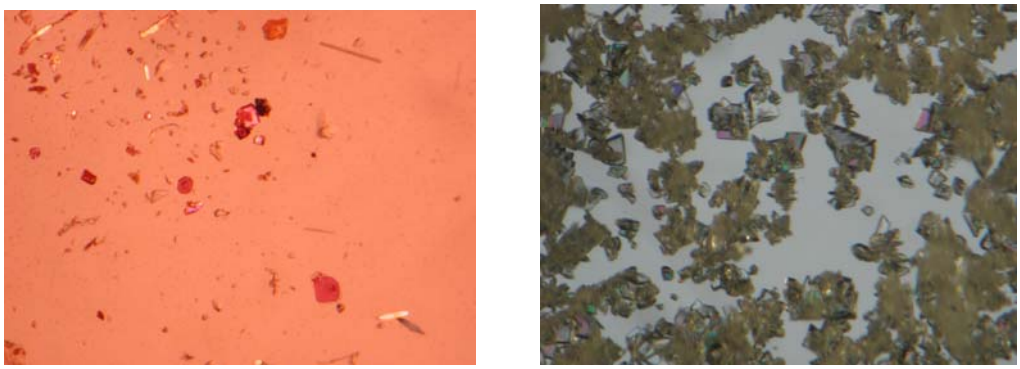

Figure 3.4 *Microscopic view of the cobalt complex **6** and colourless zinc complex **9**.*

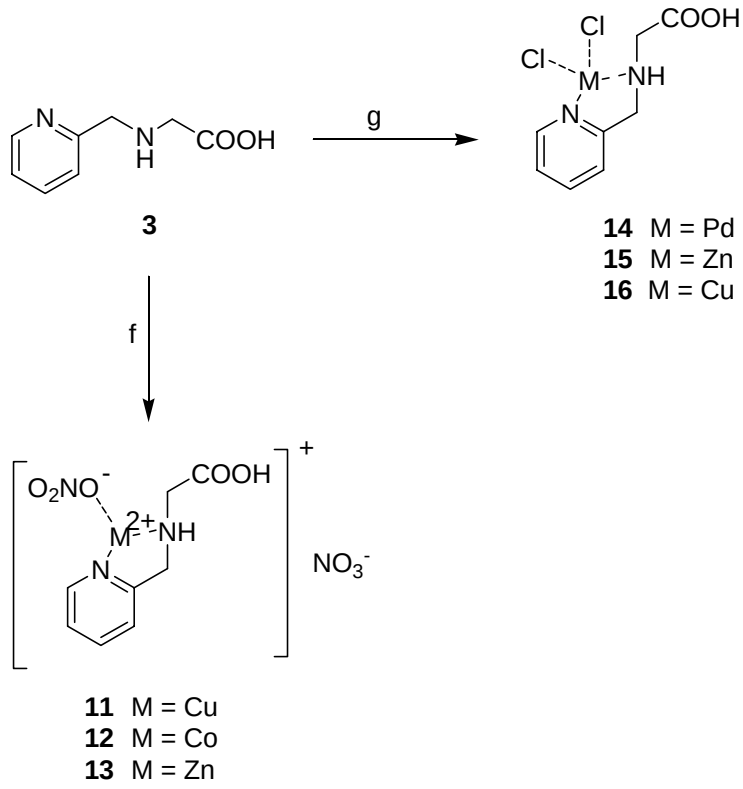

Scheme 3.4 *Synthesis of the metal complexes of the ligand **3**: f) $M(NO_3)_2$ x nH2O in hot MeOH; g) Na_2PdCl_4 in hot MeOH for **14**; MCl_2 in hot MeOH for **15** and **16**.*

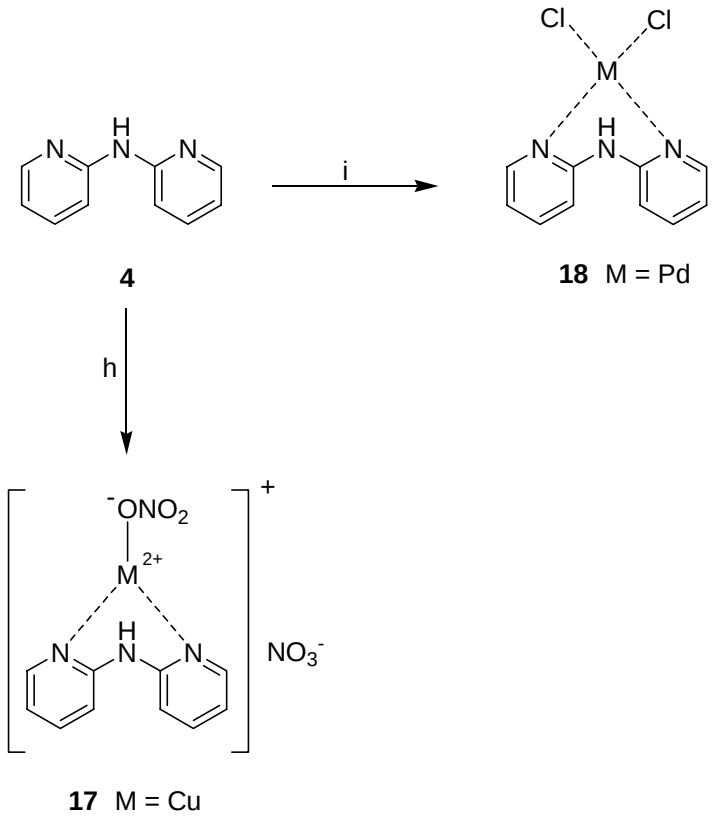

Scheme 3.5 *Synthesis of the metal complexes of the ligand **4**: h) $Cu(NO_3)_2$ x 3H2O in hot MeOH; i) Na_2PdCl_4 in hot MeOH.*

NMR spectra were obtained for Pd and Zn complexes. In comparison to the ^{1}H NMR spectrum of the ligand **2**, the major difference in the ^{1}H NMR spectrum of corresponding metal complexes was downfield shift in the case of picolyl and benzyl methylene groups H_7 and H_9 in **8**. The downfield shift is 0.42 and 0.33 ppm, respectively. In **2** these methylene groups showed two singlets, which changed to an AB system in the case of **8** because of the magnetic inequivalence of the hydrogen atoms in those methylene groups.

The FAB-MS spectra of **5-7** exhibited signals of the corresponding molecular ions after loss of one or both nitrate counterions, $[LMNO_3]^+$ and $[LM]^+$. The ESI-MS spectra were dominated by $[LM]^+$, $[LM + solvent]^+$ and $[LM + Na/K]^+$, the first being the base peak. All metal containing peaks showed the expected isotopic pattern.

A good example is the ESI-MS spectra of the Pd(II) complex **8**, where it is easy to find peaks corresponding to $[LM + Na]^+$ and $[LM + DMSO]^+$. Those peaks showed also the typical Pd(II) isotopic pattern (Figure 3.5).

The ESI-MS spectra of Co(II) complex **6** (Figure 3.6) showed peaks corresponding to $[LM + DMSO]^+$ as well as $[LM + 2DMSO]^+$, but without NO_3^-. This spectra showed expected isotopic pattern of Co(II).

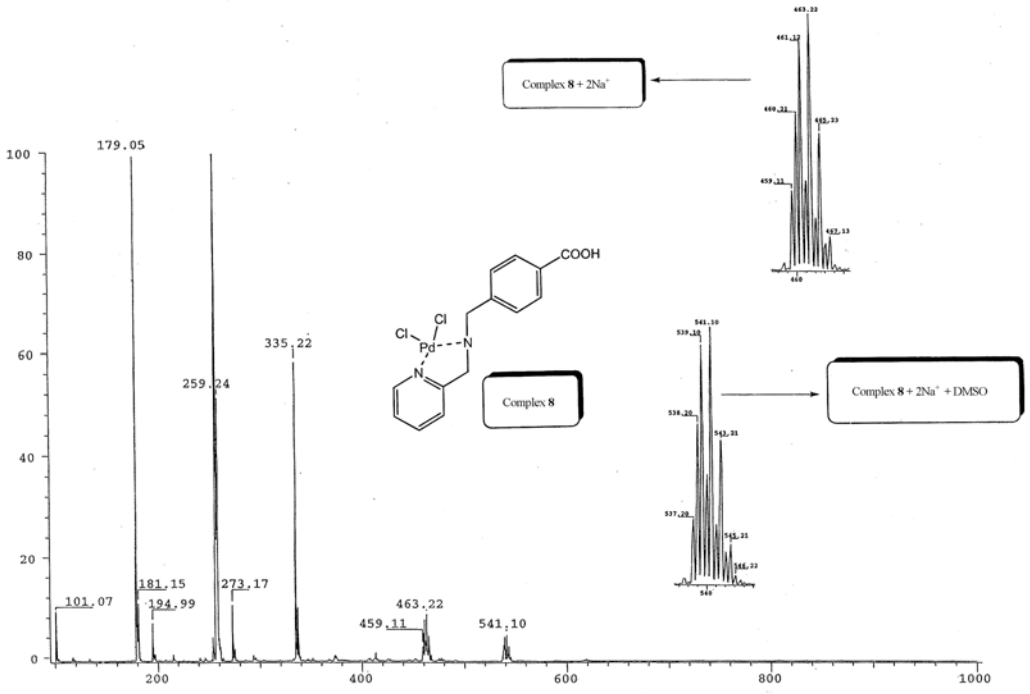

Figure 3.5 *ESI-MS spectra of Pd(II) complex* ***8****.*

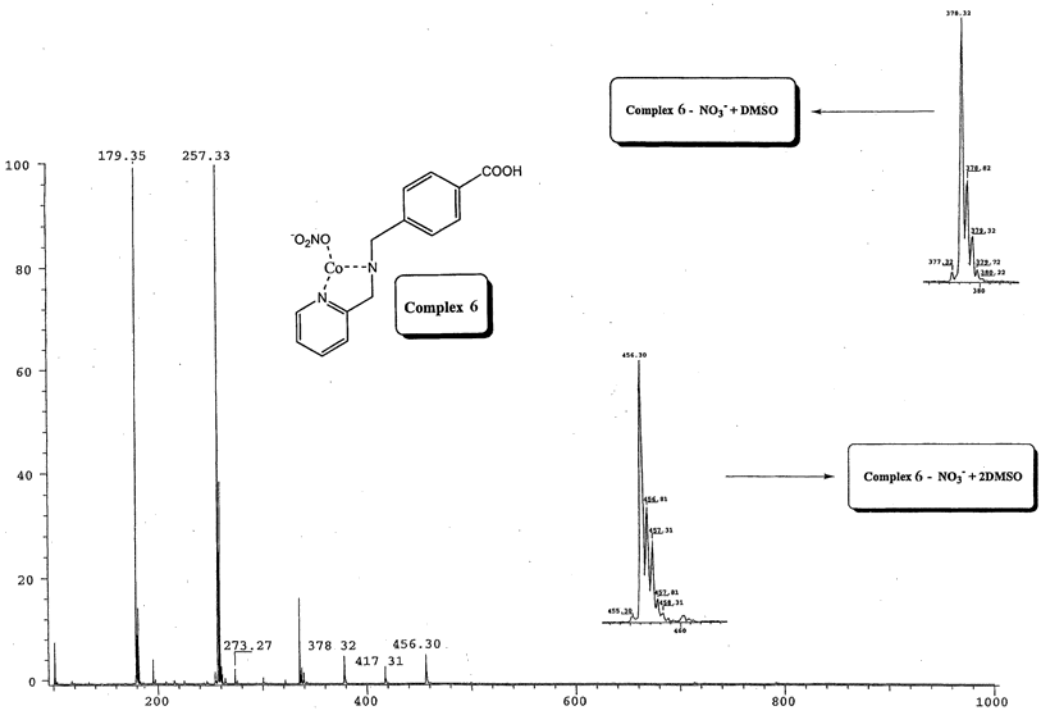

Figure 3.6 *ESI-MS spectra of Co(II) complex* ***6****.*

3.1.2 Derivatives of 8-Aminoquinoline

In the synthesis of the ligand **20**, 8-aminoquinoline **19** was dissolved in THF in the presence of triethylamine and over the next 30 minutes chloroacetic acid was added (Scheme 3.6). As a solvent THF was chosen because of good solubility of 8-aminoquinoline in this solvent. The reaction mixture refluxed for 5 days and the solvent removed under reduced pressure. The brown solid left was further purified by coloumn chromatography (DCM : MeOH, 7 : 3) resulting with a pure compound **20** as a yellow solid.

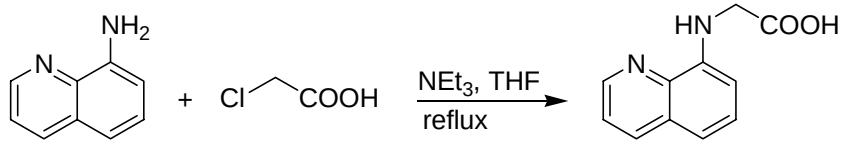

19 **20**

Scheme 3.6 *Synthesis of compound **20.***

Ligand **21** was synthesized by nucleophilic substitution from 8-aminoquinoline and α-bromotoluic acid methyl ester in the presence of NEt_3 in THF (Scheme 3.7).

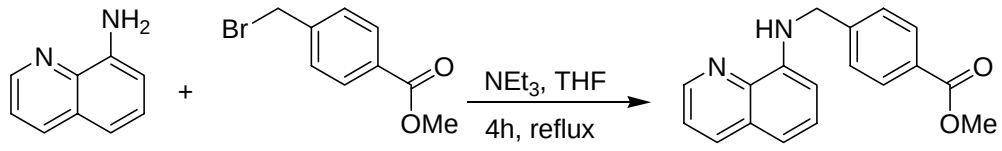

21

Scheme 3.7 *Synthesis of compound **21***

To avoid dialkylation, we took two equivalents of 8-aminoquinoline and one equivalent of α-bromotoluic acid methyl ester, which was slowly added over 2h. The TLC showed no evidence of dialkyl product. After one hour of reaction, a white precipitate of triethylammonium bromide formed, which was in later step removed by filtration. The solvent was then removed under reduced pressure and the product **21** purifed with coloumn chromatography (DCM : n-Hexane, 8 : 2). For further purification the product **21** was dissolved in a mixture of MeOH and HCl and the resulting hydrochloride was recrystalized from MeOH in the form of very intensive orange-coloured crystals (Figure 3.7).

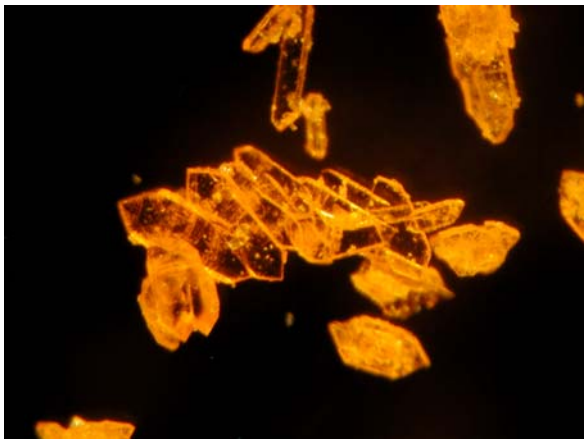

Figure 3.7 *Microscopic view of the ligand **21** monohydrochloride.*

Its intense colour was obtained in acidic medium and only in the form of monochloride, showing a halochromic effect (Scheme 3.8). This effect depends on the pH of the medium or, better to say, on protonation state of the compound. In this case, the protonation occurred on the aromatic amine, causing strong π-electron delocalisation and absorbtion of the light, resulting as an intensive orange colour. The whole system shows also the + mesomeric (+M) effect, where the p-orbital of the aliphatic amine overlaps with p-orbitals of the rest of the entity, and electronic charge may flow from the substituent to quinoline ring, adding also local electron density. The +M effect affects not only the intensive colour of this compound, but also its great stability.

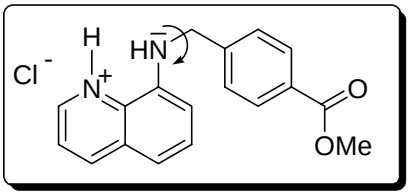

Scheme 3.8 *Halochromic effect of the ligand **21** hydrochloride.*

Upon addition of excess HCl to the monohydrochloride, the colour changed from intensive orange to colourless. This indicated the formation of dihydrochloride, where the protonation occurred on both aromatic and alyphatic amine, breaking the +M effect.

In the synthesis of the ligand **23**, the first step was condensation of the 8-aminoquinoline with salicylaldehyd giving intense yellow-coloured Schiff base **22**. Schiff base was further treated with two equivalents of sodium trisacetoxyborhydride at room temperature during 20 hours (Scheme 3.9).

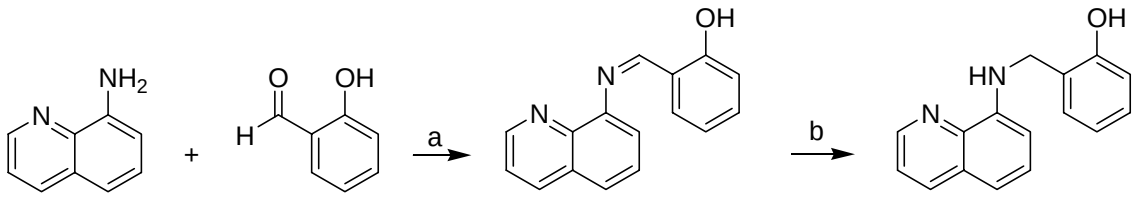

22 **23**

Scheme 3.9 *Synthesis of Schiff base **22** and ligand **23**: a) EtOH, Na_2SO_4, 1h, reflux; b) 2 eq $Na[BH(OAc)_3]$, 20 h, rt.*

The final product **23** was isolated as a hydrochloride, recrystalized from MeOH and crystals suitable for X-ray analysis were obtained by the slow evaporation of MeOH at room temperature (Figure 3.8).

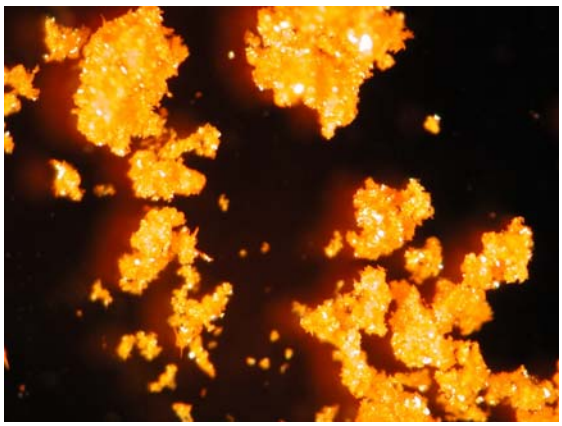

Figure 3.8 *Microscopic view of the ligand **23**.*

The ^{1}H NMR spectrum of the ligand **20** showed, in comparison to the starting compound 8-aminoquinoline **19**, one new singlet at 2.77 ppm, which can be attributed to the methylene group H_{12}. Because of the influence of the neighbouring benzyl ring the signal of methylene group in the ^{1}H NMR spectrum of the ligands **21** and **23** shifted from 2.77 to 4.66 and 4.48, respectively. The new singlet at 3.82 ppm in ^{1}H NMR spectrum of the ligand **21**, in comparison to the spectrum of ligand **20**, was attributed to the methyl group of the ester moiety. Signals appearing in the range from 5.5–9.0 ppm were attributed to the aminoquinoline unit, which is the case of **20** slightly downfield shifted comparing to the starting compound 8-aminoquinoline (Figure 3.9). The singlet at 5.9 ppm corresponding to the amino group of the 8-aminoquinoline **19**, appeared as a weak signal around 6.9 ppm in **20**.

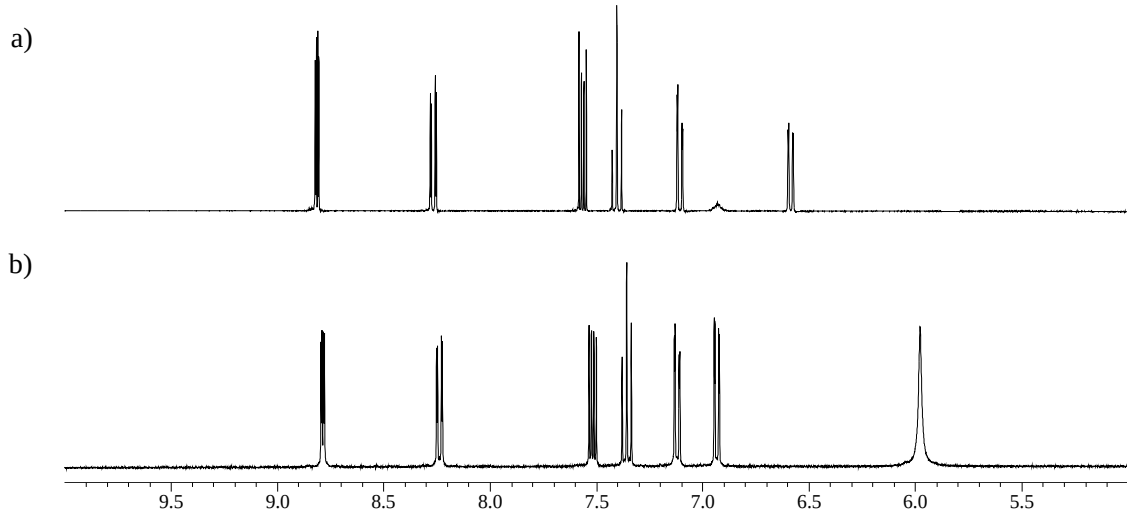

Figure 3.9 *^{1}H NMR spectra of a) ligand **20** and b) 8-aminoquinoline **19**.*

The protons H_{14} and H_{18} in the ^{1}H NMR spectrum of ligand **21** appeared as doublet at 7.91 ppm with a coupling constant of 8.0 Hz, similiar as protons H_{15} and H_{17} giving a doublet at 7.55 ppm with *J*=8.40 Hz. In the case of ligand **23**, where the hydroxy group is in 2-position, the proton H_{17} (which corresponds to H_{15} in ligand **7**) appeared together with H_6 at 7.24 ppm as a pseudo triplet. Similar happened with H_{14} of ligand **23** (which is the one corresponding to H_{14} in ligand **5**): this signal appeared with the signal of H_8 at 6.87 ppm also as a pseudotriplet.

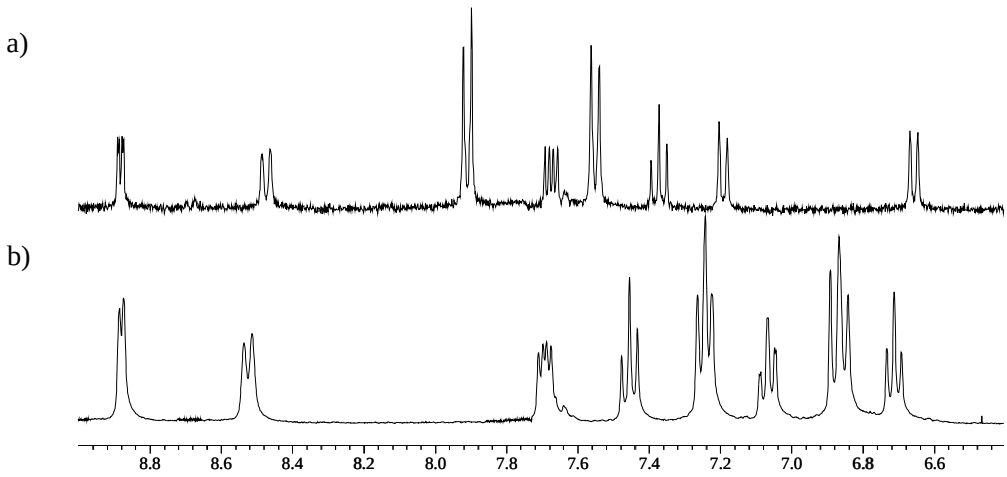

Figure 3.10 *^{1}H NMR spectra in the 6.4 – 9.0 ppm range of a) compound **21** and b) compound **23**.*

In the ^{13}C NMR spectrum of the ligands **20**, **21** and **23** methylene group was observed at 46.9, 45.9 and 41.9 ppm, respectively.

ESI-MS spectra of synthesized ligands **20**, **21** and **23** (Figure 3.11) showed the molecular peaks at *m/z* 203, 293 and 251, respectively, which corresponded exactly to $[M + H]^+$ ion.

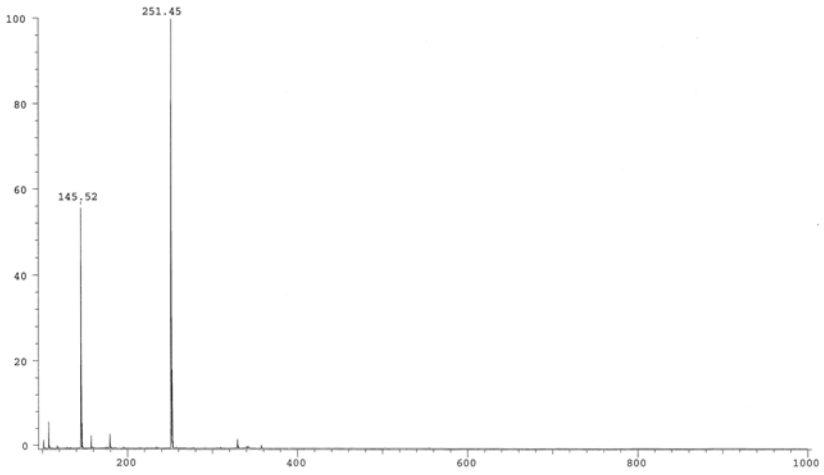

Figure 3.11 *ESI-MS spectra of the ligand **23**.*

Complexes **24 - 39** were prepared by the reaction of equimolar amounts of the ligands **19 - 23** and corresponding metal(II) nitrates/chlorides in hot methanol (Scheme 3.10). The reaction mixture was left for a few hours at room temperature and then for next few days at 7^oC. Precipitate/crystals obtained were isolated by filtration and dried in air. Yields were in the range 48-58 %.

In the reaction of 8-aminoquinoline **19** with metals, precipitation was observed immediately. An exception was the crystallization of the complexes **25** and **33**, of which crystals were suitable for a X-ray structure analysis.

Complexation of the ligand **21** with $CuCl_2$ resulted in blueish green crystal plates (Figure 3.12) suitable for the X-ray crystal analysis.

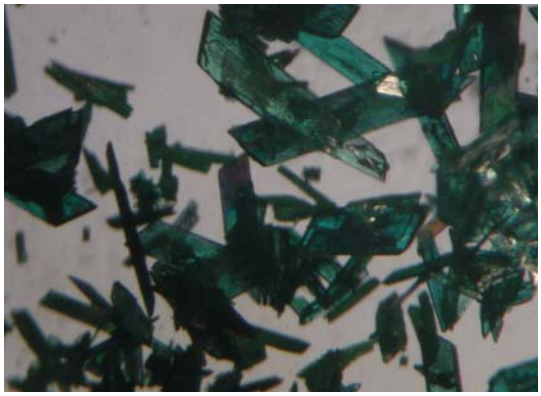

Figure 3.12 *Microscopic view of the crystals suitable for X-ray structure analysis: copper complex **36**.*

a)

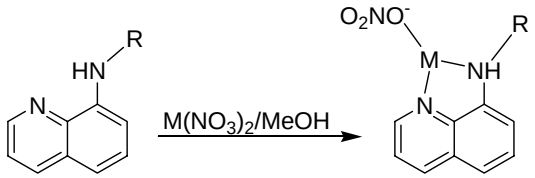

24 R = H; M = Cu(II).

25 R = H; M = Zn(II).

26 R = H; M = Cd(II).

27 R = H; M = Ni(II).

28 R = H_2C–C$_6$H$_4$–COOMe; M = Cu(II).

29 R = H_2C–C$_6$H$_4$–COOMe; M = Ni(II).

30 R = H_2C–C$_6$H$_4$(HO); M = Cu(II).

31 R = H_2C–C$_6$H$_4$(HO); M = Ni(II).

32 R = H_2C–C$_6$H$_4$(HO); M = Co(II).

b)

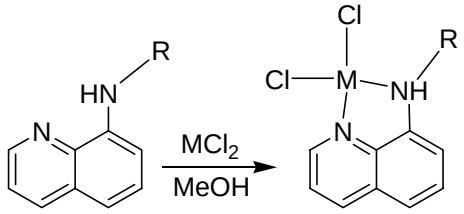

33 R = H; M = Cu(II).

34 R = H; M = Zn(II).

35 R = H; M = Pd(II).

36 R = H_2C–C$_6$H$_4$–COOMe; M = Cu(II).

37 R = H_2C–C$_6$H$_4$–COOMe; M = Pd(II).

38 R = H_2C–C$_6$H$_4$(HO); M = Cu(II).

39 R = H_2C–C$_6$H$_4$(HO); M = Pd(II).

Scheme 3.10 *Synthesis of the metal complexes **24** – **39**: a) metal(II) nitrates; b) metal(II) chlorides.*

It is interesting to note the result from the El-Bahnasawy et al.[107], who characterized this complex as the complex in dimeric form with bridging chloride ions by many other methods (elemental analysis, molar conductance, IR and electronic spectra and magnetism), but did not obtain a crystal structure. The data which we obtained by the X-ray analysis is in good agreement with these published results. Another crystal structure data obtained from complexation with this ligand, was the complexation with $Cu(NO_3)_2$, whose ORTEP plot and structural data are presented in Chapter 3.3.2.2.

When the same ligand **21** was mixed with Na_2PdCl_4 in MeOH, after a few hours needle-like dark yellow crystals were obtained (Figure 3.13). Unfortunately, during isolation

of the crystals from solution and drying in air, the crystals of **37** lost their morphology because of the loss of the solvent. Therefore, the X-ray structure could not be obtained.

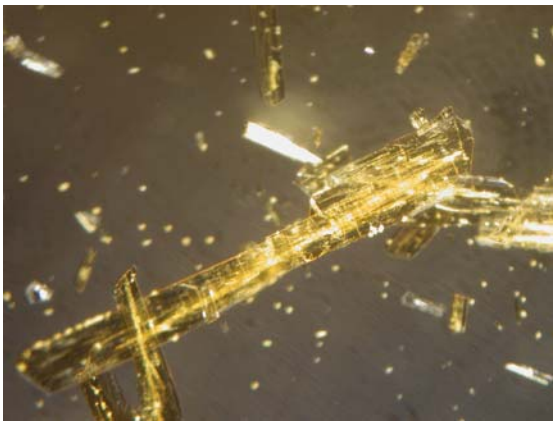

Figure 3.13 *Microscopic view of the palladium(II) complex **37**.*

Crystals of the complexes with the ligand **23** were obtained following the same procedure as described above. Intensely green crystals of the Cu(II) complex **39** (Figure 3.14) were grown from MeOH during 5 days at –7^{o}C, and then isolated by the filtration.

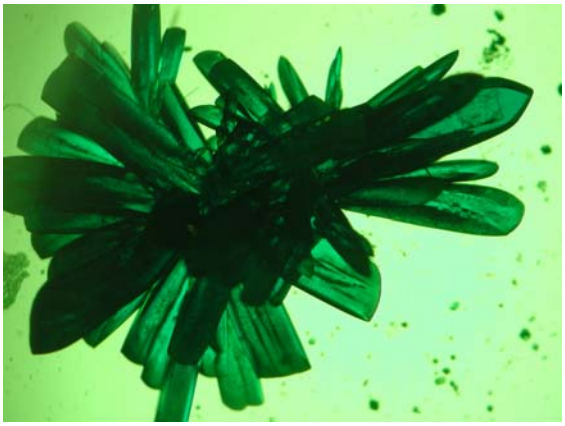

Figure 3.14 *Microscopic view of the crystals suitable for X-ray structure analysis: copper(II) complex **38**.*

After standing at –7^{o}C after a few days, plate-like crystals of the Pd(II) complex **38** (Figure 3.15) were isolated by the filtration from MeOH solution. Their ORTEP plot and crystal structure properties will be discussed in the Chapter 3.3.2.3.

Figure 3.15 *Microscopic view of the crystals suitable for X-ray structure analysis: palladium(II) complex **39**.*

The same problem as for the isolation of the Pd(II) complex **37** (Figure 3.16) occurred for the Co(II) complex from solution. Brown/orange crystals became turbid after drying in air, and therefore no crystal structure could be obtained.

Figure 3.16 *Microscopic view of the complex **37**.*

The ^{1}H NMR spectra of the complexes **24**-**39** showed a downfield shift, what is typical for the coordination of the ligand to the metal center.

In comparison to the ^{1}H NMR spectrum of the ligand **23**, the major difference in the ^{1}H NMR spectrum of the Pd(II) complex **39** is the downfield shift of H_{14} –H_{17}. For example, the downfield shift of the protons H_{14} and H_{17} was 0.76 and 0.73 ppm, respectively, suggesting major changes in the structure of the ligand **23** after coordinating the Pd(II) center. This was indeed confirmed with the crystal structure of both – ligand **23** and its Pd complex **39**, where the benzyl ring was turned away from the quinoline moiety (see Chapter 3.3.2.3).

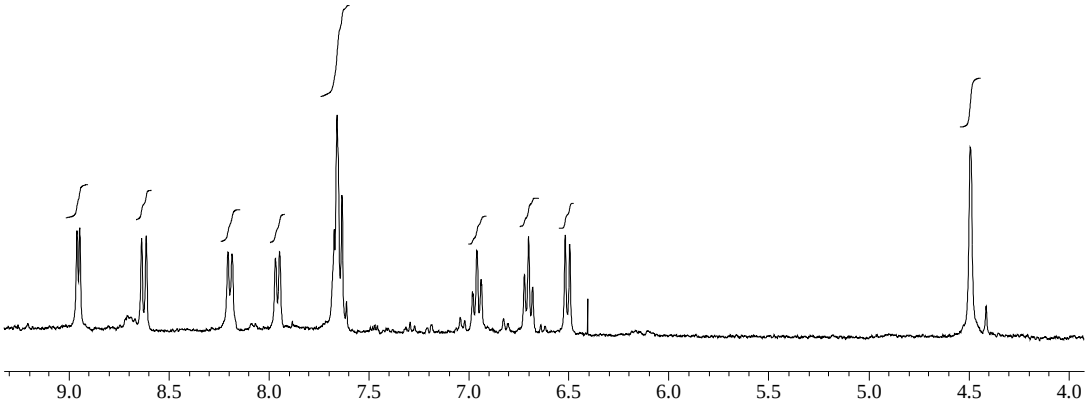

Figure 3.17 *^{1}H NMR spectra of the Pd(II) complex **39**.*

In the ^{13}C NMR spectrum of the ligand **21**, in comparison to the corresponding Pd(II) complex **37**, the carbon atoms $C_{bz\text{-}14,\ 18}$ and $C_{bz15,\ 17}$ shifted 1.9 and 1.4 ppm, respectively. A significant difference between those two ^{13}C NMR spectra was observed by the C_{12} signal, which appeared at 45.9 ppm in the ligand **21**, and was shifted to 56.6 ppm after complexation with Pd(II).

For the recording of ESI-MS spectra, metal complexes **24**-**39** were dissolved in MeOH. They showed the corresponding molecular ions after loss of nitrate/chloride counter ions $[LM]^{+}$, with an isotopic pattern typical for the metal ion in the complex. One of examples is the ESI-MS spectra of the Cu(II) complex **38**, with peak assigned to $[LM]^{+}$, showing expected isotopic patter of Cu(II) (Figure 3.18).

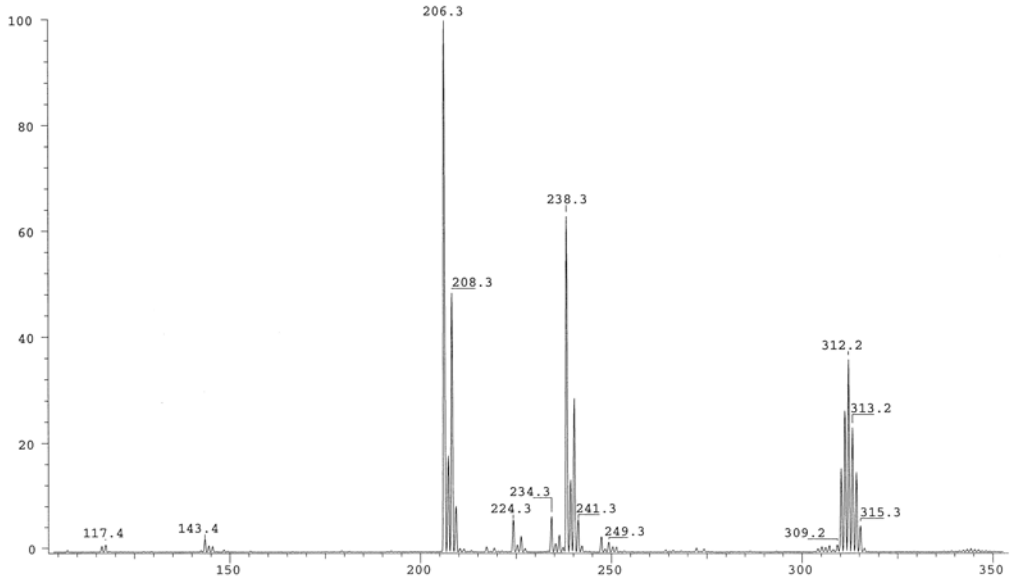

Figure 3.18 *ESI-MS spectra of the Cu(II) complex **38**.*

3.2 *N*-Nitrilotriacetic Acid (NTA) Derivatives

The six-histidine tag serves as a high affinity binding sequence for the purification of peptides and proteins via metal chelating adsorbents (Chapter 1.4). One of the most important chelators for the oligo-histidine tag is the *N*-nitrilotriacetic acid (NTA) derivative *N*-(1-carboxy-5-aminopentyl)iminodiacetic acid (see Chapter 1.4; Figure 1.8).

In ordrer to have a compound which would contain NTA moiety as a binding site to an oligo-histidine sequence and a ligand whose metal complex could act as a peptidase, compound **42** was synthesized (Figure 3.19).

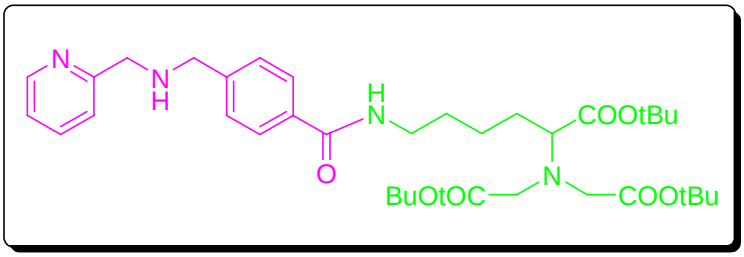

42

Figure 3.19 *Compound **42** containing NTA moiety (green) as a binding site to an oligo-histidine sequence and a ligand (purple) whose metal complex could act as a peptidase.*

In the synthesis of **42** a key step was the formation of the amide bond between acid (ligand **2**) and the amino group of the NTA derivative **41**. The synthesis of the compound **2** is already described and discussed above in the Chapter 3.1.1, while NTA derivative **41** (N^{α},N^{α}-Bis[(*tert*-butyloxycarbonyl)methyl]-L-lysine tert-butyl ester was synthesized in a two step reaction.

The NTA derivative **41** was synthesized according to a procedure proposed by Dorn et al.[108], but with some modifications. The starting compound H-Lys(Z)-tBu (N^{ε}-benzyloxycarbonyl-L-lysine *tert*-butyl ester hydrochlorid) was dissolved in DMF in the presence of NEt_3. Then bromoacetic acid *tert*-butyl ester was added and the reaction mixture was stirred at 50°C for 3 days. The excess bromoacetic acid *tert*-butyl ester and the solvent were evaporated *in vacuo* and the remaining oily residue was extracted with hexane, the organic phases collected and hexane was removed *in vacuo*. The residue was the expected Z-protected amine **40** (Scheme 3.11).

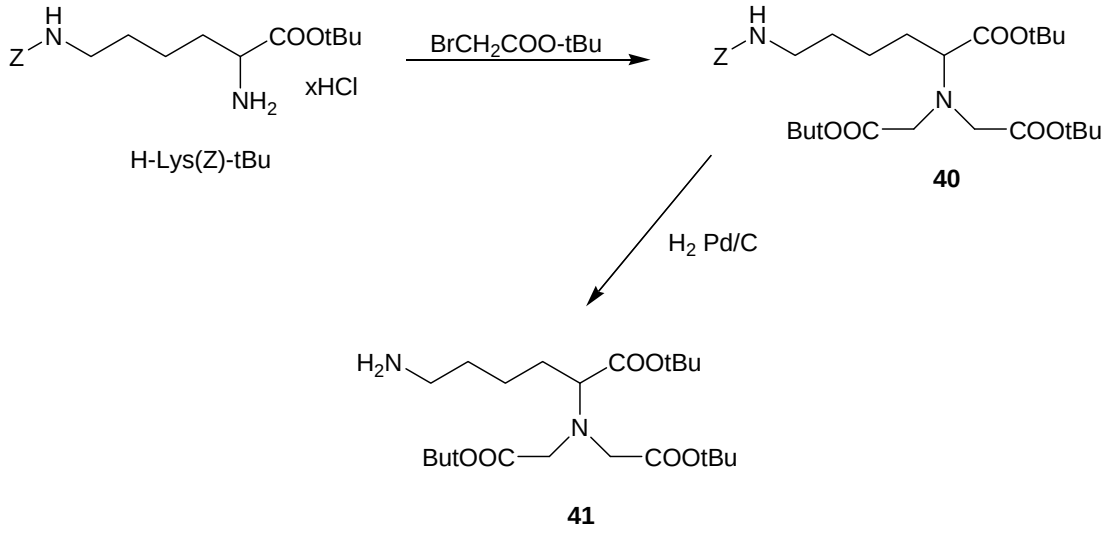

Scheme 3.11 *Synthesis of NTA derivative **41**.*

The amino group of the side chain in the starting compound and carboxy group were protected by the Z-group (benzyloxycarbonyl) and *tert*-butyl esters, respectively. The reason for such a choice of protecting groups was that the Z-group is easy to remove by the hydrogenation, while *tert*-butyl groups led to the better solubility of the compound in organic solutions.

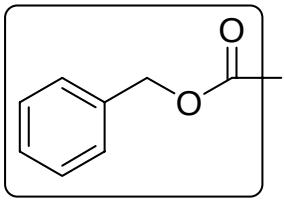

Figure 3.20 *Structure of the Z-protecting (benzyloxycarbonyl) group.*

In order to obtain the free amino group in compound **41**, the Z-protecting group was removed by hydrogenation at room temperature and atmospheric pressure. However, following the procedure proposed by Dorn et al.[108] we obtained very poor yields of the final compound **41**. Therefore, instead of $CHCl_3$:AcOH solvent mixture and 5% Pd/C, we used a mixture of MeOH, EtOH and H_2O and 10% Pd/C as a catalyst. In such reaction conditions, we could observe the reduction of the Z-group already after 2 h, with a yield of 88%. As we can see in the ^{13}C NMR spectrum of **40** in DMSO (Figure 3.21), signals of the Z-group appeared in the range 127.6-128.3 ppm, while after the hydrogenation these signals dissapeared.

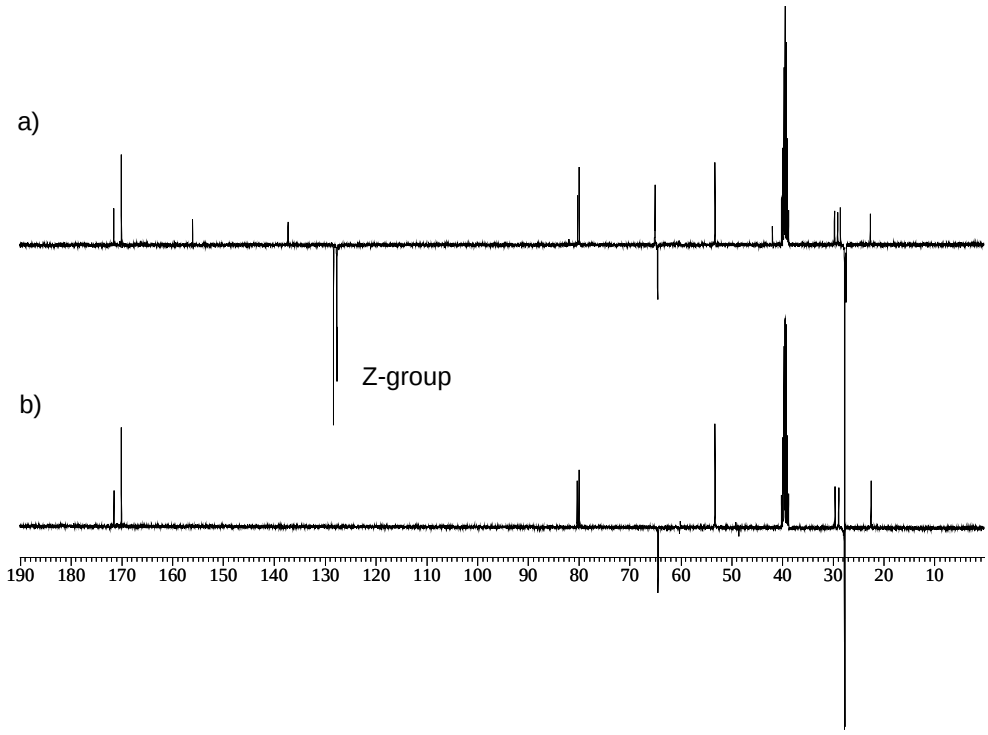

Figure 3.21 *^{13}C NMR spectra of amine: a) amino group of the **40** protected with Z-group; b) NTA derivative **41** after reduction of Z-group via hydrogenation.*

After the successful synthesis and spectroscopic characterization of both acid **2** and NTA derivative **41**, the next step was the formation of the amide bond between these two compounds. This required the activation of a carboxylic acid, which was carried out using the coupling reagents. For our purpose we chose four main methods/coupling reagents and checked their reproducibility:

- Carbodiimide method: coupling with DCC
- Mixed anhydride method: coupling with iBCF
- Disuccinimidyl (DSC) method
- Coupling with TBTU/HOBt/DIPEA

3.2.1 Carbodiimide Method: Coupling with DCC

One equivalent of *N*-4-benzylic acid-*N*-2-picolylamine **2** was dissolved in a mixture of DCM and EtOH and a solution of NHS, DCC and DMAP in acetone was added. After 15 min. stirring at room temperature, white precipitate of *N*,*N*`-dicyclohexylurea was obtained (Scheme 3.12). The reaction mixture was stirred for 4 h, then the precipitate was filtered, the solvent evaporated *in vacuo* and the residue was dissolved in EtOAc . The raw product was worked up according to the washing procedure described above. The EtOAc phase was dried with Na_2SO_4, filtered and evaporated to dryness *in vacuo*.

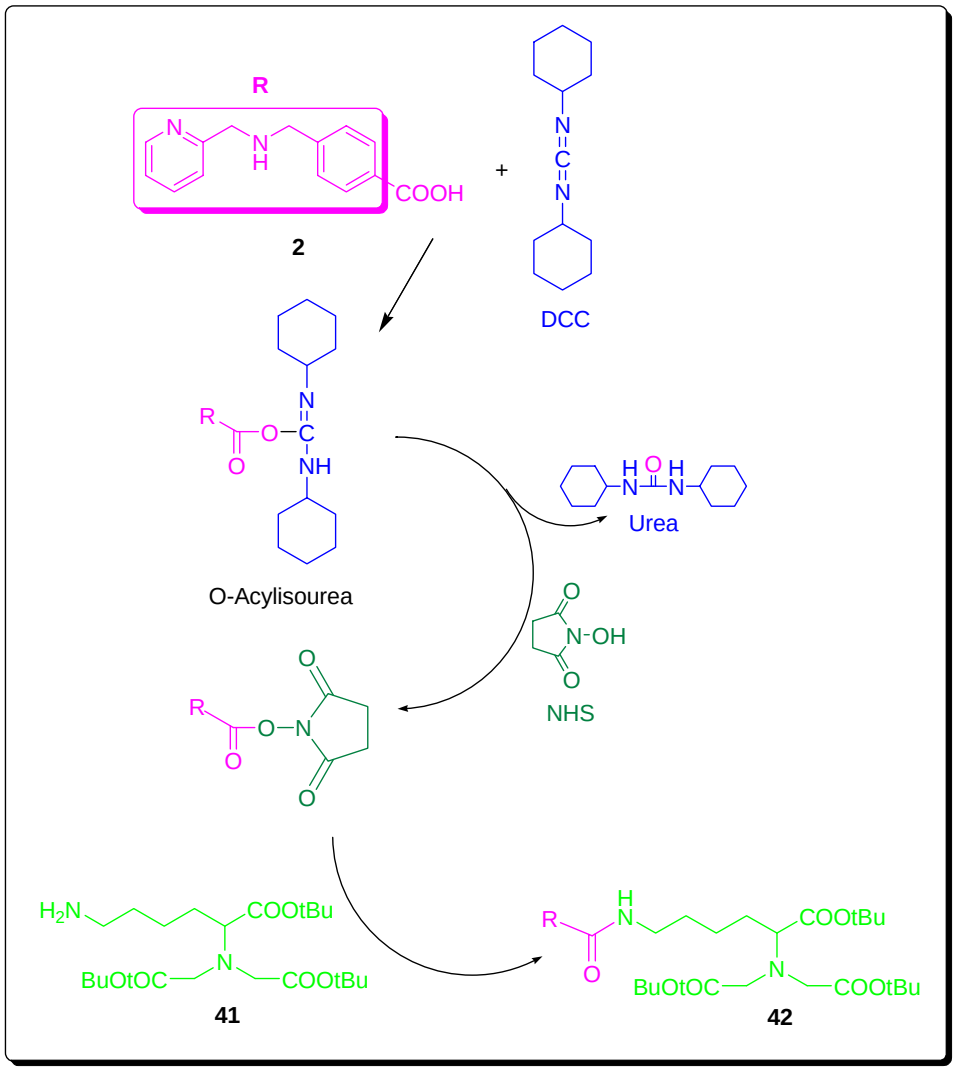

Scheme 3.12 *Mechanism of peptide bond formation through carbodiimide activation*

.

The carbodiimides, primarly DCC, were the coupling reagents of choice for many years[109, 110]. *N*-Hydroxysuccinimide (NHS) is often used to assist the carbodiimide coupling in

the presence of DCC to prevent racemization. If the reaction is carried out without NHS, the alpha carbon of the acid is very prone to racemization/epimerization. With NHS, the mixed anhydride is immediately attacked by the *N*-hydroxy alcohol to give the NHS ester, which is still very reactive towards amines, but not very prone towards racemization. NHS can be removed by washing with weak base. Beside NHS, at the beginning of the 70`s, 1-hydroxybenzotriazole (HOBt)[111] was proposed as an additive to DCC to reduce racemization and from then on other benzotriazole like 1-hydroxy-5-chlorobenzotriazole (Cl-HOBt)[112] or 1-hydroxy-7-azabenzotriazole (HOAt) [113] have also been used.

DCC reacts with the carboxyl group first and forms a very reactive intermediate, O-acylisourea. This is the most reactive species that can attack the amino component to give the corresponding amide.

However, the O-acylisourea can undergo a rearrangment to give the *N*-acylurea (Scheme 3.13), which is less reactive.

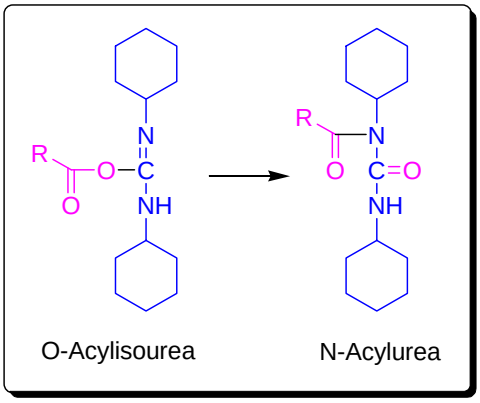

Scheme 3.13 *The reactive O-acylisourea undergoes a rearrangement to give less reactive N-acylurea.*

To overcome this problem, it is necessary to stabilize the intermediate O-acylisourea using NHS. The major drawback encountered is the precipitation of the dicyclohexylurea, which is hard to remove out from the reaction mixture even after several filtrations through 0.2 μm pore filters. Also, the use of solvents of low dieletric constant such as DCM or chloroform, should minimize the racemization.

Beside filtration through 0.2 μm pore filter, we tried to remove the urea and unreacted compound **41** by precipitation in acetone. Therefore, the compound **42** was dissolved in acetone, and white precipitate collected by the filtration.

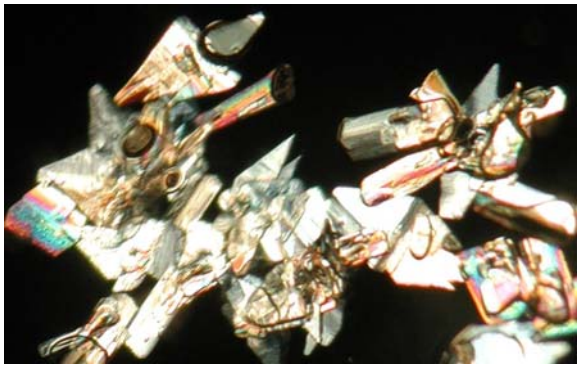

Figure 3.22 *Microscopic view of the precipitated dicyclohexylurea.*

FAB-MS spectra showed that the precipitation was indeed: urea + unreacted **41** (Figure 3.23), and the expected product **42** (Figure 3.24) was left in filtrate.

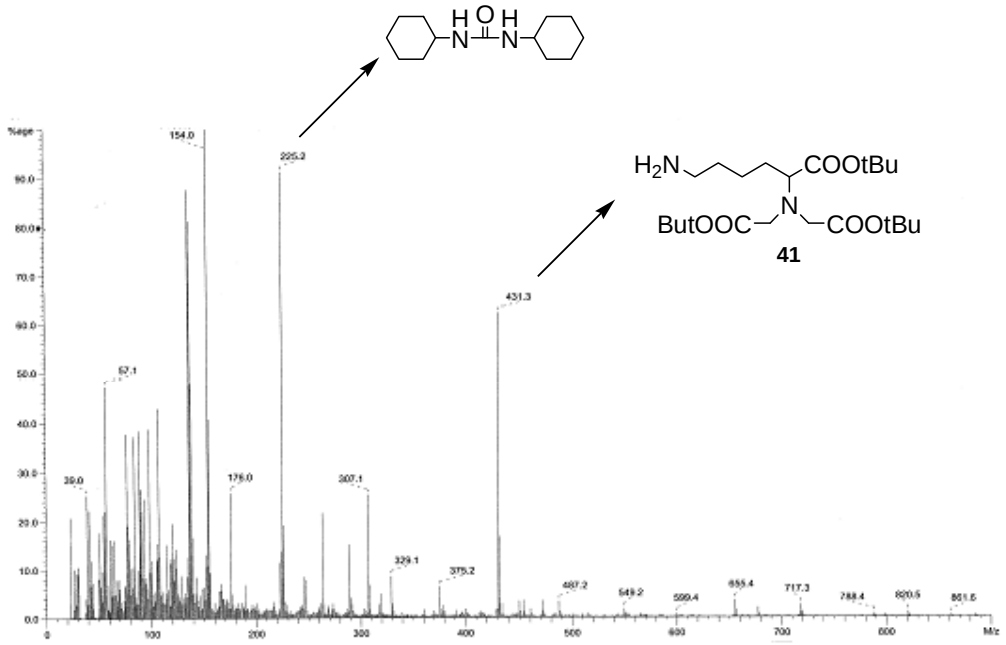

Figure 3.23 *FAB-MS spectra of the precipitate: dicyclohexylurea and unreacted **41**.*

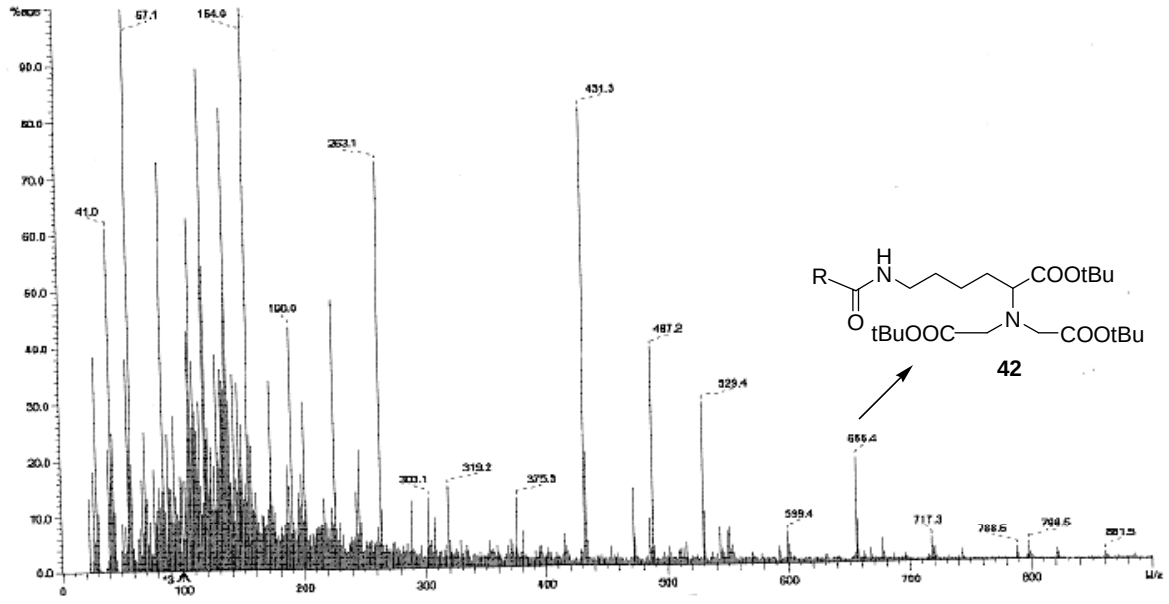

Figure 3.24 *FAB-MS of the filtrate: expected compound **42**.*

3.2.2 Mixed Anhydride Method: Coupling with iBCF

For the synthesis of the compound **42** following the mixed anhydride method, one equiv. of *N*-4-benzylic acid-*N*-2-picolylamine **2** was dissolved in DMF and then 1 equiv. NEt_3 was added. The solution was cooled to -7^oC and one equiv. of iBCF was slowly added. The activation time was about 30 min. The solution of one equiv. of the compound **41** with one equiv. of NEt_3 in DMF at $-7\ ^oC$ was added. The reaction mixture was stirred on ice for 1 h, and then at room temperature for the next 42 h. The green residue left after evaporation of the solvent *in vacuo*, was dissolved in EtOAc, filtered and then worked up according to the washing procedure: 3 times washed with 50-100 ml of 10% acetate buffer (pH 4.0), 3 times with 50-100 ml of 5% NaCl solution, three times with saturated $NaHCO_3$ solution and then again 3 times with 50-100 ml of 5% NaCl solution. The EtOAc phase was dried with Na_2SO_4, filtered and evaporated to dryness *in vacuo*. The purity was checked with TLC (EtOAc : MeOH, 8 : 2) and the compound was characterized with NMR and FAB-MS, which showed expected results (see Chapter 4.5).

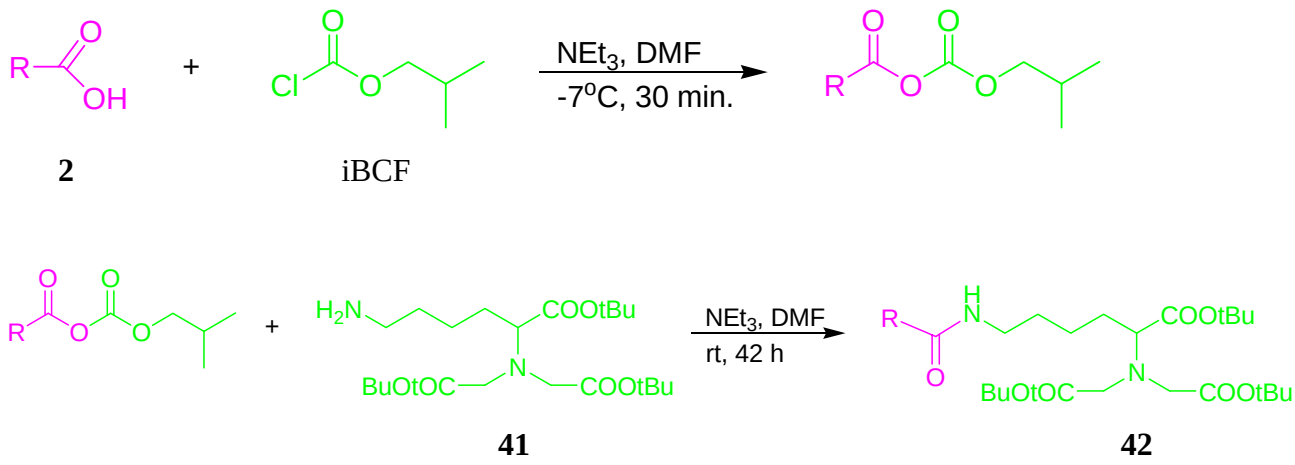

Scheme 3.14 *Formation of the amide bond by the mixed anhydride method.*

3.2.3 Disuccinimidyl (DSC) Method and Coupling with TBTU, HOBt and DIPEA

To avoid the problems concerning formation of urea and its filtration, an alternative is the coupling method using disuccinimidyl (DSC)[114, 115]. In the direct reaction of the compound **2** and DSC, the active ester formed is easy to isolate from the reaction mixture, and to go on with a coupling with **41** in the next step.

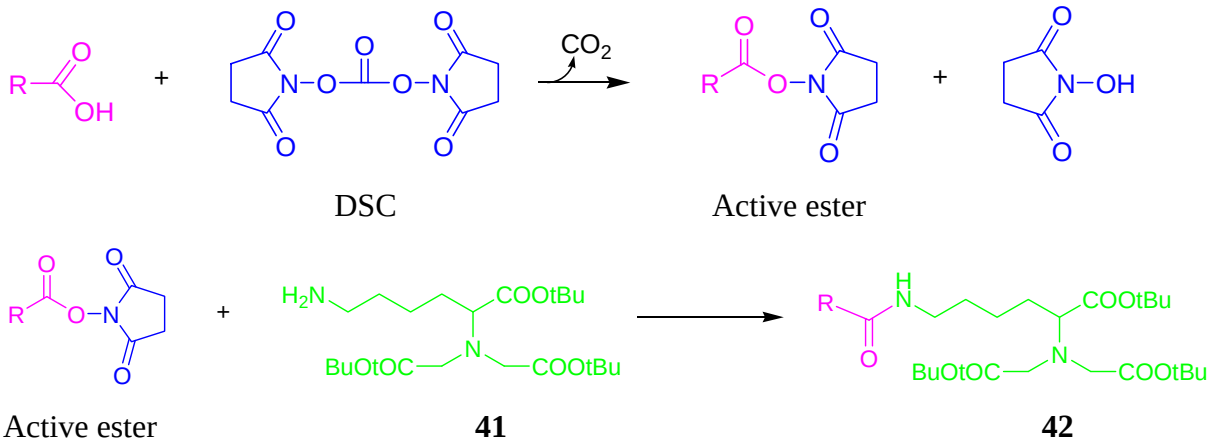

Scheme 3.15 *Coupling with DSC.*

For coupling with TBTU/HOBt/DIPEA compound **2** was dissolved in a mixture of DMF and MeOH, then TBTU, HOBt and DIPEA were added.

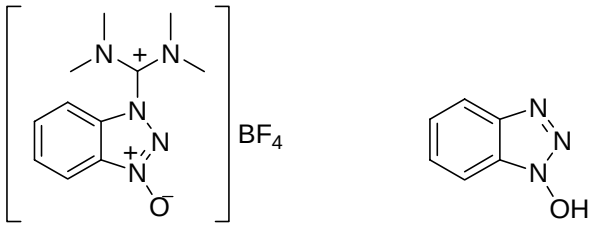

TBTU HOBt

Figure 3.25 *Structures of the coupling reagents TBTU and HOBt.*

The activation time was about 20 minutes at room temperature. The colour changed from pale yellow to orange. Then solution of **41** in DMF was added, and the reaction mixture was stirring for 24 h at room temperature. The reaction was followed by TLC in the solvent system EtOAc : MeOH, 8 : 2. The orange/brown oil left after evaporation of the solvent *in vacuo*, was dissolved in EtOAc, filtrated and then worked up according to the washing procedure: 2 times washed with 50-100 ml of 10% $NaHCO_3$ solution, once with acetate buffer (pH 4.0), and then again twice with 10% $NaHCO_3$ solution. The EtOAc phase was dried with Na_2SO_4, filtrated and evaporated to dryness *in vacuo*. The compound was characterized with NMR and FAB-MS. Similar as the NHS in the coupling procedure with DCC, HOBt is a benzotriazole, additive whose addition leads to the formation of the benzotriazole active ester, reducing racemization and avoiding the formation of other derivatives less reactive.

However, in both methods, the one using DSC[114] and in the other one using TBTU[116], the yields of the final product **42** were too low to be accepted. Therofore, the coupling method recommended from these four methods, were DCC method and mixed anhydride method using iBCF, although both resulting in yields too low to be applied.

3.3 Crystal Structures

Following structural criteria, there are two main groups of compounds, whose X-ray crystal structure was obtained during this research:

- Structures containing 2-picolylamine unit
- Structures containing 8-aminoquinoline unit.

All crystals were grown by slow evaporation of MeOH solution, either at room temperature or at –7^{o}C. Selected bond lengths and angles are summarized in tables in the end of each chapter.

3.3.1 Crystal Structures of 2-Picolylamine Derivatives

Crystal structures obtained for the derivatives of 2-picolylamine were the complexes of Zn(II) and Cu(II) coordinated with the ligand **2**. Both structures form five-membered rings M-N(1)-C(6)-C(7)-N(8)-M as showed on Figure 3.26 and Figure 3.27. They both crystallize in the triclinic crystal system, space group P-1. Two nitrogen atoms of the ligand **2** coordinate to the metal center. However, there are marked differences between these two structures. Zinc complex **9** is a *dimer* with a coordinated chloride and methanol with a bridging ligand **2** between two Zn centers. The unit cell consists of two crystallographically independent molecules around the center of inversion, which means two dimers in one unit cell Figure 3.28). Copper complex **10** is also a dimer. However, beside two nitrogen atoms from the ligand, remaining coordination sites at the metal center of the complex **10** are filled with two chlorides, one of them bridging two copper centers.

The bond distances and angles gave further insight into the properties of these two complexes. The Cu-Cu distance of 3.472 Å in the complex **10** is too long for metal-metal binding. The Cl-Cl distance of 3.357 Å is also nonbonding. The Cu-Cl distances are 2.306 Å and 2.519 Å showing that chlorides do not bridge symmetrically. Although these two complexes structures are bridged in different ways, it is interesting to see that the angles between N-Cu-N and N-Zn-N are very simmilar, 81.50 and 79.17, respectively. The phenyl rings of **9** are fairly close to each other, they are 3.738 Å apart. The fact that the distance Zn-CH_2(benzyl) (3.185 Å) is shorter than the distance between the aromatic rings (3.738 Å) shows that the weak electronic stacking interactions, common for aromatic systems, are present as well. The angles C(7)-N(8)-C(9) in both complexes **9** and **10** are almost the same: 110.72^{o} and 110.81^{o}, respectively.

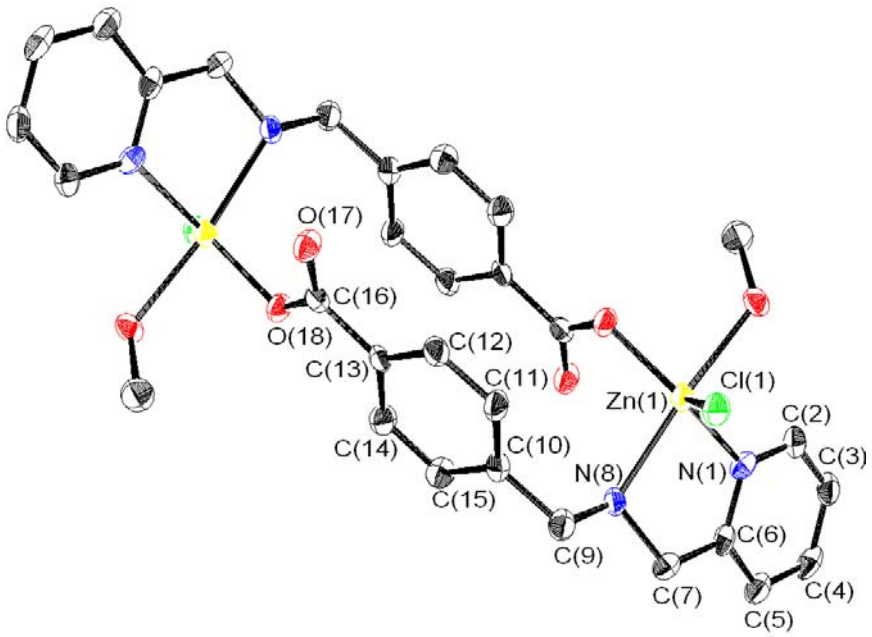

Figure 3.26 *ORTEP plot of* ***9*** *(50% probability). Hydrogen atoms have been omitted for clarity.*

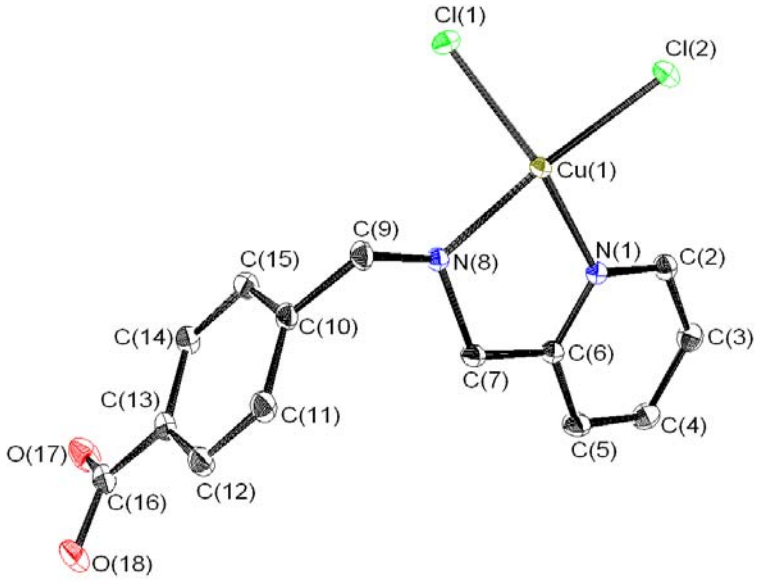

.

Figure 3.27 *ORTEP plot of* ***10*** *(50% probability). Hydrogen atoms have been omitted for clarity.*

Although these two complexes were both dimers, their two metal centers were bridged in different manner: in one case there is a benzyl part of the ligand turned in a way to take a part in the bridging two Zn centers (**9**) and in the other case benzyl part of the molecule turned *away* from the chloride bridges, not taking part in the bridging two copper centers (**10**). Figures 3.28 and 3.29 present packing in the unit cell of the complexes **9** and **10**.

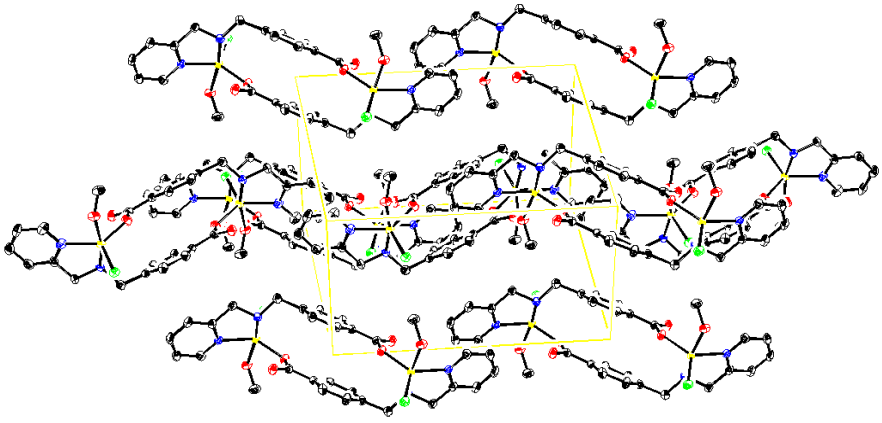

Figure 3.28 *Unit cell contents of complex **9**.*

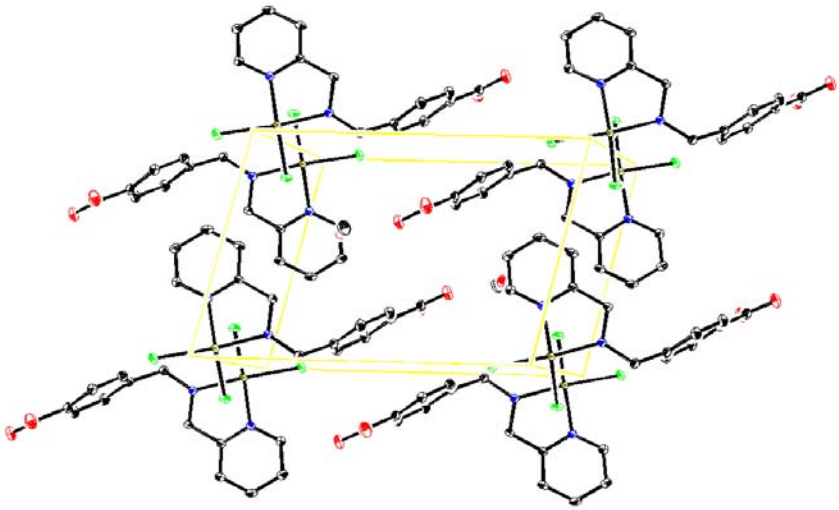

Figure 3.29 *Unit cell contents of complex **10**.*

Complex 9		**Complex 10**	
Zn(1)-O(18)#1	1.966(4)	Cu(1)-N(1)	2.0277(11)
Zn(1)-N(1)	2.099(4)	Cu(1)-N(8)	2.0371(11)
Zn(1)-O(20)	2.176(4)	Cu(1)-Cl(1)	2.3039(4)
Zn(1)-N(8)	2.185(4)	Cu(1)-Cl(2)	2.3063(3)
Zn(1)-Cl(1)	2.273(2)	Cu(1)-Cl(2)#1	2.5188(4)
		Cl(2)-Cu(1)#1	2.5187(4)
O(18)#1-Zn(1)-N(1)	131.6(2)		
O(18)#1-Zn(1)-O(20)	85.2(2)	N(1)-Cu(1)-N(8)	81.50(4)
N(1)-Zn(1)-O(20)	89.1(2)	N(1)-Cu(1)-Cl(1)	144.69(3)
O(18)#1-Zn(1)-N(8)	97.0(2)	N(8)-Cu(1)-Cl(1)	90.73(3)
N(1)-Zn(1)-N(8)	78.7(2)	N(1)-Cu(1)-Cl(2)	93.63(3)
O(20)-Zn(1)-N(8)	165.6(2)	N(8)-Cu(1)-Cl(2)	174.77(3)
O(18)#1-Zn(1)-Cl(1)	113.77(13)	Cl(1)-Cu(1)-Cl(2)	94.361(13)
N(1)-Zn(1)-Cl(1)	114.58(13)	N(1)-Cu(1)-Cl(2)#1	105.57(3)
O(20)-Zn(1)-Cl(1)	93.98(12)	N(8)-Cu(1)-Cl(2)#1	91.40(3)
N(8)-Zn(1)-Cl(1)	98.02(13)	Cl(1)-Cu(1)-Cl(2)#1	109.029(13)
		Cl(2)-Cu(1)-Cl(2)#1	88.069(12)
C(2)-N(1)-Zn(1)	127.5(4)		
C(6)-N(1)-Zn(1)	114.3(4)	Cu(1)-Cl(2)-Cu(1)#1	91.932(12)
C(9)-N(8)-Zn(1)	120.4(3)	C(7)-N(8)-Cu(1)	108.23(8)
C(7)-N(8)-Zn(1)	105.4(3)	C(9)-N(8)-Cu(1)	121.89(8)
C(16)-O(18)-Zn(1)#1	123.5(3)		
C(21)-O(20)-Zn(1)	124.5(3)		

Table 3.1 *Selected bond lengths (Å) and angles (°) for **9** and **10**.*
Symmetry transformations used to generate equivalent atoms: #1 -x,-y,-z

3.3.2 Crystal Structures of 8-aminoquinoline Derivatives

From this series of compounds, the crystal structures obtained were the metal complexes **33** and **25** with 8-aminoquinoline **19**, metal complexes **28** and **36** with ligand **21** and finally metal complexes **38** and **39** with ligand **23** as well as the crystal structure of the ligand **23** itself. All crystals were grown by slow evaporation of MeOH solution, and selected bond lengths and angles are summarized in tables in the end of chapter.

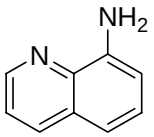

19

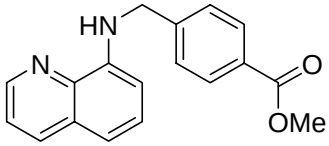

21

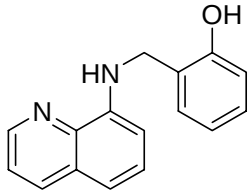

23

Figure 3.30 *8-aminoquinoline **19** and its derivatives **21** and **23**.*

3.3.2.1 Crystal structures of metal complexes with unsubstituted 8-aminoquinoline

In the crystal structure of the pale green crystals of Cu(II) complex **33,** as well as in the crystal structure of Zn(II) complex **25**, the motif of the five-membered ring, present also in the crystal structures of previously described complexes **9** and **10**, appeared between M-N(1)-C(10)-C(9)-N(11)-M. Angles in this five-membered ring by these two structures **21** and **23** of the same class were very similar, as expected.

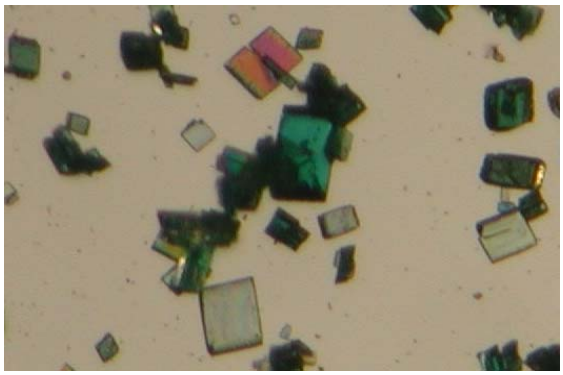

Figure 3.31 *Crystals of the Cu(II) complex **33**.*

All atoms were in the same plane as a consecquence of the rigid quionoline ring. But, in comparison to the angles of the five-membered ring in the structures of the complexes **9**

and **10**, in the complexes **33** and **25** we expected slight difference as well, because of non-rigidness of this ring in the first two structres caused by the aliphatic amine group. Indeed, the angle between C(6)-C(7)-N(8) in the structures **9** and **10** was only 109°, caused by the non-planarity of the 5-membered ring, and the corresponding angle N(11)-C(9)-C(10) in the planar motif in the structures **33** and **25** is 116-117°.

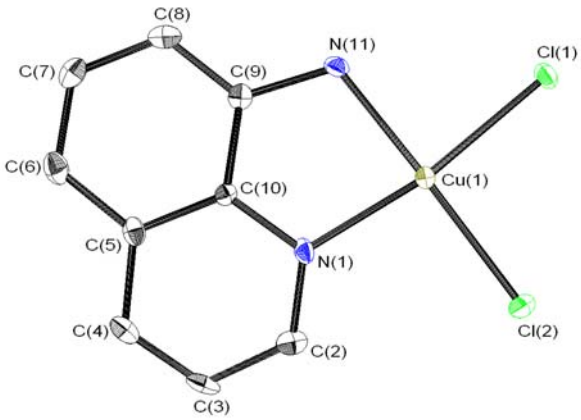

Figure 3.32 *ORTEP plot of **33** (50% probability). Hydrogen atoms have been omitted for clarity.*

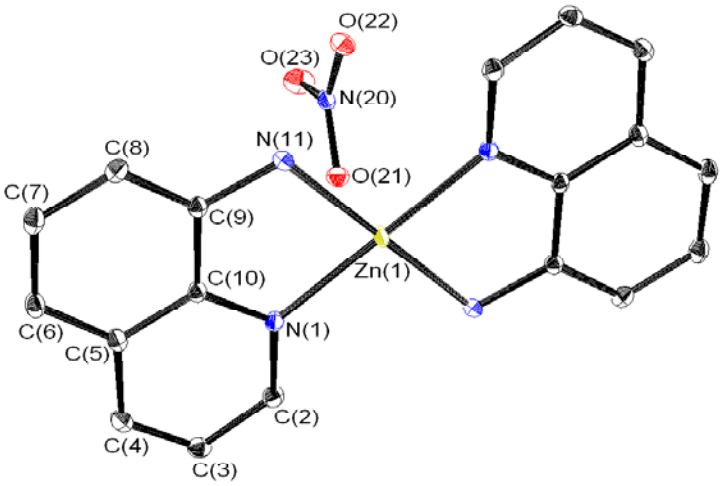

Figure 3.33 *ORTEP plot of **25** (50% probability). Hydrogen atoms have been omitted for clarity.*

While in complex **33** no hydrogen bond interactions were found, in the complex **25** there were intermolecular hydrogen bond interactions present between N(11) and O(23) of a neighbouring molecule (N····O contact = 3.047 Å), and intermolecular interactions between O(22) and O(22) of the neighbouring molecule (O····O contact = 2.989 Å). The distance between Zn(1) and O(21) from nitrate group is 2.253 Å, suggesting that nitrate did coordinate metal center. Simmilar crystal structure was obtained in 1972 by Kerr M. C. S.[117], where this complex was also described as a dimer, but with aqua ligand and not nitrate filling one coordination site.

Compound 33		**Compound 25**	
Cu(1)-N(1)	2.016(4)	Zn(1)-N(1)	2.1016(13)
Cu(1)-N(11)	2.027(4)	Zn(1)-N(1)#1	2.1016(13)
Cu(1)-Cl(2)	2.2713(12)	Zn(1)-N(11)	2.1418(13)
Cu(1)-Cl(1)	2.2870(12)	Zn(1)-N(11)#1	2.1418(13)
Cu(1)-Cl(1)#1	2.7082(13)	Zn(1)-O(21)#1	2.2531(11)
Cl(1)-Cu(1)#1	2.7082(13)	Zn(1)-O(21)	2.2531(11)
N(1)-Cu(1)-N(11)	82.88(15)	N(1)-Zn(1)-N(1)#1	180.0
N(1)-Cu(1)-Cl(2)	95.46(11)	N(1)-Zn(1)-N(11)	80.54(5)
N(11)-Cu(1)-Cl(2)	177.37(11)	N(1)#1-Zn(1)-N(11)	99.46(5)
N(1)-Cu(1)-Cl(1)	166.51(11)	N(1)-Zn(1)-N(11)#1	99.46(5)
N(11)-Cu(1)-Cl(1)	87.77(10)	N(1)#1-Zn(1)-N(11)#1	80.54(5)
Cl(2)-Cu(1)-Cl(1)	93.52(5)	N(11)-Zn(1)-N(11)#1	180.0
N(1)-Cu(1)-Cl(1)#1	94.34(11)		
N(11)-Cu(1)-Cl(1)#1	86.46(11)	N(1)-Zn(1)-O(21)#1	92.24(5)
Cl(2)-Cu(1)-Cl(1)#1	95.71(4)	N(1)#1-Zn(1)-O(21)#1	87.75(5)
Cl(1)-Cu(1)-Cl(1)#1	94.75(4)	N(11)-Zn(1)-O(21)#1	89.55(5)
Cu(1)-Cl(1)-Cu(1)#1	85.25(4)	N(11)#1-Zn(1)-O(21)#1	90.45(5)
		N(1)-Zn(1)-O(21)	87.76(5)
C(2)-N(1)-Cu(1)	129.0(3)	N(1)#1-Zn(1)-O(21)	92.24(5)
C(10)-N(1)-Cu(1)	112.4(3)	N(11)-Zn(1)-O(21)	90.45(5)
C(9)-N(11)-Cu(1)	110.3(3)	N(11)#1-Zn(1)-O(21)	89.55(5)
		O(21)#1-Zn(1)-O(21)	180.0
		C(2)-N(1)-Zn(1)	127.87(11)
		C(10)-N(1)-Zn(1)	113.67(10)
		C(9)-N(11)-Zn(1)	109.71(9)
		N(20)-O(21)-Zn(1)	126.18(9)

Table 3.2 *Selected bond lengths (Å) and angles (°) for **33** and **25**.*

Symmetry transformations used to generate equivalent atoms: #1 -x,-y,-z

3.3.2.2 Crystal structures of metal complexes with *N*-(4-carboxymethyl)benzyl-*N*--8-aminoquinoline

Two crystal structures were obtained with substituted aminoquinoline ligand **21**, namely Cu(II) complexes **36** and **28**. Both complexes crystallize in the triclinic crystal system, space group P-1.

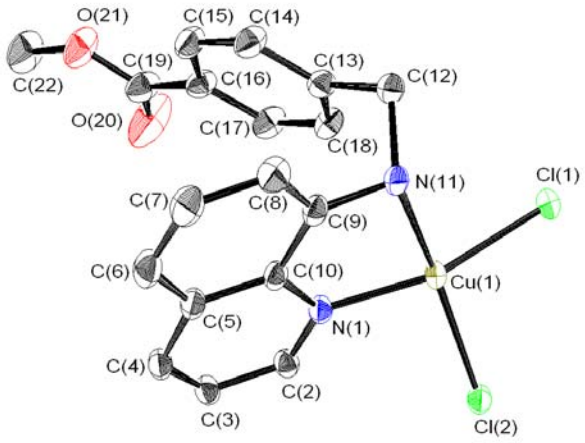

Figure 3.34 *ORTEP plot of monomer **36** (50% probability). Hydrogen atoms have been omitted for clarity.*

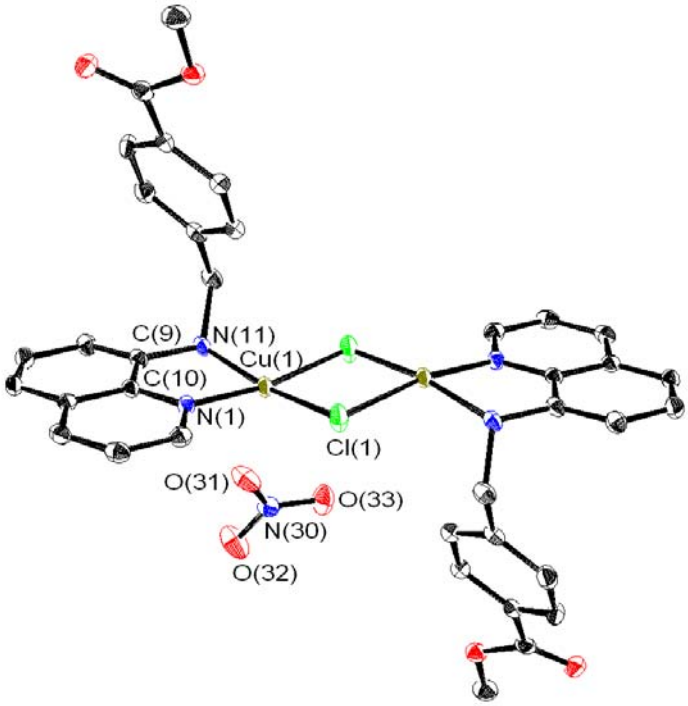

Figure 3.35 *ORTEP plot of dimer **28** (50% probability). Hydrogen atoms have been omitted for clarity.*

Complex **36** was a monomer whose Cu(II) center was coordinated by two nitrogen atoms and two chloride ions. Complex **28** was a dimer with center of inversion, whose Cu(II) center was also coordinated with two nitrogens, and remaining coordination sites were occupied with chlorides, coming from ligand *hydrochloride* itself, as a bridge between two metal centers. Distance between Cu(1) and O(31) was 2.230 Å, meaning that two coordination sites of Cu were occupied with nitrate groups.

Intermolecular hydrogen bond interactions in **36** were present between Cl(1) and N(11) of a neighbouring molecule and Cl(2) and N(11) of neighbouring molecule (Cl···N contacts were 3.250 Å and 3.297 Å, respectively).

All quinoline rings in dimer **28** were planar, and the benzyl parts of the monomers were located downwards and upwards from the quinoline plane. The Cu-Cu distance of 3.330 Å in the complex **28** is too long for metal-metal binding. Intermolecular hydrogen bond interactions in **28** were present between N-H(11) and O(32) of the nitrate group (N-H···O contact = 2.827 Å).

Compound 36		**Compound 28**	
Cu(1)-N(1)	1.9792(14)	Cu(1)-N(1)	1.9904(18)
Cu(1)-N(11)	2.0478(15)	Cu(1)-N(11)	2.0353(19)
Cu(1)-Cl(1)	2.2385(5)	Cu(1)-O(31)	2.2297(18)
Cu(1)-Cl(2)	2.2573(5)	Cu(1)-Cl(1)#1	2.2967(7)
		Cu(1)-Cl(1)	2.3000(7)
N(1)-Cu(1)-N(11)	82.97(6)	Cl(1)-Cu(1)#1	2.2967(7)
N(1)-Cu(1)-Cl(1)	161.53(5)		
N(11)-Cu(1)-Cl(1)	92.80(4)	N(1)-Cu(1)-N(11)	84.29(7)
N(1)-Cu(1)-Cl(2)	94.91(5)	N(1)-Cu(1)-O(31)	86.74(7)
N(11)-Cu(1)-Cl(2)	160.52(5)	N(11)-Cu(1)-O(31)	88.73(8)
Cl(1)-Cu(1)-Cl(2)	94.888(18)	N(1)-Cu(1)-Cl(1)#1	170.04(5)
		N(11)-Cu(1)-Cl(1)#1	92.29(5)
C(2)-N(1)-Cu(1)	128.15(12)	O(31)-Cu(1)-Cl(1)#1	102.57(5)
C(10)-N(1)-Cu(1)	112.22(11)	N(1)-Cu(1)-Cl(1)	94.51(6)
C(9)-N(11)-Cu(1)	107.19(11)	N(11)-Cu(1)-Cl(1)	169.67(6)
C(12)-N(11)-Cu(1)	117.09(12)	O(31)-Cu(1)-Cl(1)	101.47(7)
		Cl(1)#1-Cu(1)-Cl(1)	87.17(3)
		Cu(1)#1-Cl(1)-Cu(1)	92.83(3)
		C(2)-N(1)-Cu(1)	128.81(16)
		C(10)-N(1)-Cu(1)	112.23(14)
		C(9)-N(11)-Cu(1)	108.47(14)
		C(12)-N(11)-Cu(1)	117.68(14)

Table 3.3 *Selected bond lengths (Å) and angles (°) for **36** and **28**.*

Symmetry transformations used to generate equivalent atoms: #1 -x,-y,-z

3.3.2.3 Crystal structures of ligand *N*-(2-hydroxy)benzyl-*N*-8-aminoquinoline and its metal complexes

An ORTEP plot for the ligand **23** is shown in Figure 3.36. It crystallized in the monoclinic crystal system, space group $P2_1/n$. The motif of the five-membered ring observed in previous crystal structures was of course missing, because of the lacking of the metal center. The angle N(11)-C(9)-C(10) is therefore more "open" (120.47°) in comparison with the same angle in the metal complexes.

Figure 3.37 shows an ORTEP plot for the Pd(II) complex **39**. It crystallized in the monoclinic crystal system, space group $P2_1/n$. The coordination of Pd(II) was square planarPd(II), with coordination sites occupied by nitrogen atoms N(1) and N(11) and two chlorides. Phenol –OH group did not participate in coordination. Cu(II) complex **38** was a monomer, it crystallized in the monoclinic crystal system as well as **23** and **39**. Cu(II) center was 5-coordinated with nitrogen atoms N(1) and N(11), oxygen atom O(19) and two chlorides.

The major difference between ligand **23** and the corresponding complexes is the torsion of the benzyl ring in comparison to the rest of the molecule (aminoquinoline part of the molecule). Therefore is the angle C(9)-N(11)-C(12) by the ligand **23** 123.11°, but 112.9° and 112.8 ° in the complexes **38** and **39**.

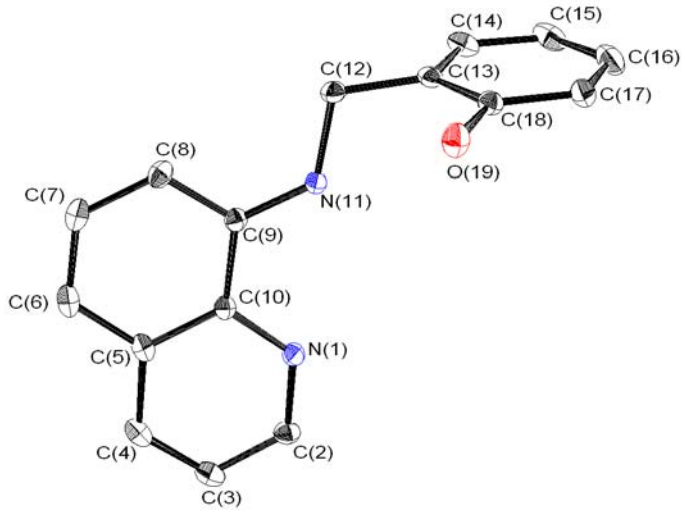

Figure 3.36 *ORTEP plot of the ligand **23** (50% probability). Hydrogen atoms have been omitted for clarity.*

The next interesting point on these crystal structures is the orientation of the –OH group (Figure 3.37; 3.38): when there was a Cu(II) present as a metal center, O(19) was

oriented *towards* this metal center Cu(1). The distance between Cu(1) and O(19) was only 2.326 Å, which means that O(19) did coordinate metal center Cu(1). On the contrary, when the metal center was Pd(II), as in the case of **39**, O(19) *turned away* from the Pd(II)/five-membered ring, giving the distance between Pd(1) and O(19) even 5.243 Å. This was also confirmed by the ^{1}H NMR spectra, where the proton signals H_{14} –H_{17} were shifted downfield.

Intermolecular hydrogen bond interactions in **39** were present between N(11) and Cl(2) of a neighbouring molecule (N····Cl contact was 3.250 Å and 3.258 Å).

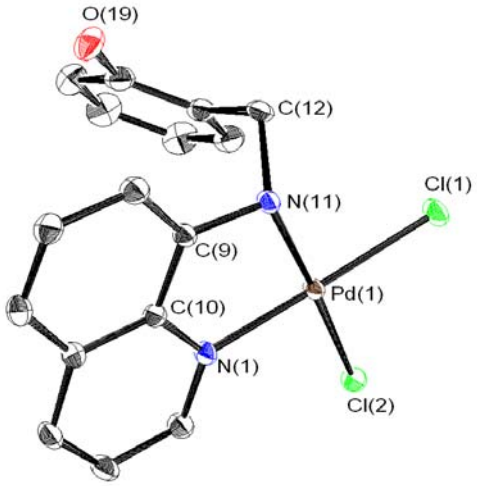

Figure 3.37 *ORTEP plot of monomer **39** (50% probability). Hydrogen atoms have been omitted for clarity*

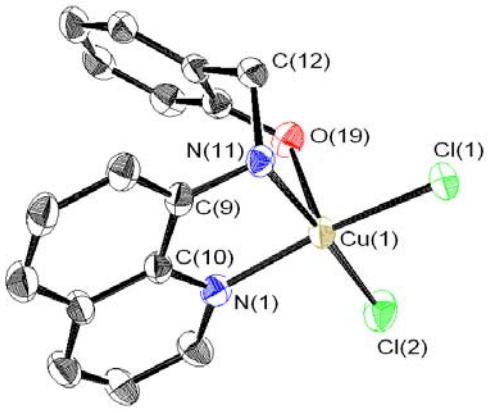

Figure 3.38 *ORTEP plot of monomer **38** (50% probability). Hydrogen atoms have been omitted for clarity.*

Compound 23		Compound 38		Compound 39	
N(1)-C(2)	1.3291(12)	Cu(1)-N(1)	1.999(3)	Pd(1)-N(1)	2.0167(15)
N(1)-C(10)	1.3745(11)	Cu(1)-N(11)	2.041(3)	Pd(1)-N(11)	2.0537(15)
C(9)-N(11)	1.3687(11)	Cu(1)-Cl(2)	2.2640(11)	Pd(1)-Cl(1)	2.3001(5)
N(11)-C(12)	1.4639(11)	Cu(1)-Cl(1)	2.2660(9)	Pd(1)-Cl(2)	2.3137(5)
		Cu(1)-O(19)	2.326(3)		
C(18)-O(19)	1.3689(12)			N(1)-Pd(1)-N(11)	83.47(6)
N(30)-O(31)	1.2317(11)	N(1)-Cu(1)-N(11)	82.90(12)	N(1)-Pd(1)-Cl(1)	173.92(5)
N(30)-O(33)	1.2463(12)	N(1)-Cu(1)-Cl(2)	94.15(9)	N(11)-Pd(1)-Cl(1)	91.46(4)
N(30)-O(32)	1.2752(11)	N(11)-Cu(1)-Cl(2)	177.05(8)	N(1)-Pd(1)-Cl(2)	94.45(5)
		N(1)-Cu(1)-Cl(1)	161.64(9)	N(11)-Pd(1)-Cl(2)	176.75(5)
C(2)-N(1)-C(10)	123.36(8)	N(11)-Cu(1)-Cl(1)	88.71(8)	Cl(1)-Pd(1)-Cl(2)	90.759(17)
N(1)-C(2)-C(3)	120.58(9)	Cl(2)-Cu(1)-Cl(1)	94.08(4)		
N(11)-C(9)-C(8)	122.69(8)	N(1)-Cu(1)-O(19)	94.29(11)	C(2)-N(1)-Pd(1)	127.94(13)
N(11)-C(9)-C(10)	120.47(8)	N(11)-Cu(1)-O(19)	87.30(10)	C(10)-N(1)-Pd(1)	112.82(12)
N(1)-C(10)-C(5)	118.06(8)	Cl(2)-Cu(1)-O(19)	93.05(8)	C(9)-N(11)-Pd(1)	109.00(11)
N(1)-C(10)-C(9)	120.60(8)	Cl(1)-Cu(1)-O(19)	101.63(8)	C(12)-N(11)-Pd(1)	113.93(11)
C(9)-N(11)-C(12)	123.12(8)				
N(11)-C(12)-C(13)	108.18(7)	C(2)-N(1)-Cu(1)	129.9(3)		
		C(10)-N(1)-Cu(1)	113.1(2)		
O(19)-C(18)-C(17)	121.59(9)	C(9)-N(11)-Cu(1)	110.0(2)		
O(19)-C(18)-C(13)	117.91(8)	C(12)-N(11)-Cu(1)	113.0(2)		
O(31)-N(30)-O(33)	122.02(10)	C(18)-O(19)-Cu(1)	117.7(2)		
O(31)-N(30)-O(32)	118.76(9)				
O(33)-N(30)-O(32)	119.21(9)				

Table 3.4 *Selected bond lengths (Å) and angles (°) for 4, 4_{Cu*} and 4_{Pd}. Symmetry transformations used to generate equivalent atoms: #1 -x,-y,-z*

3.4 Hydrolysis of Dipeptides Promoted by Transition Metal Complexes

In hydrolytically active Pd(II) complexes at least two of four coordination sites must be available for the hydrolytic cleavage of the amide bond in peptides[21-25]: one for anchoring to the side chain of the amino acid in the peptide and another one for interaction with the peptide bond to be cleaved. Therefore, two coordination sites should be occupied by a bidentate ligand to forestall additional substitution and hydrolysis equilibria, and other two coordination sites in the complex should be occupied by weak ligands that can be readily replaced.

In order to examine the hydrolysis of the small peptides promoted by the metal complexes, equimolar amounts of a substrate dipeptide (AcHisGly or AcβAlaHis) and one of metal complexes **5 – 18** (Figure 3.39), both dissolved in D_2O, were mixed rapidly in an NMR tube. The solution was 50 mM in each, and the final volume was 550 μl. The hydrolysis of dipeptide was monitored by the following the appearance of the free Gly and the disappearance of the dipeptide by ^{1}H NMR spectroscopy. Acqusition of ^{1}H NMR began as soon as possible, and 48 scans were taken at each time. The temperature was kept at 50^{o}C. The pD value was adjusted to 2.0-3.5 and measured before and after the hydrolysis experiment. The difference was less than 0.10. The methylene signals of free glycine and of peptide-bound glycine were integrated with errors estimated to be +/-5%. In all cases only the amide bond between histidine and glycine was hydrolyzed, not the amide bond to the acetyl group. If this bond had been hydrolyzed, acetic acid would have been formed, what was not detected.

Hydrolysis of AcHisGly by the pD 2.0 – 3.5 at 60^{o}C in a D_2O solution, but in the absence of metal complexes **5 – 18** was less than 10% after 5 days.

3.4.1 Promoters of Hydrolysis

Selective cleavage of peptide bond requires the formation of the complex in which the metal(II) ion can approach the scissile amide bond. Binding of the structurally simple Pd(II) complexes, such as $(PdCl_4)^{2-}$ or analogues aqua Pd(II) complex, $Pd(en)Cl_2$ and corresponding aqua complexes etc, has been studied in some laboratories[17, 18, 31, 32, 118-120].

We examined the influence of rigidness and different structures of ligands on the formation of the corresponding metal complexes and their role as peptidases. Ligands **2** and **3** contain the pyridine ring substituted at the 2-position leaving a two carbon atoms spacer between the aromatic amine and the aliphatic amine. This permits a structurally preferred N_2O square planar bipyrimidal complexation to form with M^{2+} ions. Ligand **4** contains also the pyridine ring substituted at the 2-position, but leaving only one carbon spacer between the aromatic and aliphatic amine bounded directly to phenyl ring. Metal complexes **5-18** were chosen in peptide hydrolysis experimetns as the promoters for the cleavage of the amide bond (Figure 3.39).

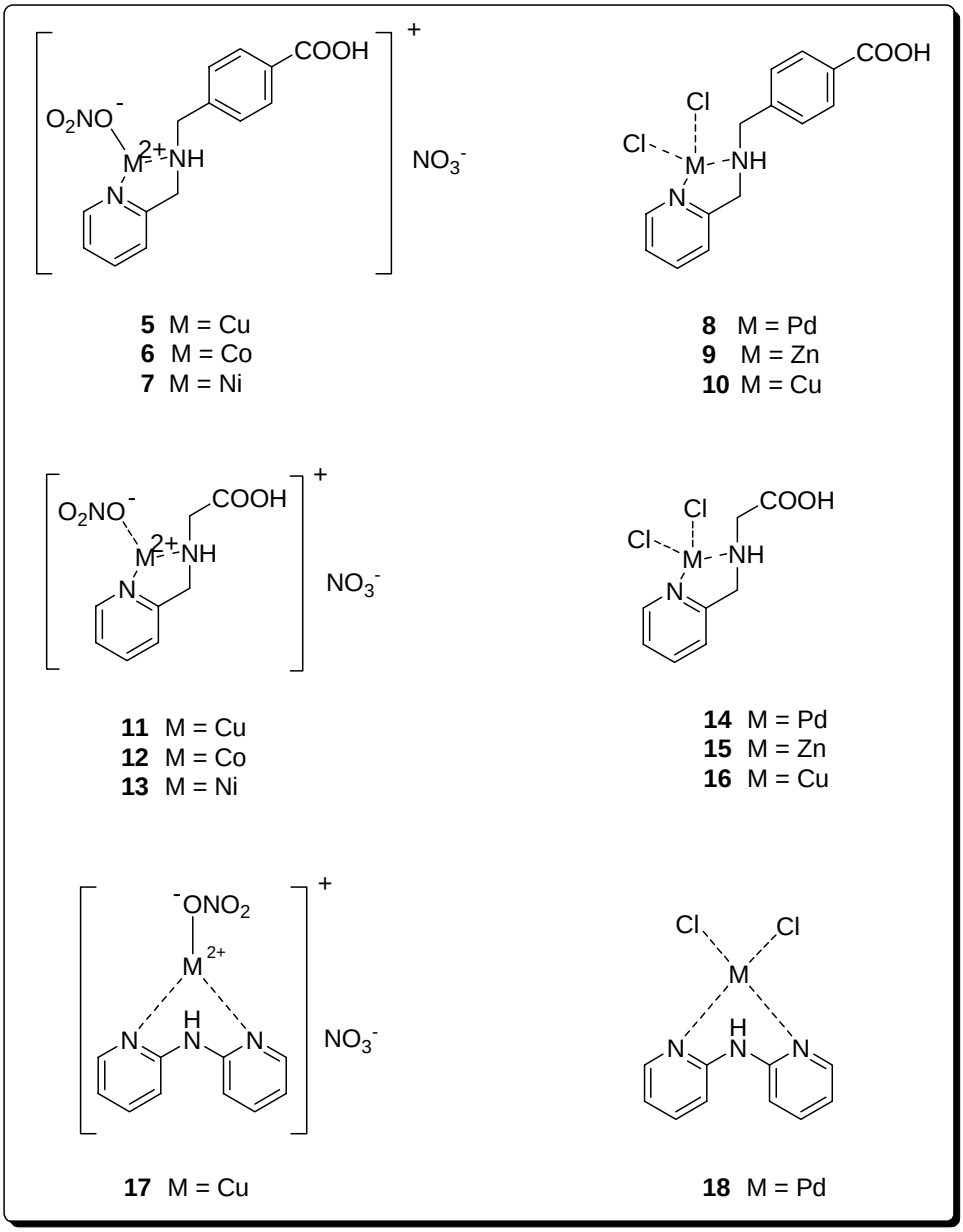

Figure 3.39 *Metal complexes as promoters of peptide hydrolysis experiments.*

3.4.2 Substrates of Hydrolysis

Histidine is commonly found as a ligand to the metal ions in metalloenzymes. The imidazole ring of histidine possesses two nitrogen atoms (N-1 and N-3), which can participate in metal binding, as well as become protonated. As a result, histidine can take on various metal-bound and protonated forms. Because of myriad of forms histidine is capable of adopting, it is not surprising that it often functions as a versatile ligand that is directly involved in the catalytic reactions.

Dipeptides HisGly and βAlaHis (Carnosine), as the substrates for the amide bond cleavage study, containe imidazol ring in the side chain of histidine (Figure 3.40).

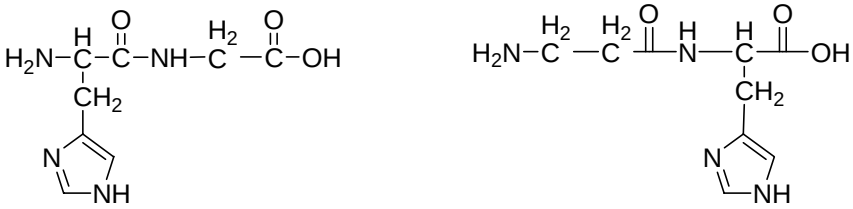

HisGly βAlaHis

Figure3.40 *Dipeptides HisGly and βAlaHis, as the substrates of hydrolysis.*

This is the anchoring side chain for the transition metal complexes, which rapidly displaces one ligand in the complexes to form substrate-promoter complexes. When a peptide, such as HisGly, containing unprotected *N*-terminal histidine residue binds to the transition metal complex, the anchored metal (II) ion displaces a proton from the terminal amino group and binds to the peptide via the terminal amino group and imidazol ring of the side chain of histidine. The resulting complex is hydrolytically inactive (Scheme 3.16), because the amidate groups coordinated to the Pd(II) ion are actually protected by this coordination against hydrolytic cleavage, and because other amide groups cannot approach the Pd(II) ion[21, 121].

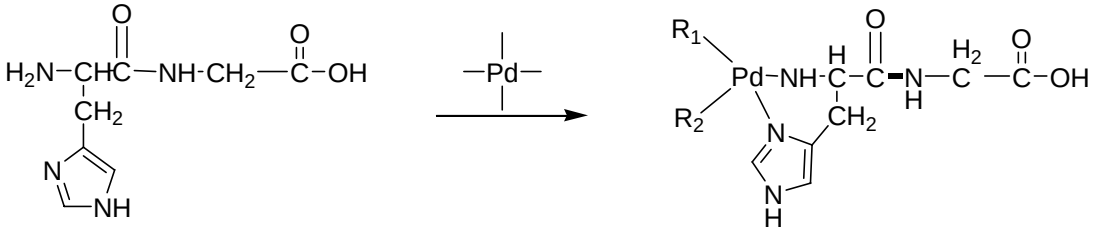

HisGly bidentate

Scheme 3.16 *Formation of hydrolytically inactive complex on the N-terminus of unprotected dipeptide.*

Similiary, when the anchoring side chain is the second residue, such as β-AlaHis, a very stable tridentate complex is formed between peptide and Pd(II) complex, where Pd(II) ion is unable to approach the amide bond.

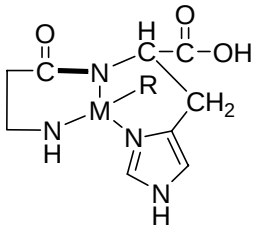

tridentate

Figure 3.41 *Structure of the hydrolytic inactive tridentate complex.*

To prevent formation of such a hydrolytically inactive promoter-substrate complexes, terminal amino group of both dipeptides was protected through acetylation of HisGly and Carnosine with acetic anhydride in glacial acetic acid (Scheme 3.17). Only then Pd(II) complexes coordinate the peptide in such a way that the Pd(II) reagent can approach the scissile peptide bond and activate it towards hydrolysis.

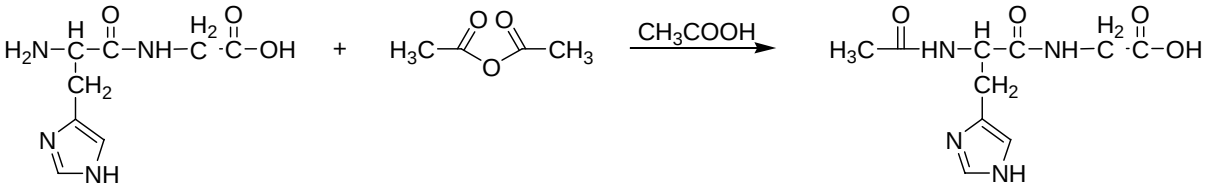

HisGly AcHisGly

Scheme 3.17 *Protection of N-terminal amino group of HisGly through acetylation.*

In the first dipeptide AcHisGly, anchoring side chain of histidine is placed on the position 1, while Gly is chosen for simplicity. βAlaHis (carnosine) is the naturally occuring dipeptide found in relatively high concentrations in body tissues – heart muscle, skeletal muscle and brain, acting as an antioxidant promoting wound healing[122]. In this acetylated dipeptide AcβAlaHis, imidazol ring of the side chain is placed on the position 2, acting as an anchor for transition metal complexes.

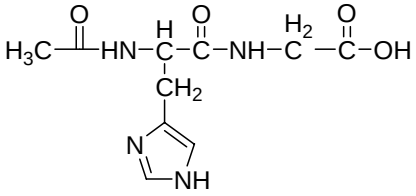

AcHisGly

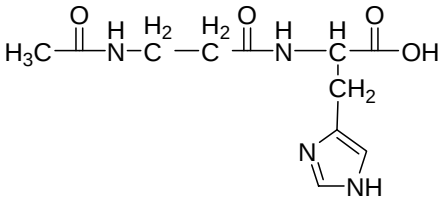

AcβAlaHis

Figure 3.42 *Dipeptides used for hydrolysis.*

3.4.3 Hydrolytic Cleavage of Peptide Bond

The subject of this study is hydrolytic cleavage of the dipeptides AcHisGly and AcβAlaHis promoted with a series of the new synthesized transition metal complexes **5 – 18**. After the reaction, in the case of AcHisGly, we expected *N*-acetylhistidine and the free glycine as the major products (Scheme 3.18).

However, in the reaction of the acetylated carnosine (AcβAlaHis) with complexes **5 – 18** we did not expect hydrolytic cleavage because the anchoring side chain of histidine is placed on the position 2. As reported before[31, 32] in the hydrolysis of dipeptides with Pd(II) complexes only the first amide bond downstream could be cleaved and not the amide bond upstream, in this case His-Gly or Ala-His bond.

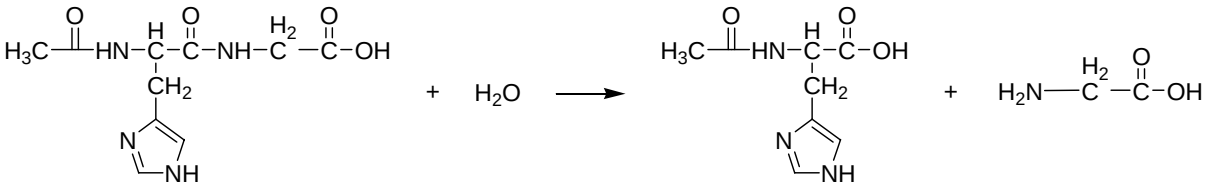

AcHisGly AcHis free Gly

Scheme 3.18 *Hydrolytic cleavage of AcHisGly into N-acetylhistidine and free Gly.*

After the synthesis of the transition metal complexes **5 – 18** and their full characterization, equimolar amounts of those complexes and AcHisGly were mixed in the NMR tube. pH was adjusted by the addition of $DClO_4$ having $2.5 < pH < 2.9$.

When some transition metal complexes **5 – 18** mixed with AcHisGly in this manner, already after 15 minutes five NMR-detectable substrate-promoter complexes spontaneously formed, analog to the reported one[31].

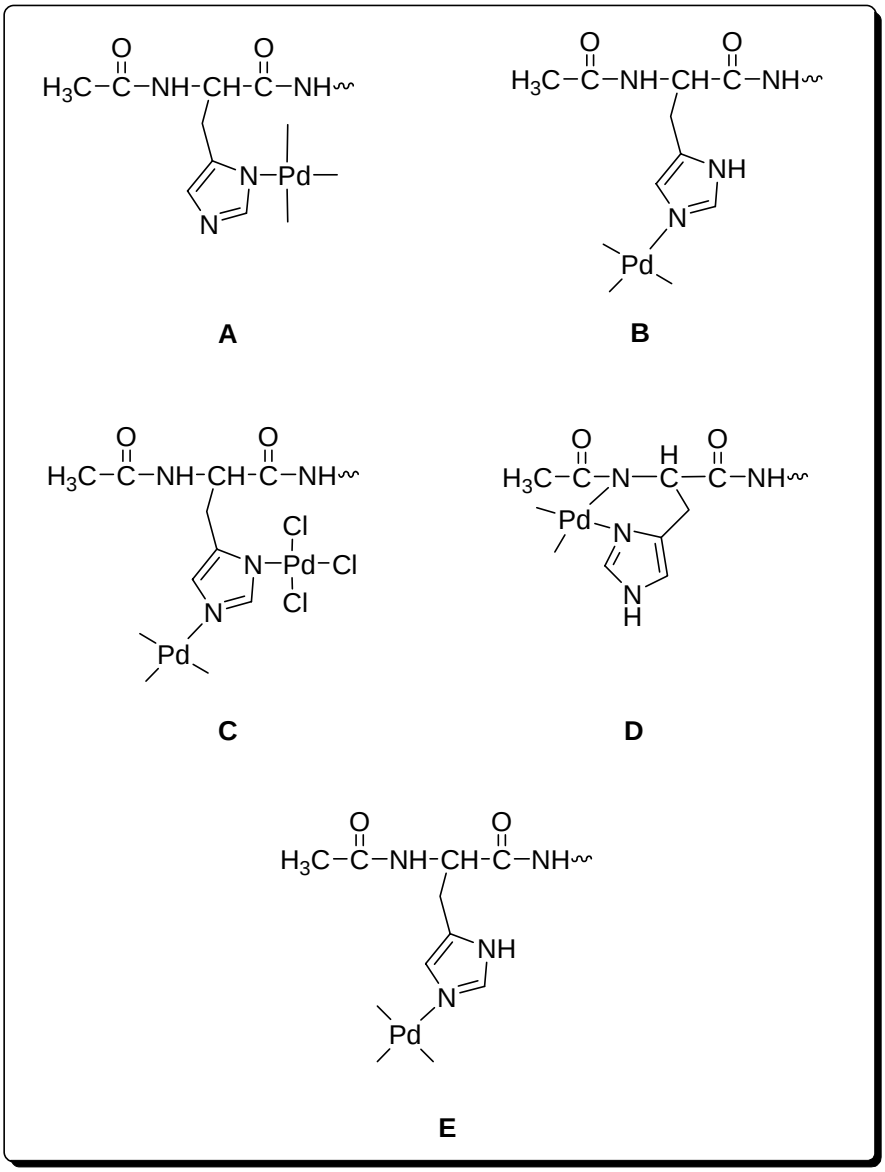

Figure 3.43 *Substrate – catalyst complexes **A**-**E** formed after ca 15 min.*

Their composition is shown on Figure 3.43 and their characteristic ^{1}H NMR resonances on Figure 3.44.

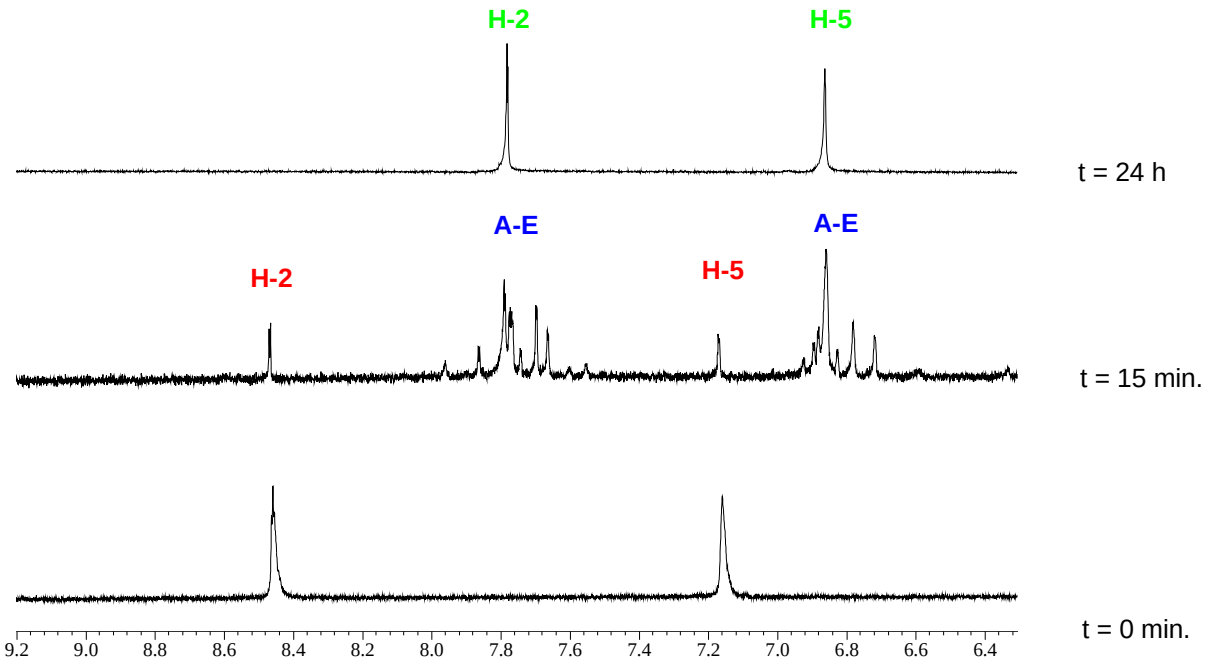

Figure 3.44 *^{1}H NMR spectra of a soultion in D_2O at pD 2.06 (red:AcHis in the uncoordinated dipeptide; blue. substrate-promoter complexes; green: free AcHis) .*

The five complexes can be distinguished on the basis of the chemical shifts of the two imidazole protons, H-2 and H-5. Their respective values in the uncoordinated dipeptides AcHisGly are 8.47 and 7.18 ppm at pD 2.06. The two major complexes are linkage isomers of each other, corresponding to two tautomers of the imidazole ring in histidine.

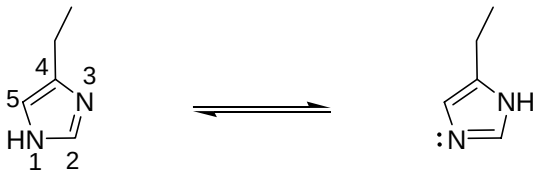

Scheme 3.19 *Tautomers of the imidazol ring in the side chain of histidine.*

In the complex **A**, unidentate coordination via the N-3 atom moves the H-2 and H-5 resonances to 7.80 and 6.87 ppm, respectively. In the complex **B**, unidentate coordination via the N-1 atom moves these resonances to 7.78 and 6.84 ppm, respectively.

The three minor complexes contain more than one palladium(II) atom per dipeptide or involve more than one donor atom in the dipeptide. The deprotonated imidazole (imidazolate anion) in the complex **C** bridges two Pd(II) atoms. This is fairly common mode of imidazole

binding, because coordination of the first nitrogen atom facilitates deprotonation, and subsequent coordination, of the other.

In the complex **D**, the substrate coordinates to Pd(II) as a bidentate ligand, via the N-3 atom of imidazole and the nitrogen atom of the acetylated amino group. The H-5 resonance occured at 6.84, as found also in a previous study[123].

In the complex **E**, coordination occured via the N-1 atom of imidazole and the carboxylate group. The experiments of another lab[32] with *N*-acetyl-3-methylhistidine giving the complex **E** in the reaction with Pd(II) complex, established that the N-3 atom of imidazole is indeed not involved. The N-1 atom and the carboxylate group probably coordinate to two Pd(II) atoms, and such binuclear complexes are well known[124, 125].

After a few hours a new signal of the methylene group of the free glycine at 3.67 ppm was monitored, suggesting the beginning of the hydrolytic cleavage of the amide bond between histidine and glycine. The cleavage was further easily monitored by following the ^{1}H NMR resonances of the free glycine signal during next few days, as shown on the Figure 3.45.

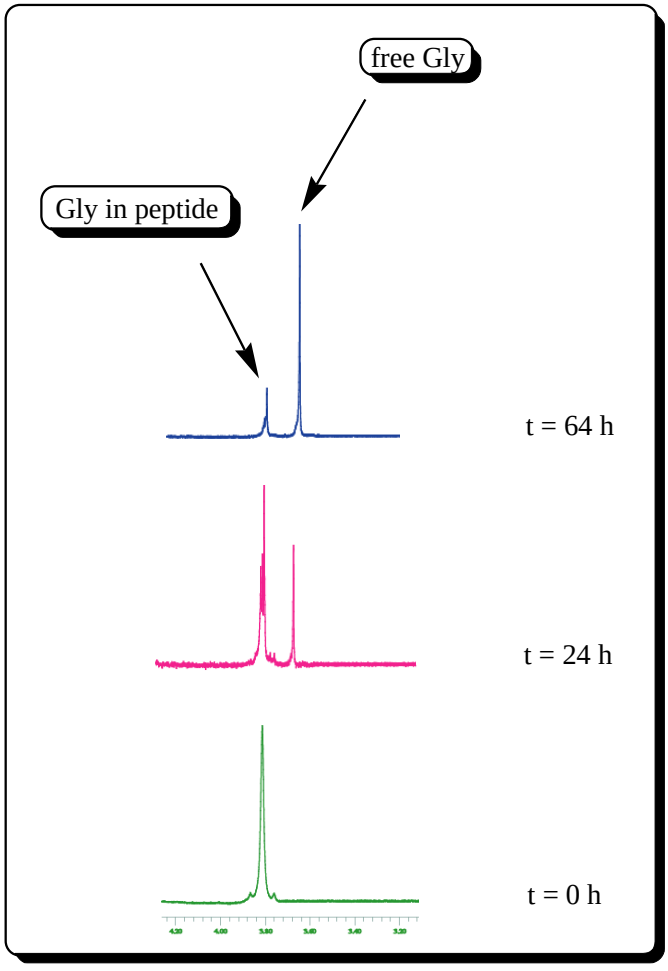

Figure 3.45 *^{1}H NMR spectra of solution AcHisGly and **14** in D_2O, at pH 2.9 and 60°C: Gly CH_2 resonances in AcHisGly (3.81 ppm) and in free Gly (3.51 ppm).*

In particulare, the best cleavage results were obtained with compounds **14**, **8** – both palladium complexes, and copper complex **17** of dipyridyl amine.

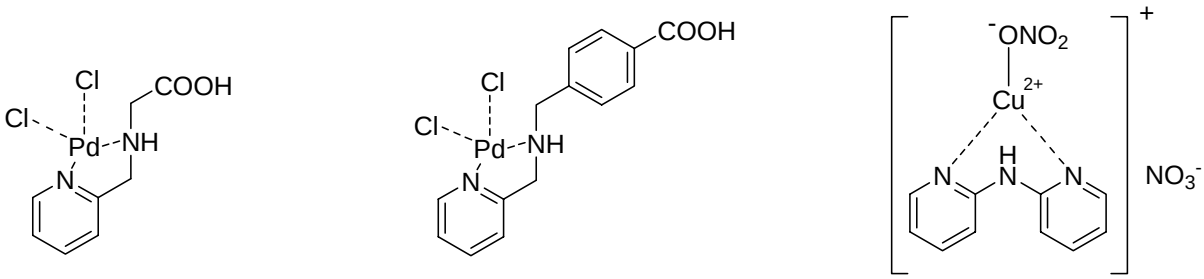

14 **8** **17**

Figure 3.46 *Pd(II) complexes **14** and **8**, and Cu(II) complex **17** showed the best result in the cleavage of the peptide bond.*

As we can see from the Figure 3.47 the background hydrolysis (hydrolysis of AcHisGly under the same conditions, but in the absence of metal complexes **5 – 18**) was less than 10% complete after 5 days. It means that metal complexes, not the acidic solvent, are responsible for the hydrolytic cleavage.

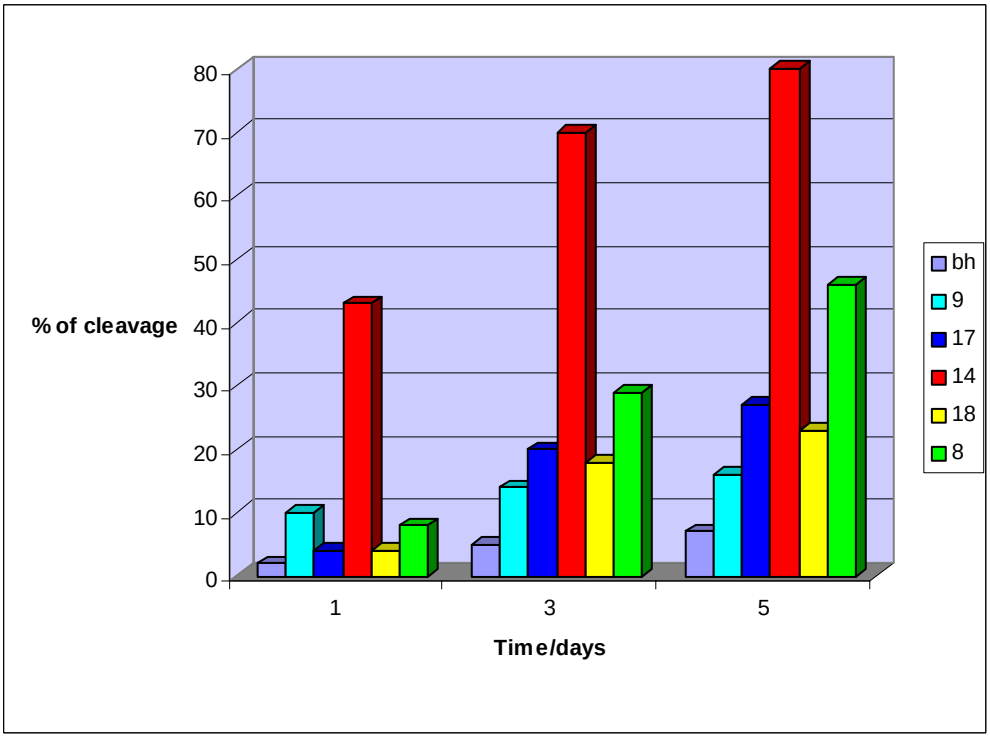

Figure 3.47 *Hydrolysis of the peptide AcHisGly with the compounds **9**, **17**, **14**, **18** and **8** during 5 days at 60°C and pH 2.9 (bh: background hydrolysis).*

The best result showed palladium(II) complex **14**: *almost 80% of the peptide was cleaved after 5 days*. This complex cleaved more than 40% of AcHisGly already after one day and almost 70% after 3 days. Disappearance of AcHisGly can be expressed in the form $v\mathrm{A} = k_{obs}\,[\mathrm{A}]^{\alpha}$, where v represents rate of reaction. The proportionality factor k_{obs} deduced from such an experiment is called the "observed rate coefficient". It was obtained as the slope of the ln plot using the linear region of the graph (2.34×10^{-2} h^{-1}). The initital rate was calculated using k_{obs} and found to be 8.21×10^{-4} $mM^{-1}h^{-1}$. A typical time course and the ln plot of c_0/c_t (c_0 and c_t denote the concentration of dipeptide at time 0 and t) versus time are shown in Figure 3.48.

a)

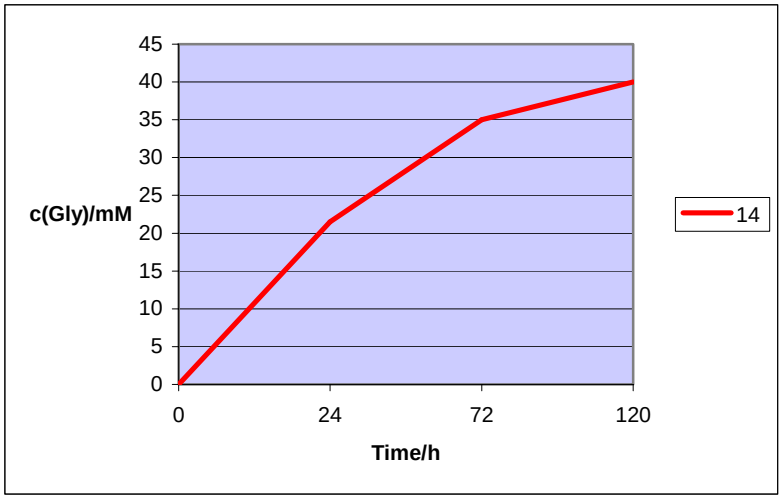

b)

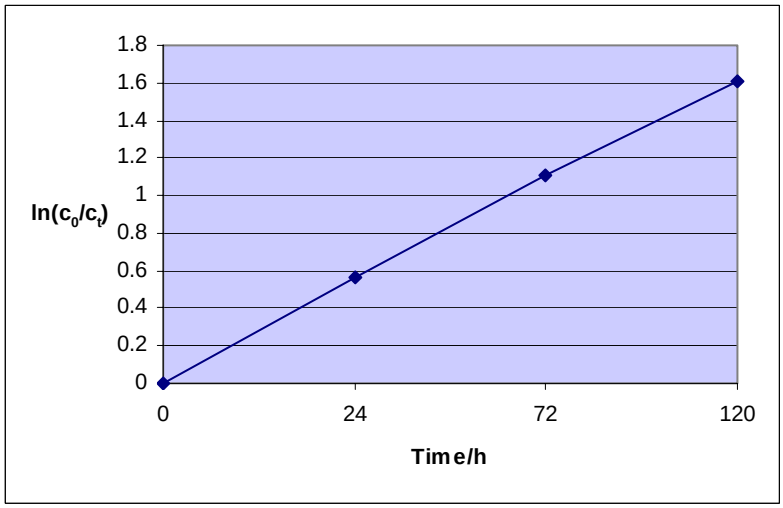

Figure 3.48 *a) Time course for the hydrolysis of AcHisGly promoted by the Pd(II) complex **14**: the concentration of free Gly as a function of time; b) ln plot for the hydrolysis of dipeptides with the compound **14**. c_0 and c_t denote the concentration of dipeptide at time 0* and t, respectively.

In this study we expected the best results from the metal complexes of the ligand **2**, because its "pocket" for the palladium(II) atom consists of the pyridine nitrogen and the nitrogen atom from the aliphatic chain on the position 2 of the pyridine ring. There is no other rigid bulky part which could disturbe approach of the metal complex to the scissile amide bond. Two other coordination sites of the palladium(II) in this complex were completed by two chlorides, which showed that not only complexes containing aqua ligands can promote a hydrolysis of the amide bond, as reported before[29-32]. The scissile amide bond is activated toward external attack by solvent water molecules by the *N*-imidazol ring, M, O chelate formation, where metal(II) atom acts as a Lewis acid.

Next best cleavage result showed palladium(II) complex **8**, which cleaved almost 50% of the same dipeptide after 5 days under the same conditions. Copper(II) complex **17** surprisingly showed its peptidase activity with almost 30% of the cleaved peptide after 5 days. In all cases the cleavage occurred only on the His-Gly bond; we did not detect acetic acid, which would be the product of the cleavage of the acetyl-histidine bond.

As an additional control experiment, we made the studies with acetylated carnosine, where the carboxylic group of histidine is free and amino group forms a genuine peptide bond. As previously described on the peptide AcHisGly, equimolar amounts of transition metal complexes **5-18** and AcAlaHis were mixed in the NMR tube under usual conditions. Even after one week we did not observe any hydrolytic cleavage.

a)

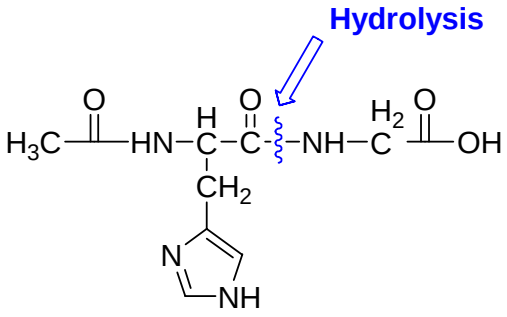

b)

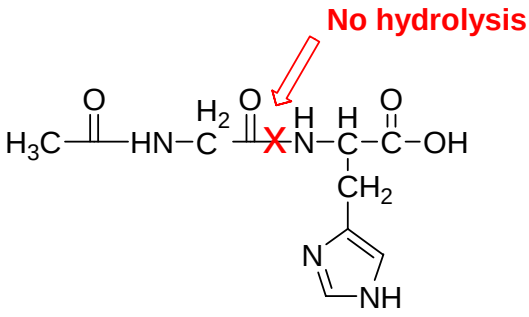

Scheme 3.20 *a) Hydrolysis of the peptide bond possible only when it is on the carboxylic side of the histidine residue; b) when the peptide bond is on the N-terminus of the anchoring histidine residue, no hydrolytic cleavage observed.*

This result suggested (Scheme 3.20) that *the scissile bond on the carboxylic side of the anchoring histidine residue is necessary for hydrolysis: when there is no scissile bond on that position, there is also no hydrolysis.* This statemet is in agreement with studies reported for some other palladium(II)complexes[31, 32].

4

Experimental Section

4.1 General Remarks

Chemicals. The solvents and NMR spectroscopic standards D_2O, DMSO-d_6, $DClO_4$, $CDCl_3$, TMS, TSPSA, as well as Pd(II), Ni(II), Zn(II), Co(II), Cu(II) and Cd(II) salts were purchased from Aldrich and used as received. Dipyridyl amine as ligand **4** and 8-aminoquinoline as ligand **19** were also purchased from Aldrich, but because of importance of their spectroscopical characterization in comparison with some other ligands, their data will be listed in this chapter as well as all other ligands synthesized in the lab. All common chemicals were of reagent grade. The amino acids and dipeptides were obtained from NovaBiochem or from Iris Biotech.

Measurements. NMR spectra, in D_2O or DMSO solution and with TSPSA or TMS as an internal standard, were recorded with a Bruker AM 360 spectrometer (^1H at 360 MHz and ^{13}C at 95.56 MHz). Individual peaks are marked as: singlet (s), doublet (d), triplet (t) and multiplet (m).

Mass spectra were recorded with Mat 8200 instrument for FAB-MS (glycerin or 3-NBA matrix) or on a Finnigan TSQ 700 for ESI-MS. Only characteristic fragments are given and the possible composition of the peaks is between brackets.

Elemental analyses were performed on a Foss Heraeus Vario EL Elementar Analysator in C, H, N mode.

The pH was measured with a membrane pH meter HI 8314 Hanna instrument (pH electrode Orion 98-26). The pD values were calculated by the standard formula pD = pH + 0.4.

X-ray crystallography. Intensity data were collected by Dr. Thomas Weyhermüller, Max-Planck Institute for Bioinorganic Chemistry, Mülheim an der Ruhr, Germany, on either a Siemens SMART CCD diffractometer or on Enraf-Nonius Kappa CCD diffractometer equipped with a Mo-target rotating anode by using Mo-Kα radiation (λ = 0.71073 Å). All crystals were grown in MeOH, picked up with glass fibers and mounted in the nitrogen cold stream of the diffractometer operating at 100K. The data were corrected for semiempirical absorption and Lorentz polarisation effects.

The structures were solved by direct and Patterson methods and refined by full-matrix least-squares on F^2 using the ShelXTL and ShelXL97 software package. All nonhydrogen atoms were refined anisotropically and all hydrogen atoms were refined isotropically in idealized positions.

Substrates for Hydrolysis. Dipeptides Histidineglycine (HisGly) and β-alanyl-L-histidine - carnosine (βAlaHis) were obtained from NovaBiochem. The peptides *N*-Acetylhistidineglycine (AcHisGly) and Acetyl-β-Alanyl-L-histidine (AcβAlaHis) were obtained by adding acetic anhydride (64.8 μl; 0.7 mmol) to a stirred solution of HisGly (150 mg; 0.7 mmol) or βAlaHis in 1.76 ml glacial acetic acid, respectively. The reaction mixtures were stirred for 3 h at room temperature. After evaporation of the solvent *in vacuo* a white powder left.

Background cleavage. Solution of dipeptide was prepared as discrebed above except that the metal complexes were missing. The solvent was always D_2O and pH value was adjusted with $DClO_4$ or NaOD. The solutions were kept at 50°C and occasionally examined by ^1H NMR spectroscopy. Over 5 days less than 10% of AcHisGly at pH 2.0 hydrolyzed.

Study of Hydrolysis. Equimolar amounts of a substrate and of metal complex, both dissolved in D_2O, were mixed rapidly in an NMR tube: The solution was 50 mM in each, and the final volume was 550 μl. Acqusition of ^1H NMR began as soon as possible, and 48 scans were taken at each time. The temperature was kept at 50°C. The pH value was adjusted by $DClO_4$ and measured before and after the hydrolysis experiment. The difference was less than 0.10. The methylene signals of free glycine and of peptide-bound glycine were integrated with errors estimated at +/-5%.

Hydrolysis Product. As one of the hydrolysis products, free glycine was identified by ^1H NMR spectroscopy and by thin-layer chromatography. Addition of pure glycine into the reaction mixture enhanced the ^1H NMR signal of the hydrolysis product. No new signal appeared. The metal complex was precipitated out from the reaction mixture by addition of diethyldithiocarbamate, filtered and the filtrate was chromatographed on silica gel with a mixture of 1-butanol, acetic acid and water in the volume ratio 40:6:15 and developed with a solution containing ninhydrin in a mixture of glacial acitic acid and 1-butanol. R_f = 0.202.

4.2 Numbering of the Ligands

***N*-(4-carboxymethyl)benzyl-*N*-(2-picolyl)amine 1.**

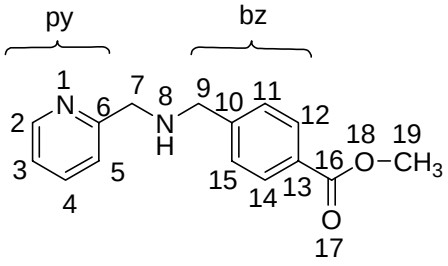

***N*-4-benzylic acid-*N*-2-picolylamine 2.**

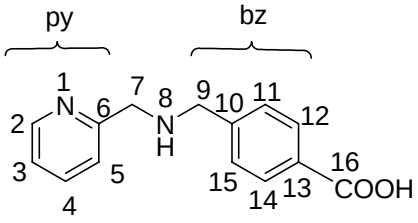

***N*-(2-pyridylmethyl)aminoacetate 3**.

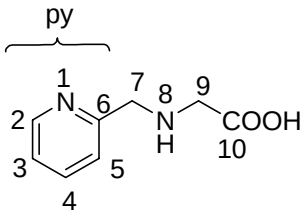

Dipyridyl amine 4.

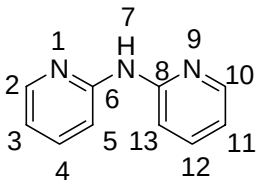

8-aminoquinoline.

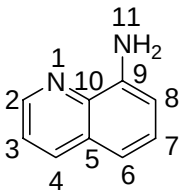

***N*-acetic acid-*N*-8-aminoquinoline 20.**

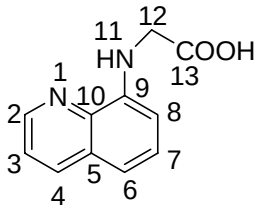

***N*-(4-carboxymethyl)benzyl-*N*-8-aminoquinoline 21.**

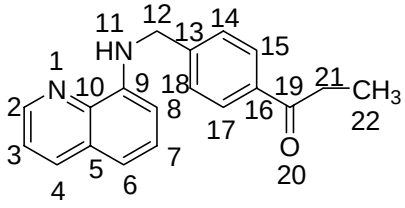

***N*-(2-hydroxy)benzyl-*N*-8-aminoquinoline 23**.

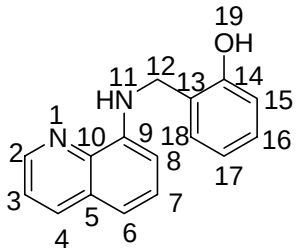

4.3 Derivatives of 2-Picolylamine

4.3.1 Ligands of 2-Picolylamine Derivatives

***N*-(4-carboxymethyl)benzyl-*N*-(2-picolyl)amine 1.** To a solution of 2-picolylamine (1.08 ml;10 mmol) and α-bromo-toluic acid methyl ester (1.15 g; 5 mmol) in THF (40 ml), NEt_3 (1.4 ml; 10 mmol) was added and the reaction mixture was refluxed for 2 hours. After cooling to room temperature, solution was filtered to remove a white precipitation. After removal of the solvent under reduced pressure, the orange/brown oily residue was purified with coloumn chromatography ($CHCl_3$: MeOH : EtOAc, 5 : 5 : 2).

$C_{15}H_{16}N_2O_2$; exact mass: 256.12.

^{1}H NMR (360 MHz, DMSO-d_6): δ (ppm) 8.47 (d, 1H, H_{py-2}), 7.82 (d, 2H, $H_{bz-12, 14}$), 7.74 (t, 1H, H_{py-4}), 7.46 (d, 1H, H_{py-5}), 7.32 (d, 2H, $H_{bz-11, 15}$), 7.24 (t, 1H, H_{py-3}), 3. 77 (s, 2H, H_7), 3.73 (s, 2H, H_9), 2.11 (s, 3H, H_{19}).

^{13}C NMR (90 MHz, DMSO-d_6): δ (ppm) 167.1 (C_{16}), 159.5 (C_{py-6}), 149.4 (C_{py}), 145.5 (C_{bz-10}), 136.4 (C_{py}), 129.7 (C_{bz}), 128.8 (C_{bz-13}), 128.1 (C_{bz}), 122.3 (C_{py}), 54.5 (C_7), 53.1 (C_9), 52.0 (C_{19}).

MS (FAB, 3-NBA): *m/z* 257 $[M + H]^+$.

***N*-4-benzylic acid-*N*-2-picolylamine 2.** To a solution of **1** in MeOH (12 ml) was added a solution of NaOH (0.2 g; 5 mmol) in H_2O (1.68 ml) and the reaction mixture was stirred for 2.5 hours at room temperature. The pH was adjusted to 7 by dropwise addition of 1M HCl, followed by removal of the solvent under reduced pressure. To the brown sticky residue CH_3CN (10 ml) was added, followed by vigorous stirring. After 30 minutes a white precipitate obtained. The solution was stored at 0^oC for 1 hour to affect precipitation and the white product was isolated by filtration.

$C_{14}H_{14}N_2O_2$; exact mass: 242.11.

^{1}H NMR (360 MHz, DMSO-d_6): δ (ppm) 8.47 (d, 1H, H_{py-2}), 7.85 (d, 2H, $H_{bz-12, 14}$), 7.75 (t, 1H, H_{py-4}), 7.45 (d, 1H, H_{py-5}), 7.34 (d, 2H, $H_{bz-11, 15}$), 7.24 (t, 1H, H_{py-3}), 3.78 (s, 2H, H_7), 3.75 (s, 2H, H_9).

^{13}C NMR (90 MHz, DMSO-d_6): δ (ppm) 174.7 (C_{16}), 157.6 (C_{py-6}), 150.0 (C_{py}), 140.0 (C_{bz-10}), 138.7 (C_{py}), 138.4 (C_{bz-13}), 130.6 (C_{bz}), 129.4 (C_{bz}), 124.1 (C_{py}), 53.4 (C_7), 52.9 (C_9).
MS (FAB, 3-NBA): *m/z* 243 $[M + H]^+$.

***N*-(2-pyridylmethyl)aminoacetate 3**. 2-Picolylamine (5.9 g; 55.0 mmol) was diluted with an aqueous solution of NaOH (0.55 g in 5 ml H2O) and mixture was heated to 60°C. Bromoacetic acid (1.29 g; 13.6 mmol), neutralised with the same aqueous solution of NaOH, was slowly added to the amine over 1 hour. After 4 hours the solvent was removed under reduced pressure and a solid was washed with diethylether. The residual solid was dried and isolated as an orange solid.

$C_8H_{10}N_2O_2$; exact mass: 166.07.
^{1}H NMR (360 MHz, DMSO): δ (ppm) 8.35 (d, 1H, H_{py-2}), 7.72 (t, 1H, H_{py-4}), 7.31 (d, 1H, H_{py-5}), 7.24 (t, 1H, H_{py-3}), 3.87 (s, 2H, H_7), 3.22 (s, 2H, H_9).
^{13}C NMR (90 MHz, DMSO-d_6): δ (ppm) 173.7 (C_{10}), 161.6 (C_{py-6}), 149.3 (C_{py-2}), 136.9 ($C_{py-3,}$ C_{py-4}), 123.1 (C_{py-5}), 53.9 (C_7), 52.6 (C_9).
MS (ESI): *m/z* 198 $[LOCH_3]^+$, 189 $[L + Na]^+$, 167 $[M + H]^+$.

Dipyridyl amine 4. Commercially available from Aldrich and used as received.

$C_{10}H_9N_3$; exact mass: 171.08.
^{1}H NMR (360 MHz, DMSO): δ (ppm) 9.63 (s, 1H, H_7), 8.20 (d, 2H, $H_{2, 10}$), 7.74 (d, 2H, $H_{5, 13}$), 7.63 (t, 2H, $H_{3, 11}$), 6.84 (t, 2H, $H_{4, 12}$).
MS (FAB): *m/z* 172 $[M + H]^+$.

4.3.2 Metal Complexes of 2-Picolylamine Derivatives

General procedure. The ligands **2**, **3** or **4** (0.25 mmol) were dissolved in methanol (5 ml) in a beaker, heated to boiling and poured to the boiling solution of corresponding metal chloride/nitrate (0.25 mmol) in methanol (5 ml). The reaction mixture was filtered and allowed to cool to room temperature. After standing overnight at room temperature and few days on the 7^{o}C, the precipitated product was collected by filtration and dried in air.

Complexes of the ligand 2.

[LCu(NO$_3$)]NO$_3$, **5.** Copper(II) nitrate trihydrate was used (60.4 mg; 0.25 mmol). Tyrkiz coloured powder obtained, yield 55%.

MS (FAB, 3-NBA): *m/z* 367 $[LCuNO_3]^+$, 305 $[LCu]^+$.

MS (ESI): *m/z* 383 $[LCu + DMSO]^+$, 344 $[LCu + K]^+$, 305 $[LCu]^+$.

[LCo(NO$_3$)]NO$_3$, **6.** Cobalt(II) nitrate hexahydrate was used (72.8 mg; 0.25 mmol). Violet crystals obtained, yield 42%.

MS (ESI): *m/z* 378 $[LCo + DMSO]^+$, 339 $[LCo + K]^+$, 300 $[LCo]^+$.

[LNi(NO$_3$)]NO$_3$, **7.** Nickel(II) nitrate hexahydrate was used (72.7 mg; 0.25 mmol). Green crystals, yield 50%.

MS (ESI): *m/z* 338 $[LNi + K]^+$, 299 $[LNi]^+$.

[LPdCl)]Cl, **8.** Sodium tetrachloropalladate was used (70 mg; 0.25 mmol). Orange powder obtained, yield 52%.

^{1}H NMR (360 MHz, DMSO-d$_6$): δ (ppm) 8.62 (d, 1H, H_{py-2}), 7.95 (t, 1H, H_{py-4}), 7.86 (d, 2H, $H_{bz-12, 14}$), 7.72 (d, 2H, $H_{bz-11, 15}$), 7.52 (d, 1H, H_{py-5}), 7.40 (t, 1H, H_{py-3}), 4.19 (m, 2H, H_7), 4.06 (m, 2H, H_9).

^{13}C NMR (90 MHz, DMSO-d$_6$): δ (ppm) 166.8 (C_{16}), 163.3 (C_{py-6}), 148.5 (C_{py}), 139.7 (C_{py}), 139.3 (C_{bz-10}), 130.5 (C_{bz-13}), 130.4 (C_{bz}), 129.2 (C_{bz}), 123.6 (C_{py}), 122.0 (C_{py}), 57.9 (C_7), 55.7 (C_9).

MS (FAB): *m/z* 347 $[LPd]^+$.

MS (ESI): *m/z* 541 $[M +2Na + DMSO]^+$, 463 $[M+ 2Na]^+$.

[LZnCl)]Cl, **9.** Zinc chloride (34.0 mg; 0.25 mmol) was used. After standing for few days in the fridge, colourless crystals formed, that were suitable for X-ray crystallography. Yield 56%. Table 4.1.

^{1}H NMR (360 MHz, DMSO-d_6): δ (ppm) 8.66 (d, 1H, H_{py-2}), 8.06 (t, 1H, H_{py-4}), 7.58 (d, 1H, H_{py-5}), 7.37 (t, 1H, H_{py-3}), 4.12 (m, 2H, H_7), 3.90 (m, 2H, H_9).

^{1}H NMR (360 MHz, D_2O): δ (ppm) 8.62 (d, 1H, H_{py-2}), 8.13 (t, 1H, H_{py-4}), 7.98 (d, 2H, $H_{bz-12, 14}$), 7.70 (d, 2H, $H_{bz-11, 15}$), 7.65 (t, 1H, H_{py-3}), 7.53 (d, 1H, H_{py-5}), 4.44 (s, 2H, H_7), 4.34 (s, 2H, H_9).

MS (FAB): *m/z* 307 $[LNi]^+$.

Elemental analysis: calc. C 48.15, H 4.58, N 7.49; found C 46.17, H 4.28, N 7.65%.

[LCuCl)]Cl, **10.** Copper(II) chloride trihydrate was used (47.1 mg; 0.25 mmol). Green crystals, suitable for X-ray crystallography, formed during slow evaporation of the reaction mixture. Yield 52%. Table 4.1.

Complexes of the ligand 3.

[LCu(NO_3)]NO_3, **11.** Copper(II) nitrate trihydrate was used (60.4 mg; 0.25 mmol). Blue/green powder obtained, yield 54%.

MS (ESI): *m/z* 306 $[LCu + DMSO]^+$, 260 $[LCuOCH_3]^+$, 228 $[LCu]^+$.

[LCo(NO_3)]NO_3, **12.** Cobalt(II) nitrate hexahydrate was used (72.8 mg; 0.25 mmol). Dark purple powder obtained, yield 46%.

MS (ESI): *m/z* 389 $[LCoL]^+$.

[LZn(NO_3)]NO_3, **13.** Zinc(II) nitrate hexahydrate was used (72.8 mg; 0.25 mmol). Colourless crystals obtained, yield 55%.

MS (ESI): *m/z* 393 $[LZnL]^+$, 291 $[LZn]^+$.

[LPdCl)]Cl, **14.** Sodium tetrachloropalladate was used (70 mg; 0.25 mmol). Dark orange powder obtained, yield 51%.

^{1}H NMR (360 MHz, DMSO-d_6): δ (ppm) 8.21 (d, 1H, H_{py-2}), 7.81 (t, 1H, H_{py-4}), 7.35 (d, 1H, H_{py-5}), 7.27 (t, 1H, H_{py-3}), 3.85 (m, 2H, H_7), 3.71 (m, 2H, H_9).

^{13}C NMR (90 MHz, DMSO-d_6): δ (ppm) 180.6 (C_{10}), 164.2 (C_{py-6}), 149.8 (C_{py-2}), 140.3, 124.4 ($C_{py-3,}$ C_{py-4}), 122.0 (C_{py-5}), 53.9 (C_7), 52.6 (C_9).

MS (ESI): *m/z* 331 [LPd OCH_3 + Na]$^+$, 277 [LPd]$^+$.

[LZnCl)]Cl, **15.** Zinc chloride (34.0 mg; 0.25 mmol) was used. Colourless crystals obtained, yield 53%.

MS (FAB): *m/z* 393 [LZnL]$^+$, 291 [LZn]$^+$.

[LCuCl)]Cl, **16.** Copper(II) chloride trihydrate was used (47.1 mg; 0.25 mmol). Green powder obtained, yield 55%.

MS (ESI): *m/z* 306 [LCu + DMSO]$^+$, 260 [$LCuOCH_3$]$^+$, 228 [LCu]$^+$.

Complexes of the ligand 4.

[LCu(NO_3)]NO_3, **17.** Copper(II) nitrate trihydrate was used (60.4 mg; 0.25 mmol). Ble/green powder obtained, yield 62%.

MS (ESI): *m/z* 296 [$LCuNO_3$]$^+$, 265 [$LCuOCH_3$]$^+$, 234 [LCu]$^+$.

[LPdCl)]Cl, **18.** Sodium tetrachloropalladate was used (70 mg; 0.25 mmol). Dark orange powder obtained, yield 50%.

^{1}H NMR (360 MHz, DMSO-d_6): δ (ppm) 8.56 (d, 2H, $H_{py\text{-}2,\ 10}$), 8.32 (s, 1H, NH), 7.96 (t, 2H, $H_{py\text{-}3,\ 11}$), 7.48 (d, 2H, $H_{py\text{-}5,\ 13}$), 7.12 (t, 2H, $H_{py\text{-}4,\ 12}$).

MS (ESI): *m/z* 622, 552, 447 [LPdL]$^+$, 311 [LPdCl]$^+$, 276 [LPd]$^+$.

4.4 Derivatives of 8-Aminoquinoline

4.4.1 Ligands of 8-Aminoquinoline Derivatives

8-aminoquinoline 19. Commercially available from Aldrich and used as received.

$C_9H_8N_2$; exact mass: 144.07.

^{1}H NMR (360 MHz, DMSO-d_6): δ (ppm) 8.79 (d, 1H, H_2), 8.24 (d, 1H, H_4), 7.52 (m, 1H, H_7), 7.36 (t, 1H, H_3), 7.12 (d, 1H, H_6), 6.99 (d, 1H, H_8), 5.98 (s, 2H, H_{11}).

^{13}C NMR (90 MHz, DMSO-d_6): δ (ppm)

MS (FAB): *m/z* 145 $[M + H]^+$.

***N*-acetic acid-*N*-8-aminoquinoline 20.** 8-Aminoquinoline (1.0 g; 6.7 mmol) was dissolved in 5 ml THF and NEt_3 (1 ml) was added. During next 30 minutes mixture of chloroacetic acid (0.63 g; 6.7 mmol) and THF (5 ml) added. After 5 days refluxing, THF was removed under reduced pressure and the brown solid left was further purified by the coloumn chromatography (DCM : MeOH, 7 : 3). The pure compound **2** was isolated as a yellow solid, yield 58%.

$C_{11}H_{10}N_2O_2$; exact mass: 202.07.

^{1}H NMR (360 MHz, DMSO-d_6): δ (ppm) 8.81 (d, 1H, H_2), 8.27 (d, 1H, H_4), 7.56 (m, 1H, H_7), 7.40 (t, 1H, H_3), 7.11 (d, 1H, H_6), 6.93 (s, 1H, H_{11}), 6.59 (d, 1H, H_8), 2.77 (s, 2H, H_{12})

^{13}C NMR (90 MHz, DMSO-d_6): δ (ppm) 173.3 (C_{13}), 146.8 (C_2), 144.2 (C_9), 137.5 (C_5), 138.7 (C_4), 134.3(C_{10}), 128.2 (C_8), 127.9 (C_7), 121.6 (C_6), 104.2 (C_3), 46.9 (C_{12}).

MS (FAB): *m/z* 203 $[M + H]^+$.

***N*-(4-carboxymethyl)benzyl-*N*-8-aminoquinoline 21.** To a solution of 8-aminoquinoline (0.629 g; 4.36 mmol) and NEt_3 (0.438 g; 4.33 mmol) in THF (40 ml) at 60°C, α-bromo-toluic acid methyl ester (0.5 g; 2.18 mmol) in THF (11 ml) was slowly added during 2 hours. The reaction mixture was refluxed for next 3 hours. After cooling to the room temperature, solution was filtered to remove a white precipitation (triethylammoniumbromid). After removal of the solvent under reduced pressure, the brown oily residue was purified with flash coloumn chromatography (DCM : n-Hexane, 8 : 2). Purifed oil was dissolved in 1 ml

solution MeOH : HCl = 5 :1, solvent removed under reduced pressure and dried during 20 minutes by the pressure of 10 mbar and 90°C. After the recrystalization from MeOH, the hydrochloride was washed with ether and dried *in vacuo*. Yellow powder (0.226 g; 0.68 mmol, 31.5%) of the ligand **3** hydrochloride was obtained.

$C_{18}H_{16}N_2O_2$; exact mass: 292.12.

^{1}H NMR (360 MHz, DMSO-d_6): δ (ppm) 8.88 (d, 1H, H_2), 8.47 (d, 1H, H_4), 7.91 (d, 2H, $H_{14, 18}$), 7.67 (m, 1H, H_7), 7.55 (d, 2H, $H_{15, 17}$), 7.37 (t, 1H, H_3), 7.19 (d, 1H, H_6), 6.66 (d, 1H, H_8), 4.66 (s, 2H, H_{12}), 3.82 (s, 3H, H_{22}).

^{13}C NMR (90 MHz, DMSO-d_6): δ (ppm) 165.9 (C_{19}), 144.7 (C_{13}), 144.5 (C_2), 141.5 (C_4), 141.2 ($C_{5, 10}$), 132.2 (C_9), 129.2 ($C_{14, 18}$), 128.9 (C_{16}), 127.2 ($C_{15, 17}$), 126.6 (C_7), 120.5 (C_6), 108.4 (C_3), 51.8 (C_{22}), 45.9 (C_{12}).

MS (FAB): *m/z* 293 $[M + H]^+$.

Elemental analysis: calc. C 65.75, H 5.21, N 8.52; found C 65.49, H 5.16, N 8.50 %.

***N*-(2-hydroxy)benzyl-*N*-8-aminoquinoline 23**. Salicylaldehyd (0.593 g; 4.85 mmol) and 8-aminoquinoline (0.700 g; 4.83 mmol) were dissolved in ethanol (10 ml) and refluxed for 40 minutes in the presence of natriumsulfat. After cooling down to room temperature natriumsulfat was removed by filtration and yellow coloured Schiff base **22** was obtained.. Natriumtrisacetoxyborhydride (2.047 g; 9.66 mmol) was slowly added to the reaction mixture and the suspension was stirred for next 20 hours at room temperature. Then 5 ml water and 2 ml conc. HCl were added and the mixture extracted with ether/ethylacetate 1:1. After removing of the organic solvent under reduced pressure, residual solid was dissolved in 2 ml EtOH : HCl, 5:1, precipitate filtered and resulting orange powder recrystalized from methanol, dried *in vacuo* giving 0.395 g (1.38 mmol; 28.6 %) of the title compound **4** as hydrochloride. Crystalls suitable for X-ray analysis were formed by slow evaporation of the solvent at room temperature. (Table 4.4).

$C_{16}H_{14}N_2O$; exact mass: 250.11.

^{1}H NMR (360 MHz, DMSO-d_6): δ (ppm) 8.88 (d, 1H, H_2), 8.53 (d, 1H, H_4), 7.69 (m, 1H, H_7), 7.45(t, 1H, H_3), 7.24 (m, 2H, $H_{6, 17}$), 7.07 (t, 1H, H_{15}), 6.87 (m, 2H, $H_{8, 14}$), 6.67 (t, 1H H_{16}), 4.48 (s, 2H, H_{12}).

^{13}C NMR (90 MHz, DMSO-d_6): δ (ppm) 155.2 (C_{18}), 145.5 (C_2), 141.9 (C_9), 139.5 (C_4), 134.2 (C_{10}), 128.8 (C_5), 128.5 ($C_{13, 15}$), 127.9 (C_7), 124.2 (C_{13}), 121.6 (C_6), 118.7 (C_{16}), 115.0 (C_8), 114.5 (C_{14}), 107.8 (C_3), 41.8 (C_{12}).

MS (ESI): *m/z* 251 $[M + H]^+$.

Elemental analysis: calc. C 67.01, H 5.27, N 9.77; found C 66.60, H 5.22, N 9.52 %.

4.4.2 Metal Complexes of 8-Aminoquinoline Derivatives

General Procedure. 8-Aminoquinoline (36.0 mg; 0.25 mmol) was dissolved in hot methanol (5 ml) and the boiling solution poured to the boiling solution of corresponding metal(II) salt (0.25 mmol) in methanol (5 ml). The final mixture was kept on the room temperature for few hours and the solvent was allowed to slowly evaporate. Precipitate/crystals formed were collected by filtration and dried in air.

Complexes of the ligand 19.

$[LCu(NO_3)]NO_3$, **24.** Copper(II) nitrate was used (0.25 mmol). Green crystals formed by the evaporation of the solvent during 2 days on the room temperautre. Yield 52 %.

MS (ESI): *m/z* 352 $[LCuL]^+$, 284 $[LCu + DMSO]^+$, 238 $[LCuOCH_3]^+$, 206 $[LCu]^+$.

Elemental analysis: calc. C 45.62, H 2.98, N 17.73; found C 45.23, H 3.53, N 17.52 %.

$[LZn(NO_3)]NO_3$, **25.** Zinc(II) nitrate was used (74.0 mg; 0.25 mmol). Colourless crystals suitable for the X-ray analysis formed after few days standing in the fridge (Table 4.2). Yield 51%.

MS (ESI): *m/z* 353 $[LZnL]^+$, 209 $[LZn]^+$.

Elemental analysis: calc. C 45.44, H 2.97, N 17.67; found C 45.16, H 3.32, N 17.47 %.

$[LCd(NO_3)]NO_3$, **26.** Cadmium(II) nitrate was used (60.0 mg; 0.25 mmol). After one day standing on the room temperature, colourless crystals obtained. Yield 49 %.

MS (ESI): *m/z* 330 $[LCd + DMSO]^+$, 286 $[LCdOCH_3]^+$, 254 $[LCd]^+$.

$[LNi(NO_3)]NO_3$, **27.** Nickel(II) nitrate was used (72.7 mg; 0.25 mmol). After one day standing at room temperature, green crystals obtained. Yield 51 %.

MS (ESI): *m/z* 345 $[LNiL]^+$, 279 $[LNi + DMSO]^+$, 233 $[LNiOCH_3]^+$, 201 $[LNi]^+$.

[LCuCl)]Cl, **33.** Copper(II) chloride trihydrate was used (47.1; 0.25 mmol). Green crystals for X-ray analysis were obtained by the slow evaporation of the solvent during one week (Table 4.2). Yield 58 %.

MS (ESI): *m/z* 284 $[LCu + DMSO]^+$, 238 $[LCuOCH_3]^+$, 206 $[LCu]^+$.

Elemental analysis: calc. C 38.80, H 2.89, N 10.05; found C 38.59, H 2.99, N 9.96 %.

[LZnCl)]Cl, **34.** Zinc(II) chloride was used (34.0 mg; 0.25 mmol). Colourless crystals formed after few days standing in the fridge. Yield 54 %.

MS (ESI): *m/z* 353 $[LZnL]^+$, 241 $[LZnOCH_3]^+$, 209 $[LZn]^+$.

[LPdCl)]Cl, **35.** Sodium tetrachloropalladate was used (70 mg; 0.25 mmol). Dark red crystals formed. Yield 54 %.

MS (ESI): *m/z* 393 $[LPdL]^+$, 281 $[LPdOCH_3]^+$, 250 $[LPd]^+$.

Metal complexes of the ligand 21.

$[LCu(NO_3)]NO_3$, **28.** Ligand **21** hydrochloride (30.0 mg; 0.091 mmol) was dissolved in 2 ml hot methanol and poured into the boling methanol solution (1 ml) of copper(II) nitrate trihydrate (60.4 mg; 0.25 mmol). After 24 hours standing on the 7^{o}C, green crystals of X-ray quality were washed with methanol and dried in air. Yield 50%. (Table 4.3).

MS (ESI): *m/z* 353 $[LCu]^+$.

Elemental analysis: calc. C 47.69, H 3.56, N 9.27; found C 49.85, H 3.56, N 6.77 %.

$[LNi(NO_3)]NO_3$, **29.** Nickel(II) nitrate was used (72.7 mg; 0.25 mmol). Green crystals obtained. Yield 51 %.

MS (ESI): *m/z* 378 $[LNiOCH_3]^+$, 347 $[LNi]^+$.

[LCuCl)]Cl, **36.** Copper(II) chloride trihydrate (47.1 mg; 0.25 mmol) was used. Green crystals, suitable for X-ray crystallography, formed during slow evaporation of the reaction mixture. Yield 52%. Table (4.3).

MS (ESI): *m/z* 432 $[LCu + DMSO]^+$, 390 $[LCuCl]^+$, 354 $[LCu]^+$.

Elemental analysis: calc. C 50.78, H 3.55, N 6.58; found C 49.89, H 3.65, N 6.56 %.

[LPdCl)]Cl, **37.** The ligand **21** as hydrochloride (30.0 mg; 0.091 mmol) was dissolved in methanol (3 ml) in a beaker, heated to boiling and poured to the boiling solution of

natriumtetrachlororpalladate (26.0 mg; 0.091 mmol) in methanol (3 ml). The reaction mixture was filtered and allowed to cool to room temperature. After standing overnight at room temperature and few days on the 7°C, the precipitated yellow product was collected by filtration and dried in air. Yield 54%.

MS (ESI): *m/z* 475 $[LPd + DMSO]^+$, 429 $[LPdOCH_3]^+$, 399 $[LPd]^+$.

Elemental analysis: calc. C 46.03, H 3.43, N 5.91; found C 44.15, H 3.61, N 5.96 %.

Metal complexes of the ligand 23.

$[LCu(NO_3)]NO_3$, **30.** Ligand **23** hydrochloride (30.0 mg; 0.104 mmol) was dissolved in 2 ml methanol and the boiling solution poured to the solution of copper(II) nitrate trihydrate (47.1 mg; 0.25 mmol) in 2 ml hot methanol. Green crystalls obtained, yield 55%

MS (ESI): *m/z* 390 $[LCu + DMSO]^+$, 343 $[LCuOCH_3]^+$, 312 $[LCu]^+$.

$[LNi(NO_3)]NO_3$, **31.** Nickel(II) nitrate was used (72.7 mg; 0.25 mmol). Green crystals obtained. Yield 48 %.

MS (ESI): *m/z* 385 $[LNi + DMSO]^+$, 338 $[LNiOCH_3]^+$, 307 $[LNi]^+$.

$[LCo(NO_3)]NO_3$, **32.** Cobalt(II) nitrate hexahydrate was used (72.8 mg; 0.25 mmol). Violet powder obtained. Yield 65%.

MS (ESI): *m/z* 389 $[LCoL]^+$.

[LCuCl)]Cl, **38.** Copper(II) chloride trihydrate (47.1 mg; 0.25 mmol) was used. After cooling down to room temperature and standing two days on 7°C, dark green crystalls of X-ray quallity formed (Table 4.5).

MS (ESI): *m/z* 343 $[LCuOCH_3]^+$, 312 $[LCu]^+$.

Elemental analysis: calc. C 43.75, H 3.90, N 6.38; found C 42.48, H 3.76, N 6.07 %.

[LPdCl)]Cl, **39.** Ligand **23** hydrochloride (30.0 mg; 0.104 mmol) was dissolved in 2 ml boiling methanol and added to the boliling solution of natriumtetrachloropalladate (29.7 mg; 0.104 mmol) in 2 ml methanol. The solution was allowed to cool down and after few hours standing on the room temperature yellow crystals suitable for X-ray crystallography formed (Table 4.5).

^{1}H NMR (360 MHz, DMSO-d_6): δ (ppm) 8.96 (d, 1H, H_{py-2}), 8.64 (d, 1H, H_{py-4}), 8.20 (d, 1H, H_{ph-6}), 7.97(d, 1H, H_{bz-17}), 7.67-7.63 (m, 3H, $H_{3,\ 7,\ 14}$), 6.96 (t, 1H, H_{bz-15}), 6.70 (t, 1H, H_{bz-16}), 6.50 (d, 1H H_{ph-8}), 4.49 (s, 2H, H_{12}).

MS (ESI): *m/z* 433 $[LPd + DMSO]^+$, 386 $[LPdOCH_3]^+$, 355 $[LPd]^+$.

Elemental analysis: calc. C 39.86, H 3.55, N 5.81; found C 35.47, H 2.86, N 5.04 %.

4.5 Derivatives of *N*-Nitrilotriacetic Acid (NTA)

N^{α},N^{α}-Bis[(*tert*-butyloxycarbonyl)methyl]-N^{ε}-benzyloxycarbonyl-L-lysine tert-butyl ester 40. Starting compound N^{ε}-benzyloxycarbonyl-L-lysine *tert*-butyl ester hydrochlorid (H-Lys(Z)-tBu) (1.07 g; 3.30 mmol) and NEt_3 (2.66 ml) were dissolved in DMF (40 ml), and bromoacetic acid *tert*-butyl ester (6.4 g; 3.30 mmol) was added. The reaction mixture was stirring at 50°C for 3 days, and then the solvent and the excess of bromoacetic acid *tert*-butyl ester were evaporated *in vacuo*. The remaining oily residue was extracted 3 times with hexane, the organic phases collected and hexane removed *in vacuo*. Yield 70%.

$C_{30}H_{48}N_2O_8$; exact mass: 564.34

^{1}H NMR (360 MHz, $CDCl_3$): δ (ppm) 7.32 (m, 5H, H_{bz}), 5.08 (s, 2H, C_6H_5-C*H*$_2$), 3.46 (dd, 4H, -N(C*H*$_2$COOtBu)$_2$), 3.31 (t, 1H, Z-NH-$(CH_2)_4$-C*H*-), 3.19 (q, 2H, Z-NH-C*H*$_2$-), 1.64 (m, 2H, Z-NH-$(CH_2)_3$-C*H*$_2$-), 1.53 (m, 4H, Z-NH-CH_2-(C*H*$_2$)$_2$-), 1.45 (s, 9H, (C*H*$_3$)$_3$COCOCH$_2$CH-), 1.42 (s, 18H, ((C*H*$_3$)$_3$COCOCH$_2$)$_2$N-).

^{13}C NMR (90 MHz, $CDCl_3$): δ (ppm) 173.1 $(CH_3)_3CO\mathit{C}OCH$), 171.4 (-N($CH_2\mathit{C}$OOtBu)$_2$), 157.1 ($C_6H_5CH_2O\mathit{C}$O-), 137.5 ($C_{Z\text{-}1}$), 128.6-128.7, 129.1 ($C_{Z\text{-}2\text{-}6}$), 81.9 ((CH$_3$)$_3$*C*OCOCH), 81.4 ((CH$_3$)$_3$*C*OCOCH$_2$)$_2$N-), 67.1 (C_6H_5-*C*H$_2$), 65.8 (-*C*HN-), 54.6 ((C*H*$_3$)$_3$COCO*C*H$_2$)$_2$N-), 41.5 (Z-NH-*C*H$_2$-), 30.7, 28.9-29.9, 28.8, 23.7 (Z-NH-CH_2-(*C*H$_2$)$_3$-), ((*C*H$_3$)$_3$COCO-).

MS (FAB): *m/z* 565 $[M + H]^+$.

N^{α},N^{α}-Bis[(*tert*-butyloxycarbonyl)methyl]-L-lysine tert-butyl ester 41. The Z-protected amine **40** (911 mg; 1.62 mmol) was dissolved in 25 ml of the mixture MeOH : EtOH : H_2O, 25 : 2 : 1, and the spatula tip of Pd/C (10% Pd) was added. The reaction mixture was hydrogenated at room temperature and atmospheric pressure for 3 h. The catalyst was filtered off, and the solvent removed in vacuo. Yield 88%.

$C_{22}H_{42}N_2O_6$; exact mass: 430.3.

^{1}H NMR (360 MHz, $CDCl_3$): δ (ppm) 3.44 (dd, 4H, -N(C*H*$_2$COOtBu)$_2$), 3.30 (t, 2H, NH_2-$(CH_2)_4$-C*H*-), 2.67 (t, 2H, NH_2-C*H*$_2$-), 1.73 (bm, 2H, NH_2-CH_2-C*H*$_2$-), 1.63 (m, 4H, NH_2-$(CH_2)_2$-(C*H*$_2$)$_2$-), 1.45 (s, 9H, (C*H*$_3$)$_3$COCOCH$_2$CH-), 1.43 (s, 18H, ((C*H*$_3$)$_3$COCOCH$_2$)$_2$N-).

^{13}C NMR (90 MHz, $CDCl_3$): δ (ppm) 173.1 $(CH_3)_3\mathit{C}OCOCH$), 171.3 (-N($CH_2\mathit{C}$OOtBu)$_2$), 157.1 ($C_6H_5CH_2O\mathit{C}$O-), 81.7 ((CH$_3$)$_3$*C*OCOCH), 81.3 ((CH$_3$)$_3$*C*OCOCH$_2$)$_2$N-), 65.8 (-*C*HN),

54.5 ($(CH_3)_3COCOCH_2)_2N$-), 42.6 (NH_2-CH_2-), 33.9, 31.2, 28.8-28.9, 23.8 (NH_2-CH_2-$(CH_2)_3$-), ($(CH_3)_3COCO$-).

MS (FAB): *m/z* 431 $[M + H]^+$.

N^{α},N^{α}-Bis[(*tert*-butyloxycarbonyl)methyl]-N^{ε}-(benzylcarbonyl-*N*-2-picolylamine)-L-lysine tert-butyl ester 42.

Coupling with DCC. Compound **2** (31.5 mg; 0.14 mmol) was dissolved in mixture of DCM and EtOH and solution of NHS (16.1 mg; 0.14 mmol), DCC (28.0 mg; 0.14 mmol) and DMAP (2-3 mg) in acetone was added. After stirring at room temperature for 4 h, the precipitated urea was filtered off and compound **41** (60.2 mg; 0.14 mmol) with NEt_3 (0.014 ml; 0.14 mmol) in ml DCM were added. The reaction was stirred over night. Thereafter the solvent was removed *in vacuo* and the residue was dissolved in EtOAc . The raw product was worked up according to the washing procedure: 3 times washed with 50-100 ml of 10% acetate buffer (pH 4.0), 3 times with 50-100 ml of 5% NaCl solution, 3 times with saturated $NaHCO_3$ solution and then again 3 times with 50-100 ml of 5% NaCl solution. The EtOAc phase was dried with Na_2SO_4, filtered and evaporated to dryness *in vacuo*. Yield 26%.

Coupling with iBCF. The compound **2** (90 mg; 0.4 mmol) was dissolved in DMF and NEt_3 (0.04 ml; 0.4 mmol) was added. The solution was cooled to -7^oC and iBCF (0.055 ml; 0.4 mmol) was slowly added. After about 30 min. of activation, a solution of **41** (172.0 mg; 0.4 mmol) with NEt_3 (0.04 ml; 0.4 mmol) in DMF at $-7\ ^oC$ was added. The reaction mixture was stirred on ice for 1 h, and then on the room temperature for next 42 h. The solution was then filtrated and evaporated *in vacuo*. The green residue was dissolved in EtOAc, filtered and then 3 times washed with 50-100 ml of 10% acetate buffer (pH 4.0), 3 times with 50-100 ml of 5% NaCl solution, 3 times with saturated $NaHCO_3$ solution and then again 3 times with 50-100 ml of 5% NaCl solution. The EtOAc phase was dried with Na_2SO_4, filtered and evaporated to dryness *in vacuo*. Yield 22%.

Coupling with DSC. Compound **2** (40 mg; 0.18 mmol) was dissolved in DMF (2 ml) and dry pyridine (0.1 ml). DSC (64 mg; 0.27 mmol) was added and the mixture was stirred at 55^oC for 90 min. After diluting the mixture with EtOAc, the supernatant was decanted. The product (ester) was dissolved in DMF and reprecipitated. Compound **41** (103.2 mg; 0.24 mmol) was dissolved in 0.1 M Na_2CO_3 (2 ml) and was added to the isolated ester. The reaction mixture

was stirred at room temperature for 1 h. The product was isolated by the extraction with EtOAc. Yield 14%.

Coupling with TBTU. Compound **2** (47 mg; 0.20 mmol) was dissolved in DMF and TBTU (64 mg; 0.20 mmol), HOBt (27 mg; 0.20 mmol) and DIPEA (130 μl; 10 mmol) were added. After 20 min. of activation the solution of **41** (86 mg; 0.2 mmol) in DMF was added. After 24 h stirring on the room temperature, the solvent was evaporated *in vacuo*, and orange/brown oil left. This residue was dissolved in EtOAc and worked up acoording to the washing procedure: 2 times washed with 50-100 ml of 10% $NaHCO_3$ solution, then one time with 50-100 ml of acetate buffer (pH 4.0), and finally 2 times with 50-100 ml of 10% $NaHCO_3$ solution. The EtOAc phase was collected and then dried with Na_2SO_4, filtered and the solvent evaporated to dryness *in vacuo*. Yield 16%.

$C_{36}H_{54}N_4O_7$; exact mass: 654.4.

^{1}H NMR (360 MHz, $CDCl_3$): δ (ppm) 8.55 (d, 1H, H_{py-2}), 7.81 (d, 2H, $H_{bz-12,\ 14}$), 7.66 (t, 1H, H_{py-4}), 7.42 (d, 1H, H_{py-5}), 7.28 (d, 2H, $H_{bz-11,\ 15}$), 7.19 (t, 1H, H_{py-3}), 3.93 (s, 2H, H_7), 3.90 (s, 2H, H_9), 3.44 (dd, 4H, -N(C*H*$_2$COOtBu)$_2$), 3.31 (t, 2H, -NH-(CH$_2$)$_4$-C*H*-), 2.64 (t, 2H, -NH-C*H*$_2$-), 1.93 (m, 2H, -NH-CH$_2$-C*H*$_2$-), 1.67 (m, 4H, -NH-(CH$_2$)$_2$-(C*H*$_2$)$_2$-), 1.45 (s, 9H, (C*H*$_3$)$_3$COCOCH$_2$CH-), 1.41 (s, 18H, ((C*H*$_3$)$_3$COCOCH$_2$)$_2$N-).

^{13}C NMR (90 MHz, $CDCl_3$): δ (ppm) 174.6 (C_{16}), 173.0 ($CH_3)_3$*C*OCOCH), 171.2 (-N(CH$_2$*C*OOtBu)$_2$), 156.6 (C_{py-6}), 150.1 (C_{py}), 140.1 (C_{bz-10}), 138.5 (C_{py}), 138.0 (C_{bz-13}), 130.6 (C_{bz}), 129.3 (C_{bz}), 124.0 (C_{py}), 81.3 ((CH$_3$)$_3$*C*OCOCH), 80.8 ((CH$_3$)$_3$*C*OCOCH$_2$)$_2$N-), 64.8 (-*C*HN-), 54.0 ((CH$_3$)$_3$COCO*C*H$_2$)$_2$N-), 53.4 (C_7), 52.9 (C_9), 42.4 (NH$_2$-*C*H$_2$-), 33.9, 28.2-28.0, 25.6, 24.9 (-NH-CH$_2$-(*C*H$_2$)$_3$-), ((*C*H$_3$)$_3$COCO-).

MS (FAB): *m/z* 655 $[M + H]^+$, 431 (**41**), 225 (dicyclohexylurea).

4.6 X-Ray Crystallographic Data

Compound	**10**	**9**
Empirical formula	C_{30} H_{36} Cl_4 Cu_2 N_4 O_6	C_{30} H_{34} Cl_2 N_4 O_6Zn_2
Formula weight	817.50	748.25
T/K	100(2)	100(2)
Wavelength/ Å	0.71073	0.71073
Crystal system	Triclinic	Triclinic
Space group	P-1	P-1
a/Å	7.9093(3)	10.2518(8)
b/Å	9.1598(3)	10.5238(8)
c/Å	12.3657(4)	15.0675(12)
$\alpha/^o$	77.493(4)	86.54(1)
$\beta/^o$	73.788(4)	86.90(1)
$\gamma/^o$	85.445(4)	81.49(1)
V/ $Å^3$	839.66(5)	1603.1(2)
Z	1	2
D_c/gcm^{-3}	1.617	1.550
Absorption coefficient/mm^{-1}	1.633	1.711
θ Range/^{o}	3.33 to 31.02	3.45 to 26.00
Reflections collected	20456	20180
Independent reflections (R_{int})	5337	6256
Data/restraints/parameters	5337/0/211	6206/1/406
Goodness-of-fit on $F^{2\alpha}$	1.042	1.030
Final R indices [I>2σ(I)]	R1 = 0.0264, wR2 = 0.0643	R1 = 0.0633, wR2 = 0.1348
R indices (all data)	R1 = 0.0302, wR2 = 0.0662	R1 = 0.1120, wR2 = 0.1578
Largest diff. peak and hole/e $Å^3$	0.828 and -0.472	1.556 and -0.530

Table 4.1 *Crystal data and structure refinement for the complexes **9** and **10** .*

Compound	**25**	**33**
Empirical formula	C_{18} H_{16} N_6 O_6 Zn	C_{18} H_{16} Cl_4 Cu_2 N_4
Formula weight	477.74	557.23
T/K	100(2)	100(2)
Wavelength/ Å	0.71073	0.71073
Crystal system	Triclinic	Triclinic
Space group	P-1	P-1
a/ Å	7.2017(3)	6.2726(5)
b/ Å	8.0801(3)	8.4865(7)
c/ Å	8.7053(3)	10.2486(9)
$\alpha/^o$	72.361(5)	108.725(8)
$\beta/^o$	70.272(5)	107.615(8)
$\gamma/^o$	69.779(5)	93.421(8)
V/ $Å^3$	437.37(3)	484.97(7)
Z	1	1
D_c/gcm^{-3}	1.814	1.908
Absorption coefficient/mm^{-1}	1.461	2.756
θ Range/^{o}	3.12 to 31.03	3.42 to 27.50
Reflections collected	12345	8585
Independent reflections (R_{int})	2784	2216
Data/restraints/parameters	2784 / 0 / 142	2216 / 0 / 127
Goodness-of-fit on $F^{2\alpha}$	1.115	1.054
Final R indices [I>2σ(I)]	R1 = 0.0300, wR2 = 0.0782	R1 = 0.0500, wR2 = 0.0839
R indices (all data)	R1 = 0.0315, wR2 = 0.0789	R1 = 0.0908, wR2 = 0.0
Largest diff. peak and hole/e $Å^3$	1.116 and -0.346	0.681 and -0.605

Table 4.2 *Crystal data and structure refinement for the complexes **25** and **33**.*

Compound	**28**	**36**
Empirical formula	C_{36} H_{32} Cl_2 Cu_2 N_6 O_{10}	C_{18} H_{16} Cl_2 Cu N_2 O_2
Formula weight	906.66	426.77
T/K	100(2)	100(2)
Wavelength/ Å	0.71073	0.71073
Crystal system	Triclinic	Triclinic
Space group	P-1	P-1
a/ Å	9.1206(5)	7.9446(3)
b/ Å	9.6731(5)	9.2046(3)
c/ Å	10.3848(6)	13.0212(4)
$\alpha/^o$	78.877(5)	86.335(5)
$\beta/^o$	80.046(5)	79.359(5)
$\gamma/^o$	79.969(5)	70.672(5)
V/ $Å^3$	876.00(8)	883.08(5)
Z	1	2
D_c/gcm^{-3}	1.719	1.605
Absorption coefficient/mm^{-1}	1.438	1.553
θ Range/^{o}	3.27 to 31.15	3.83 to 30.97
Reflections collected	24074	28514
Independent reflections (R_{int})	5585	5556
Data/restraints/parameters	5585 / 0 / 254	5556 / 0 / 227
Goodness-of-fit on $F^{2\alpha}$	1.057	1.040
Final R indices [I>2σ(I)]	R1 = 0.0446, wR2 = 0.1012	R1 = 0.0358, wR2 = 0.0716
R indices (all data)	R1 = 0.0582, wR2 = 0.1076	R1 = 0.0486, wR2 = 0.0765
Largest diff. peak and hole/e $Å^3$	0.974 and -0.875	0.459 and -0.432

Table 4.3 *Crystal data and structure refinement for the complexes **28** and **36**.*

Compound	**23**
Empirical formula	$C_{16}\ H_{17}\ N_3\ O_5$
Formula weight	331.33
T/K	100(2)
Wavelength/ Å	0.71073
Crystal system	Monoclinic
Space group	$P2_1/n$
a/ Å	6.6827(2)
b/ Å	18.4101(6)
c/ Å	12.4654(4)
$\alpha/^o$	90
$\beta/^o$	101.786(5)
$\gamma/^o$	90
V/ $Å^3$	1501.27(8)
Z	4
D_c/gcm^{-3}	1.466
Absorption coefficient/mm^{-1}	0.111
θ Range/^{o}	3.30 to 31.50
Reflections collected	43403
Independent reflections (R_{int})	4978
Data/restraints/parameters	4978 / 3 / 229
Goodness-of-fit on $F^{2\alpha}$	1.056
Final R indices [$I>2\sigma(I)$]	R1 = 0.0425, wR2 = 0.1094
R indices (all data)	R1 = 0.0489, wR2 = 0.1140
Largest diff. peak and hole/e $Å^3$	0.446 and -0.256

Table 4.4 *Crystal data and structure refinement for the ligand **23**.*

Compound	**39**	**38**
Empirical formula	C_{19} H_{26} Cl_2 N_2 O_4 Pd	C_{16} H_{14} Cl_2 Cu N_2 O * 1.5 MeOH * 0.5 H_2O
Formula weight	523.72	441.80
T/K	100(2)	100(2)
Wavelength/ Å	0.71073	0.71073
Crystal system	Monoclinic	Monoclinic
Space group	$P2_1/c$	$P2_1/n$
a/ Å	14.4044(4)	11.4862(6)
b/ Å	8.5670(2)	14.1744(9)
c/ Å	18.5054(4)	12.5915(6)
$\alpha/^o$	90	90
$\beta/^o$	101.777(5)	108.180(5)
$\gamma/^o$	90	90
V/ $Å^3$	2235.54(9)	1947.69(19)
Z	4	4
D_c/gcm^{-3}	1.556	1.507
Absorption coefficient/mm^{-1}	1.095	1.414
θ Range/^{o}	3.11 to 30.99	3.34 to 30.56
Reflections collected	34995	40808
Independent reflections (R_{int})	7107	5931
Data/restraints/parameters	7107 / 1 / 269	5931 / 1 / 254
Goodness-of-fit on $F^{2\alpha}$	1.034	1.160
Final R indices [$I>2\sigma(I)$]	R1 = 0.0298, wR2 = 0.0639	R1 = 0.0830, wR2 = 0.2444
R indices (all data)	R1 = 0.0410, wR2 = 0.0687	R1 = 0.0961, wR2 = 0.2565
Largest diff. peak and hole/e $Å^3$	1.281 and -0.742	2.801 and -0.798

Table 4.5 *Crystal data and structure refinement for the complexes **38** and **39** .*

5

Conclusion

Regioselective cleavage of peptides and proteins is a very common procedure in protein sequencing and other biochemical applications. However, the half-life for the hydrolysis of amide bond is very long at room temperature and pH 7. For GlyGly, for example, it is 350 years, and for AcGlyGly, 500 years. Because uncatalyzed hydrolysis of peptides is extremely slow, artificial cleavage methods are needed in analytical biochemistry and molecular biology for studies of unnatural proteins, sequencing of large or blocked proteins, analysis of protein domains, studies of protein association, and synthesis of new drugs, among other tasks.

The aim of this research was to examine the influence of different structures of ligands on the formation of the corresponding metal complexes and their role as synthetic peptidases.

To this end, three series of the ligands and corresponding metal complexes were synthesized and structurally charaterized. Synthesized ligands contain either a pyridine ring or quinoline ring, both substituted at the aliphatic amino group, leaving one or two carbon spacer between the aromatic and the aliphatic amine. In that way, a structurally preferred N_2O octahedral complexation to form with various divalent metal ions, such as Pd(II), Zn(II), Cu(II), Co(II), Ni(II) and Cd(II), was permitted. The ligands were obtained in high purity and good yield.

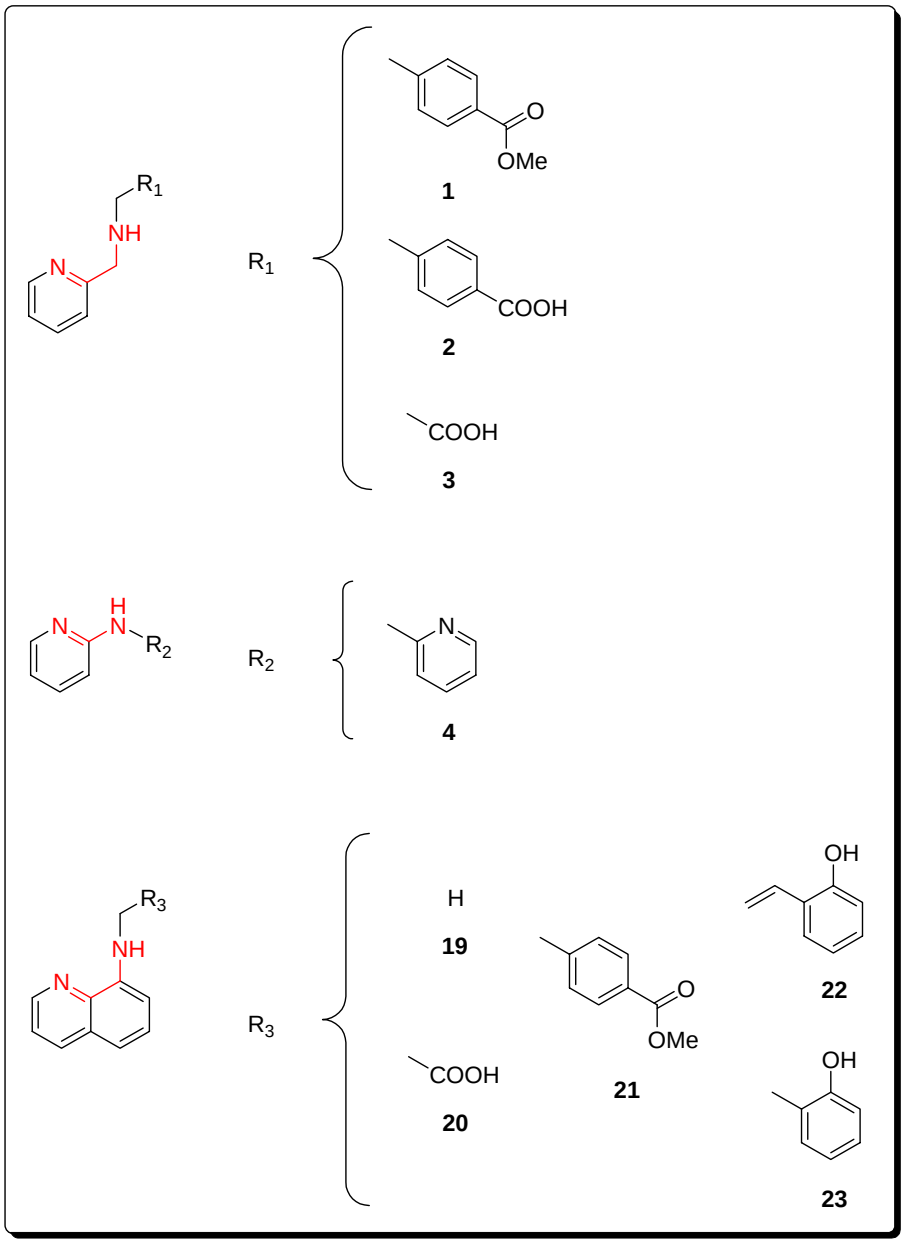

Figure 5.1 *Overview of the general structures of the synthesized ligands.*

To complete the characterization of the metal complexes, beside ^{1}H and ^{13}C NMR data, FAB/ESI-MS data and elemental analysis, crystal structure data for nine compounds (crystal structure of eight metal complexes and one crystal structure of the ligand) have been obtained. They gave further insight into the nature of binding in the metal complexes. All X-ray analysis data obtained suggested that the complexation of the synthesized ligands with Zn(II) gave dimers with two different modes of dimerization depending on the metal salt and structure of the ligand used for the complexation. For example, complexation of $ZnCl_2$ with ligand **2** gave a dimer with coordinated chloride, solvent (MeOH) and a bridging ligand between two Zn centers (Figure 5.2a). Complexation with $Zn(NO_3)_2$ gave a dimer with only one Zn(II) center, coordinated with four nitrogen atoms N(1) and N(11) from two ligands, and nitrate groups (Figure 5.2b).

a) b)

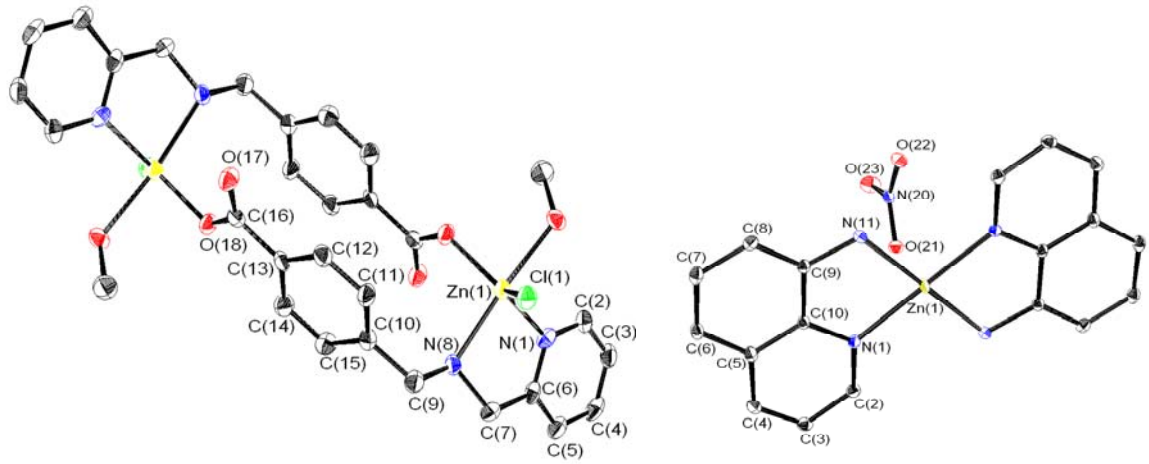

Figure 5.2 *ORTEP plot of Zn(II) complexes: a) dimer* ***9*** *(50% probability); b)* ***25*** *(50% probability). Hydrogen atoms have been omitted for clarity.*

After synthesis and structural characterization of ligands and their metal complexes, their role as promotores in the cleavage of amide bond in small peptides was examined. Two peptides were chosen as substrates for the hydrolysis. Each peptide contained one histidine residue, whose imidazol ring in the side chain serves as an anchor for the metal complexes. To supress the formation of hydrolytically inactive promoter-substrate complexes, the *N*-terminus of the dipeptides was protected by acetylation. The histidine residue was placed either on the *N*- (AcHisGly) or C-terminus (AcβAlaHis) of dipeptides.

The reaction of dipeptide and one of the metal complexes **5-18** at pH 2.9 was monitored by ^{1}H NMR over five days. Already after 15 minutes five NMR-detectable

substrate-promoter complexes spontaneously formed. After a few hours a new signal of the methylen group of the free glycine at 3.67 ppm was monitored, indicating the beginning of hydrolytic cleavage of the amide bond between histidine and glycine. The cleavage was further monitored following the ^{1}H NMR resonances of the free glycine signal during 5 days.

The major products of the hydrolysis of AcHisGly promoted by our metal complexes were *N*-acetylhistidine and free glycine, as expected. Background hydrolysis was less than 10% after 5 days, showing that the metal complexes were responsible for hydrolytic cleavage, and not the acidic solvent.

Of all tested complexes, the most efficient cleavage agents were Pd(II) complexes **14** and **8**, and Cu(II) complex **17** (Figure 5.3).

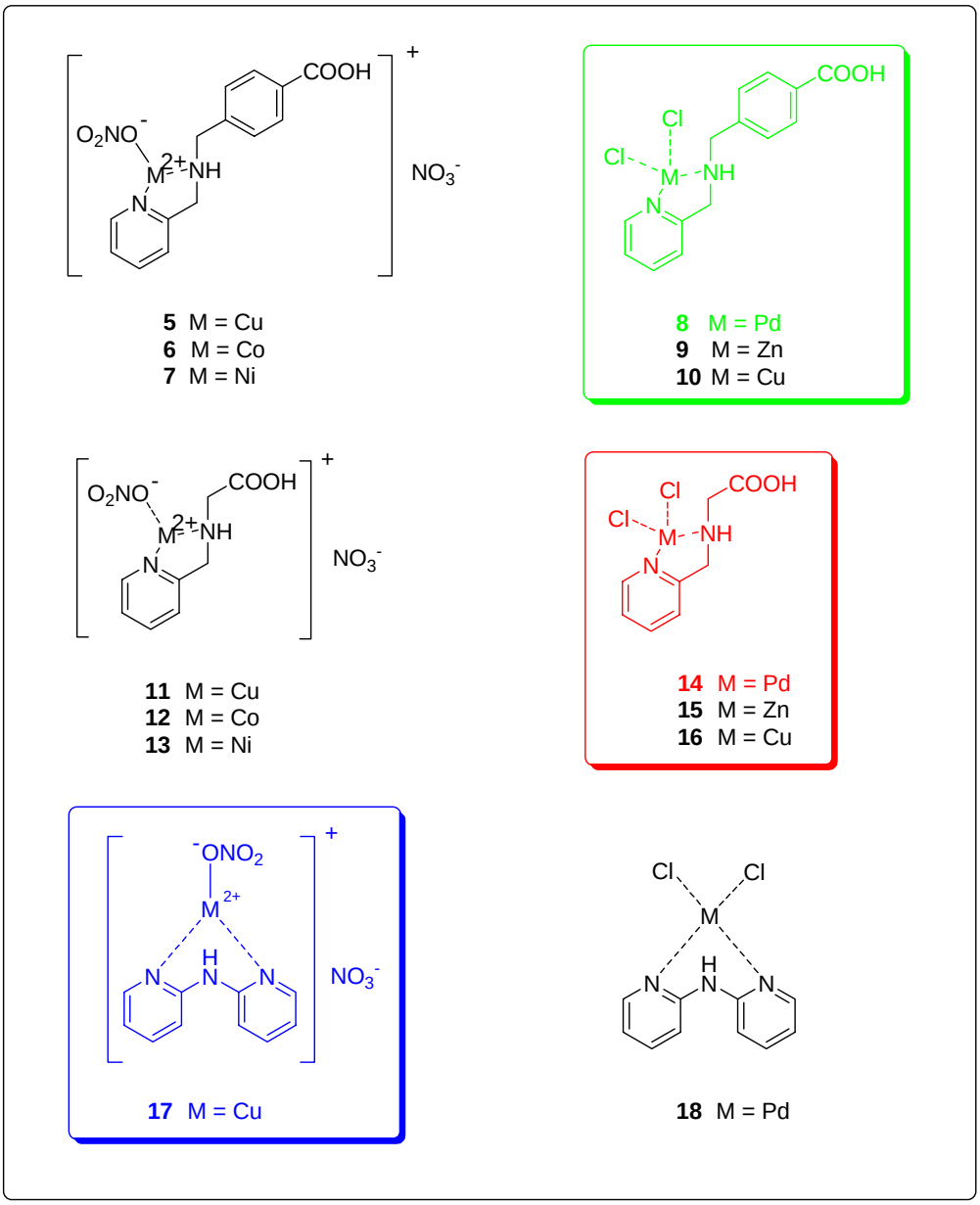

Figure 5.3 *Substrates tested in peptide hydrolysis experiments: compounds **14**, **8** and **17** showed the best peptide cleavage results.*

Palladium(II) complex **14** showed the best result in amide bond cleavage in AcHisGly: *almost 80% of the peptide was cleaved after 5 days*. Palladium(II) complex **8** cleaved almost 50% of the same dipeptide after 5 days under the same conditions. Copper(II) complex **17** showed its peptidase activity with almost 30% of the cleaved peptide. In all cases the cleavage occurred only on the His-Gly bond; we did not detect acetic acid, which would be the product of the cleavage of the acetyl-histidine bond.

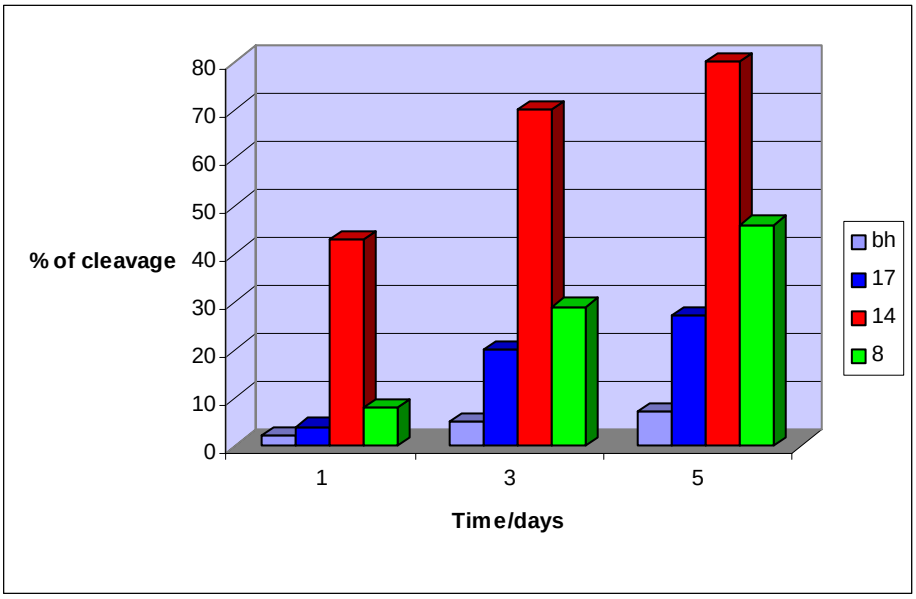

Figure 3.4 *Hydrolysis of the peptide AcHisGly with the compounds **17**, **14** and **8** during 5 days at 60°C and pH 2.9 (bh: background hydrolysis).*

As expected, in the reaction of the acetylated carnosine (AcβAlaHis) with synthesized metal complexes we did not observe hydrolytic cleavage, because the anchoring side chain of histidine is placed on the C-terminus.

a) b)

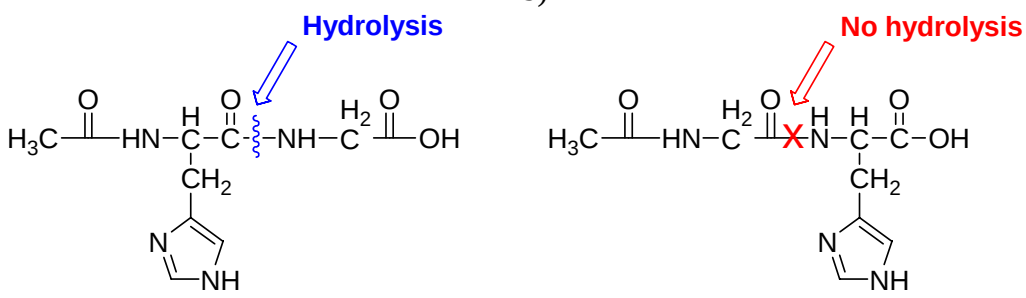

Scheme 3.1 *a) Hydrolysis of the peptide bond is possible only when it is on the carboxylic side of the histidine residue; b) when the peptide bond is on the N-terminus of the anchoring histidine residue, no hydrolytic cleavage observed.*

In the hydrolysis of dipeptides promoted by Pd(II) complexes, our results proved that:

- *A scissile bond on the carboxylic side of the anchoring histidine residue is necessary for hydrolysis;*
- *when the peptide bond is on the N-terminus of the anchoring histidine residue, no hydrolytic cleavage was observed;*
- *simple and readily available palladium(II) complex* ***14*** *acts with useful regioselectivity in promoting hydrolytic cleavage of dipeptides, comparable with one described by Kostić*[31, 32]*:*
- *palladium(II) complex* ***14*** *cleaved almost 80% of the dipeptide after 5 days.*

The ability of Pd(II) complexes to cleave peptides at relatively few sites, with explicable selectivity and good yields bodes well for their use in biochemical and bioanalytical practice.

In addition, in order to synthesize a compound which could take a part in IMAC (Immobilised metal-ion affinity chromatography), in this study we also investigated the possibilities to couple one of the synthesized ligands, whose metal complex could act as a peptidase, with NTA (*N*-nitrilotriacetic acid) moiety, known as an important and well characterized chelator for the oligo-histidine tag.

Therefore, different coupling methods were investigated in the synthesis of the compound **42**:

- Carbodiimide method: coupling with DCC
- Mixed anhydride method: coupling with iBCF
- Disuccinimidyl (DSC) method
- Coupling with TBTU/HOBt/DIPEA

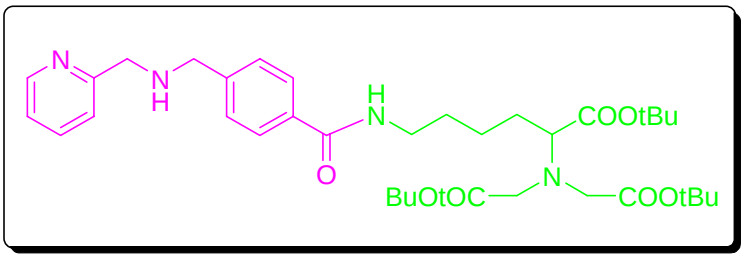

42

We showed that the carbodiimide method and mixed anhydride method could be applied in the synthesis of compound such as compound **42**.

6

References

(1) Best S. L., Chattopadhyay T. K., Djuran M. I., Palmer R. A., Sadler P. J., Sovago I., Varnagy K. *J. Chem. Soc. Dalton Trans*. **1997**, 2587.

(2) Sigel H., Martin R. B. *Chem. Rev*. **1982**, *82*, 385.

(3) Radzicka A., Wolfenden R. *J. Am. Chem. Soc*. **1996**, *118*, 6105.

(4) Sayre L. M., *J. Am. Chem. Soc*. **1986**, *108*, 1632.

(5) Pollack R. M., Bender M. L. *J. Am. Chem. Soc.* **1970**, *92*, 7190.

(6) Kershner L. D., Schowen R. L. *J. Am. Chem. Soc.* **1971**, *93*, 2014.

(7) Pocker Y., Deits T. L. *J. Am. Chem. Soc.* **1982**, *104*, 2424.

(8) Gensmantel N. P., Proctor P., Page M. I. *J. Chem. Soc., Perkin Trans.* 2 **1980**, 1725.

(9) Ramachandran K. L., Witkop B. *Methods Enzymol*. **1976**, *11*, 283.

(10) Walker J. M., *The Protein Protocol Handbook* **1996** Humana Press, Totowa, NJ.

(11) Fontana A. *Methods Enzymol.* **1972**, *25*, 419.

(12) Hendry P., Sargeson A. M., *Prog. Inorg. Chem.* **1990**, *38*, 201.

(13) Sutton P. A., Buckingham D. A., *Acc. Chem. Res.*, **1987**, *20*, 357.

(14) Chin J., *Acc. Chem. Res.*, **1991**, *24*, 145.

(15) Suh J., *Acc. Chem. Res.*, **1992**, *25*, 273.

(16) Rosenberg B., VanCamp L., Trosko J. E., Mansour V. H. *Nature*, **1969**, *222*, 385.

(17) Pettit L. D., Bezer M. *Coord. Chem. Rev.* **1985**, *61*, 97.

(18) Appleton T. G. *Coord. Chem. Rev.* **1997**, *166*, 313.

(19) Kozlowski H., Pettit L. D. *Stud. Inorg. Chem. Rev.* **1999**, *171*, 190.

(20) Burgeson, I. E., Kostić, N. M.. *Inorg. Chem.* **1991**, *30*, 4299.

(21) Zhu, L., Kostić, N. M. *Inorg. Chem.* **1992**, *31*, 3994.

(22) Zhu, L., Kostić, N. M. *J. Am. Chem. Soc.* **1993**, *115*, 4566.

(23) Zhu, L., Qin, L., Parac, T. N., Kostić, N. M. *J. Am. Chem. Soc.* **1994**, *116*, 5218.

(24) Zhu, L., Kostić, N. M. *Inorg. Chim. Acta* **1994**, *217*, 21.

(25) Kostić, N. M., Zhu, L., U.S. **1994**, 17 pp.

(26) Milovic N. M., Kostić, N. M. *J. Am. Chem. Soc.* **2002**, *124*, 4759.

(27) Parac T. N., Ullmann G. M., Kostić N. M *J. Am. Chem. Soc.* **1999**, *121*, 3127.

(28) Milovic, N. N., Dutca L. M., Kostić N. M. Chem. Eur. J. **2003**, *9*, 5097.

(29) Kaminskaia, N. V., Kostić N. M. *Inorg. Chem.* **2001**, *40*, 2368.

(30) Korneeva E. N., Ovchinnikov M. V., Kostić N. M. *Inorg. Chim. Acta* **1996**, *243*, 9.

(31) Parac T. N., Kostić N. M. *J. Am. Chem. Soc.* **1996**, *118*, 51.

(32) Parac T. N., Kostić N. M. *J. Am. Chem. Soc.* **1996**, *118*, 5946.

(33) Milovic N. M., Kostić, N. M. *Inorg. Chem.* **2002**, *41*, 7053.

(34) Chin, J. *Acc. Chem. Res.* **1991**, *24*, 145.

(35) Sigel, H., Martin, R. B. *Chem. Rev.* **1982**, *82*, 385..

(36) Newton, R. A. *Ph.D. Dissertation,* Department of Chemistry, University of Washington, Seattle, **1953**.

(37) Meriwether W., Westheimer F. H. *J. Am. Chem. Soc.* **1956**, *78*, 5119.

(38) Groves J. T., Baron L. A. *J. Am. Chem. Soc.* **1989**, *111*, 5442.

(39) Hegg E. L., Burstyn J. N. *J. Am. Chem. Soc.* **1995**, *117*, 7015.

(40) Nakahara A., Hamada K., Miyachi I., Sakurai K.-I. *Bull. Chem. Soc. Jap.* **1967**, *40*, 2826.

(41) Nakahara A., Hamada K., Nakao Y., Higashiyama T. *Coord. Chem. Rev.* **1968**, *3*, 207.

(42) Buckingham, D. A., Collman J. P., Happer D. A. R., Marzill L. G. *J. Am. Chem. Soc.* **1967**, *89*, 1082.

(43) Marzill L. G., Buckingham, D. A. *Inorg. Chem.* **1967**, *6*, 1042.

(44) Buckingham, D. A., Marzill L. G., Sargeson A. M. *J. Am. Chem. Soc.* **1967**, *89*, 2772.

(45) Collman J. P., Kimura E. *J. Am. Chem. Soc.* **1967**, *89*, 6096.

(46) Collman J. P., Buckingham D. A. *Inorg. Chem.* **1967**, *6*, 1803.

(47) Kimura E., Young S., Collman J. P. *Inorg. Chem.* **1970**, *9*, 1183.

(48) Oh S. K., Storm C. B. *Bioinorg. Chem.* **1973**, *3*, 89.

(49) Vallee B. L., Auld D. S. *Biochemistry* **1990**, *29*, 5647.

(50) Auld D. S. *Structure Bond.* **1997**, *89*, 29.

(51) Lipscomb W. N., Sträter N. *Chem. Rev.* **1996**, *96*, 2375.

(52) Coleman J. E. *Curr. Opin. Chem. Biol.* **1998**, *2*, 222.

(53) Mills C. F., *Zinc in Human Biology*, Springer-Verlag, New York, **1989**.

(54) Vallee B. L., Auld D. S. *Acc. Chem. Res.* **1993**, *26*, 543.

(55) Alberts I. L., Nadassy K., Wodak S. J. *Protein Sci.* **1998**, *7*, 1700.

(56) Wilcox D. E. *Chem Rev.* **1996**, *96*, 2435.

(57) Sträter N., Lipscomb W. N., Klabunde T., Krebs B. *Angew. Chem.-Int. Edit. Engl.* **1996**, *35*, 2024.

(58) Berg J. M. *Acc. Chem. Res.* **1995**, *28*, 14.

(59) Lindskog S. *Pharmacol. Ther.* **1997**, *74*, 1.

(60) Kimura E. *Progress in Inorganic Chemistry*, John Wiley and Sons, New York, **1994**, *41*, 443.

(61) Vahrenkamp H. *Acc. Chem. Res.* **1999**, *32*, 589.

(62) Vahrenkamp H. *Bioinorganic Chemistry-Transition Metals in Biology and Their Coordination Chemistry*, Wiley-VCH, Weinheim, **1997**, 540.

(63) Kimura E., Koike T. Shionoya M. *Structure and Bonding*, Springer-Verlag, Berlin, **1997**.

(64) Parkin G. *Adv. Inorg. Chem.* **1995**, *42*, 291.

(65) Jairam R., Potvin P. G., Balsky S. *J. Chem. Soc. Perkin Trans.* **1999**, *2*, 363.

(66) Itoh T., Fujii Y., Tada T., Yoshikawa Y., Hisada H. *Bull. Chem. Soc. Jpn.* **1996**, *69*, 1265.

(67) Greener B., Moore M. H., Walton P. H. *Chem. Commun.* **1996**, 27.

(68) Hannon M. J., Mayers P. C., Taylor P. C. *Tetrahedron Lett.* **1998**, *39*, 8509.

(69) Scrimin P., Tecilla P., Tonellato U., Valle G., Veronese A. *J. Chem. Soc. Chem. Commun.* **1995**, 1163.

(70) Ruf M., Vahrenkamp H. *Inorg. Chem.* **1996**, *35*, 6571.

(71) Bergquist C., Parkin G. *J. Am. Chem. Soc.* **1999**, *121*, 6322.

(72) Kimblin C., Allen W. E., Parkin G. *J. Chem. Soc. Chem. Commun.* **1995**, 1813.

(73) Dowling C., Parkin G. *Polyhedron* **1996**, *15*, 2463.

(74) Dowling C., Murphy V. J., Parkin G. *Inorg. Chem.* **1996**, *35*, 2414.

(75) Hammes B. S., Carrano C. J. *Inorg. Chem.* **1999**, *38*, 4593.

(76) Cheng X., Zhang X., Pflugrath J. W., Studier F. W. *Proc. Natl. Acad. Sci. USA* 1994, *91*, 4034.

(77) Jaffe E. K. *Acta Crystallogr. Sect. D: Biol. Crystallogr.* **2000**, *56*, 115.

(78) Myers L. C., Terranova M. P., Ferentz A. E., Wagner G., Verdine G. L. *Science* **1993**, *261*, 1164.

(79) Porath J., Carlsson J., Olsson I., Belfrage G. *Nature* **1975**, *258*, 598.

(80) Ritter S., Komenda J., Setlikova E., Setlik I., Welte W. *J. Chrom.* **1992**, *625*, 21.

(81) Hansen P., Lindeberg G., Andersson L. *J. Chrom.* **1992**, *627*, 125.

(82) Hubert P., Porath J. *J. Chrom.* **1980**, *198*, 247.

(83) Sulkowski E. *Trends Biotechnol.* **1985**, *3*, 1.

(84) Kagedal L in: Janson J. C., Ryden L. *Protein Purification*, VCH, Weinheim, **1989**, 227.

(85) Zachariou M., Hearn M. T. W. *Biochemistry* **1996**, *35*, 202.

(86) Winzerling J. J., Berna P., Porath J. J. *Methods* **1992**, *4*, 14.

(87) Hochuli E. Gen. Eng. **1990**, *12*, 87.

(88) Arnold F. H. *Bio/Technology* **1991**, *9*, 151.

(89) Ho C. H., Limberis L., Caldwell K. D., Stewart R. J. *Langmuir* **1998**, *14*, 3889.

(90) Dietrich C. *Ph. D. Thesis*, TU-München **1995**.

(91) Pack D. W., Arnold F. H. *Chem. Phys. Lipid.* **1997**, *86*, 135.

(92) Schmitt L., Dietrich C., Tampe T. *J. Am. Chem. Soc.* **1994**, *116*, 8485.

(93) Ng K., Pack D. W., Sasake D. Y., Arnold F. H. *Langmuir* **1995**, *11*, 4048.

(94) Sigal B. G., Bamdad C., Barberis A., Strominger J., Whitesides G. M. *Anal. Chem.* **1996**, *68*, 490.

(95) Schmid E. L., Keller T. A., Dienes Z., Vogel H. *Anal. Chem.* **1997**, *69*, 1979.

(96) Gritsch S., Neumeier K., Schmitt L., Tampe R. *Biosens. Bioelect*. **1995**, *10*, 805.

(97) Maloney K. M., Shnek D. R., Sasaki D. Y., Arnold F. H. *Chem. Biol.* **1996**, *3*, 185.

(98) Shnek D. R., Pack D. W., Sasaki D. Y., Arnold F. H. *Langmuir* **1994**, *10*, 2382.

(99) Dietrich C., Scmitt L., Tampe R. *Proc. Natl. Acad. Sci. U.S.A.* **1995**, *92*, 9014.

(100) Dietrich C., Boscheinen O., Scharf K. D., Scmitt L., Tampe R. *Biochemistry* **1996**, *35*, 1100.

(101) Kubalek E. W., Le Grice F. J., Brown P. O. *J. Struct. Biol*. **1994**, *113*, 117.

(102) Frey W., Schief W. R., Pack D. W., Chen C. T., Chilkoti A., Stayton P., Vogel V., Arnold F. H. *Proc. Natl. Acad. Sci. U.S.A.* **1996**, *93*, 4937.

(103) Pack D. W., Chen G., Maloney K. M., Chen C., Arnold F. H. *J. Am. Chem. Soc*. **1997**, *119*, 2479.

(104) Barklis E., McDermott J., Wilkens S., Schabtach E., Scmid M. F., Fuller S., Karanjia S., Love Z., Jones R., Rui Y., Zhao X., Thompson D. *EMBO J.* **1997**, *16*, 1199.

(105) O`Shannessy D. J., O`Donnell K. C., Martin J., Brigham-Burke M. *Anal. Biochem*. **1995**, *229*, 119.

(106) Chaouk H, Hearn M. T. W. *J. Chrom.* A **1999**, *852*, 105.

(107) El-Bahnasawy R. M., Khidr, M., Mokhtar, N. *Delta Journal of Science* **1993**, *17*, 141.

(108) Dorn I. T., Neumaier K. R., Tampe R. *J. Am. Chem. Soc*. **1998**, *120*, 2753.

(109) Sheehan J. C., Hess G. P. *J. Am. Chem. Soc.* **1955**, *77*, 1067.

(110) Khorana H. G. *J. Chem. Soc*. **1952**, 2081.

(111) König W., Geiger R. *Chem. Ber.* **1970**, *103*, 788.

(112) Ueki M., Yanagihira T. *Peptides* (Proceedings of the 25th European Peptide symposium), Akademiai Kiado, Budapest, **1998**, 252.

(113) Carpino L. A. *J. Am. Chem. Soc*. **1993**, *115*, 4397.

(114) Ogura H., Kobayashi T., Shimizu K., Kawabe K., Takeda K. *Tetrahedron Lett.* **1979**, *49*, 4745.

(115) Mujumdar R. B., Ernst L. A., Mujumdar S. R., Lewis C. J., Waggoner A. S. *Bioconj. Chem*. **1993**, *4*, 105.

(116) Dourtoglou V., Ziegler J. C., Gross B. *Tetrahedron Lett.* **1978**, 1269.

(117) Kerr, M. C. S. *Diss. Abstr. Int. B* **1972**, *33*, 664.

(118) Karet, G. B.; Kostić, N. M. *Inorg. Chem*. **1998**, *37*, 1021.

(119) Djuran, M. I.; Milinkovic, S. U. *Polyhedron* **1999**, *18*, 3611.

(120) Tsiveriotis; P.; Hadjiliadis, N. *Coord. Chem. Rev*. **1999**, *190*, 171.

(121) Siebert, A. F. M.; Sheldrick, W. S. *J. Chem. Soc., Dalton Trans.* **1997**, 385.

(122) Bonfanti, L., Peretto, S., de Marchis, S., Fasolo, A. *Prog. Neurobiol*., **1999**, *59*, 333.

(123) Rabenstein, D. L., Isab A. A., Shoukry, M. M. *Inorg. Chem*. **1982**, *21*, 3234.

(124) Appleton, T. G., Pesch, F. J., Wienken, M., Menzer S., Lippert B. *Inorg. Chem*. **1992**, *31*, 4410.

(125) Letter, J. E., Jr., Jordan, R. B. *Inorg. Chem*. **1974**, *13*, 1152.